SANDIA REPORT

SAND2006-3485
Unlimited Release

Small Scale Closed Brayton Cycle Dynamic Response Experiment Results

Steven A. Wright, Milton E. Vernon, Paul Pickard

Prepared by
Sandia National Laboratories
Albuquerque, New Mexico 87185 and Livermore, California 94550

Sandia is a multiprogram laboratory operated by Sandia Corporation,
a Lockheed Martin Company, for the United States Department of Energy's
National Nuclear Security Administration under Contract DE-AC04-94AL85000.

Approved for public release; further dissemination unlimited.

Sandia National Laboratories

Issued by Sandia National Laboratories, operated for the United States Department of Energy by Sandia Corporation.

Printed in the United States of America. This report has been reproduced directly from the best available copy.

Available to DOE and DOE contractors from
U.S. Department of Energy
Office of Scientific and Technical Information
P.O. Box 62
Oak Ridge, TN 37831

Telephone: (865) 576-8401
Facsimile: (865) 576-5728
E-Mail: reports@adonis.osti.gov
Online ordering: http://www.osti.gov/bridge

Available to the public from
U.S. Department of Commerce
National Technical Information Service
5285 Port Royal Rd.
Springfield, VA 22161

Telephone: (800) 553-6847
Facsimile: (703) 605-6900
E-Mail: orders@ntis.fedworld.gov
Online order: http://www.ntis.gov/help/ordermethods.asp?loc=7-4-0#online

Abstract

The DOE Generation IV Program is investigating advanced power conversion cycles for next generation nuclear power plants. Brayton cycles using inert or other gas working fluids have the potential for operation at the higher outlet temperatures characteristic of Gen IV reactors and can potentially provide higher efficiency and more compact power conversion systems than current steam cycles. Although open Brayton cycle are in use for many applications (combined cycle power plants, aircraft engines), only a few closed Brayton cycles have been tested. Experience with closed Brayton cycles coupled to nuclear reactors is even more limited. Current projections of Brayton cycle performance are based on analytic models developed in at the National Labs, Universities or NASA. There is relatively limited experimental data to use for model comparisons or validation. This report describes the results of a series of test performed using the recently constructed Sandia Brayton Loop (SBL-30) to develop steady state data, transient data, flow data and control information data for a closed loop gas Brayton cycle. The Sandia Brayton loop is capable of operating with ideal gases or gas mixtures including helium and argon, nitrogen and carbon dioxide. (far from the critical point). The data from the non-CO2 tests are presented in this report, and a subsequent report will be submitted that includes the CO2 Brayton data and analysis. The mix of gases used in the experiments reported here was selected to span the range of gas properties from ideal gases to non-ideal gases such as CO2. This data provides a basis for comparing and validating aspects of the various steady state and dynamic models being used to design Brayton cycles for next generation reactors.

Table of Contents

ABSTRACT **3**

TABLE OF CONTENTS **4**

LIST OF FIGURES **6**

LIST OF TABLES **8**

1 INTRODUCTION **9**

1.1 SUPERCRITICAL CO2 BRAYTON CYCLES 9
1.2 CLOSED BRAYTON CYCLE TEST MATRIX 10
1.3 REPORT CONTENTS 10

2 SANDIA BRAYTON TEST LOOP **11**

2.1 SANDIA BRAYTON LOOP SUMMARY DESIGN DESCRIPTION 11
2.2 DUCTING AND INSTRUMENTATION DESCRIPTION 14

3 MEASURED TEST DATA FROM THE SANDIA CLOSED BRAYTON LOOP **17**

3.1 TEST MATRIX 17
3.1.1 Characteristic Flow Test *18*
3.1.2 Static Operating Power Curve Test *19*
3.1.3 Dynamic Tests *20*
3.1.4 Inventory Control Tests *20*
3.2 TEST CONDUCT 21
3.2.1 Fill and Purge Sequence *21*
3.2.2 Startup Sequence *21*
3.2.3 Inventory Control *22*
3.2.4 Turbine Inlet Temperature Changes, (Transient and Steady State Data) *22*
3.2.5 Fill Gas Change *23*
3.2.6 RPM Changes at Constant TIT (Static Power Operating Curve Tests and Pressure Operating Lines or Flow Curves) *23*
3.2.7 Transient effects of rpm level changes *23*
3.2.8 System Shutdown *23*
3.3 STEADY STATE FLOW CURVE VALIDATION TEST RESULTS 25
3.4 STATIC CLOSED LOOP TEST 29
3.5 STEADY STATE INVENTORY CONTROL TEST DATA 32
3.6 TRANSIENT TEST DATA 34

4 SUMMARY DESCRIPTION OF GEOMETRY, DIMENSIONS AND TEST CONDITIONS **39**

4.1 GEOMETRY AND TEST CONDITIONS FOR STEADY STATE FLOW DATA 39
4.2 TEST CONDITIONS FOR STEADY STATE INVENTORY CONTROL DATA 41
4.3 GEOMETRY AND TEST CONDITIONS FOR ALL TESTS 42
4.3.1 Detailed Description of the Capstone C30 Radial Turbine and Compressors *42*
4.3.1.1 Capstone C-30 Compressor and Turbine 42
4.3.2 Summary Description of the Sandia Brayton Loop Geometry and Dimensions *45*
4.3.2.1 Description of ducting and piping 45
4.3.2.2 Watlow heater description 47
4.3.2.3 Precooler or waste heat gas chiller description 48

5 DETAILED DESCRIPTION OF THE SANDIA BRAYTON TEST LOOP DESCRIPTION **49**

5.1 CLOSED BRAYTON CYCLE TEST-LOOP DESCRIPTION 49
5.2 CAPSTONE TURBO-ALTERNATOR-COMPRESSOR MODIFICATIONS 50

5.3 GAS HEATER DESCRIPTION 59
5.3.1 Electrical Power Description 65
5.4 GAS COOLER DESCRIPTION 67
5.5 DUCTING AND INSTRUMENTATION DESCRIPTION 72

6 SUMMARY AND OBSERVATIONS 77

REFERENCES 79

List of Figures

FIGURE 2.1: SCHEMATIC BLOCK DIAGRAM OF SANDIA BRAYTON LOOP. THE MEASURED GAS TEMPERATURE, PRESSURE AND POWER LEVELS FOR A TEST THAT USED N2 30%HE AS THE WORKING FLUID IS ILLUSTRATED. RED NUMBERS INDICATE COOLANT STATE POINT IDENTIFIERS FOR THE HARDWARE:MODELS. 12
FIGURE 2.2: ASSEMBLY DRAWING OF THE SANDIA CLOSED-BRAYTON-CYCLE TEST-LOOP (SBL-30). 13
FIGURE 2.3: SANDIA BRAYTON LOOP AS INSTALLED AT SANDIA. THE LOOP IS UN-INSULATED IN THIS FIGURE. THE HEATER IS ON THE LEFT, THE GAS CHILLER ON THE RIGHT, AND THE TAC IN THE MIDDLE. 13
FIGURE 2.4: FULLY INSTALLED AND INSULATED SANDIA BRAYTON LOOP. 14
FIGURE 2.5: TOP VIEW SCHEMATIC OF SANDIA BRAYTON LOOP AND LOCATION OF MAJOR TEMPERATURE AND PRESSURE SENSORS, AND THE CONTROLLERS. 15
FIGURE 3.1: COMPARISON OF THE MEASURE OPERATING CURVE (PRESSURE RATIO VERSUS FLOW MEASURED FROM TEST TT4) FOR THE CAPSTONE C30 TURBINE AND COMPRESSOR VERSUS PREDICTED CURVES (SOLID LINES) BASED ON THE MEAN LINE FLOW ANALYSIS OFF-DESIGN PERFORMANCE MODELS FOR A 285 K COMPRESSOR INLET TEMPERATURE AND A 700 K TURBINE INLET TEMPERATURE. THE MEASURED DATA (BLUE TRIANGLES) CORRESPONDS TO A SHAFT SPEED OF 40, 46, 57, AND 62 KRPM 19
FIGURE 3.2: OPERATIONAL CURVE OF SANDIA BRAYTON LOOP SHOWING POWER PRODUCED BY THE ALTERNATOR VERSUS SHAFT SPEED FOR TURBINE INLET TEMPERATURES OF 600 K, 650 K, THROUGH 880 K. NOTE THE TURBINE INLET TEMPERATURE MUST BE ABOVE 650 K BEFORE SELF SUSTAINING OPERATIONS CAN BE MAINTAINED AT ANY TURBINE INLET TEMPERATURE. 20
FIGURE 3.3: TYPICAL OPERATIONAL TRANSIENT OF THE SANDIA BRAYTON LOOP. THE TOP IMAGE SHOWS THE RECORDED GAS TEMPERATURE DATA (DEGREES K) ALONG WITH THE HEATER POWER (SHOWN AS THE BLUE LINE IN PERCENT THERMAL POWER). BASED ON RESISTANCE MEASUREMENTS 100% POWER IS 62.5 KW OF HEATER POWER. THE LOWER SET OF CURVES SHOWS THE PRESSURE DATA FOR ALL PRESSURE TAPS ON THE HIGH AND LOW PRESSURE LEGS OF THE LOOP. 24
FIGURE 3.4: TYPICAL MEASURED DATA WITH A BLOW UP OF THE TURBOMACHINERY SHAFT SPEED AND THE MEASURED ALTERNATOR POWER. THIS IS THE SAME DATA AS SHOWN IN THE PREVIOUS FIGURE EXCEPT THAT THE LOWER PLOT IS EXPANDED TO SHOW THE SHAFT SPEED AND ALTERNATOR POWER. 25
FIGURE 3.5: MEASURED COMPRESSOR AND TURBINE PRESSURE RATIO AS FUNCTION OF MASS FLOW RATE. MASS FLOW RATE IS IN KG/S OF FLUID BEING TESTS. 26
FIGURE 3.6: OPERATING COMPRESSOR PRESSURE RATIO LINES PLOTTED AS A FUNCTION OF DIMENSIONLESS FLOW. ..28
FIGURE 3.7: OPERATING COMPRESSOR PRESSURE RATIO LINES PLOTTED AS A FUNCTION OF DIMENSIONLESS FLOW WITH DATA FOR CO2 INCLUDED AND ON AN EXPANDED SCALE. 29
FIGURE 3.8: POWER OPERATING CURVE FOR VARIOUS GASES AND FOR FIXED TURBINE INLET TEMPERATURES PLOTTED AS A FUNCTION OF SHAFT SPEED. 31
FIGURE 3.9: LARGER SCALE PLOT OF THE OPERATING POWER CURVE FOR VARIOUS GASES AND FOR FIXED TURBINE INLET TEMPERATURES..32
FIGURE 3.10: MEASURED RESULTS OF INVENTORY CONTROL TESTS SHOWING THE ALTERNATOR POWER AS A FUNCTION OF FILL GAS PRESSURE. THESE DATA WERE TAKEN AT STATE POINTS NEAR ZERO NET POWER GENERATION AS THE POWER LEVELS ARE SMALL (A FEW HUNDRED WATTS) COMPARED TO MAXIMUM POWER LEVELS ATTAINABLE OF 10-30 KWE. 33
FIGURE 3.11: PLOT OF INVENTORY COEFFICIENT (ELECTRICAL POWER PER KPA) WHEN MEASURED OVER THE RANGE OF -250 - + 250 WE AND PLOTTED AS A FUNCTION OF MOLECULAR WEIGHT. NOTE THAT THE ARGON DATA IS AT 700 K NOT AT 650 K. 34
FIGURE 3.12: SCREEN IMAGES OF MEASURED TEMPERATURE AND PRESSURE DATA FOR N2 AND N2-10%AR. TEST DATE WAS 06-01-11...36
FIGURE 3.13: SCREEN IMAGES OF MEASURED TEMPERATURE AND RPM AND ALTERNATOR POWER DATA FOR N2 AND N2-10%AR. TEST DATE WAS 06-01-11. 36
FIGURE 3.14: SCREEN IMAGES OF MEASURED TEMPERATURE AND PRESSURE DATA FORARGON AND ARGON 10%HE. TEST DATE WAS 06-03-16. 37
FIGURE 3.15: SCREEN IMAGES OF MEASURED TEMPERATURE AND RPM AND ALTERNATOR POWER DATA FOR ARGON AND AR-20%HE. TEST DATE WAS 06-03-16. 37
FIGURE 3.16: SCREEN IMAGES OF MEASURED TEMPERATURE AND PRESSURE DATA FOR N2-30%HE TEST DATE WAS 06-03-23. 38
FIGURE 3.17: SCREEN IMAGES OF MEASURED TEMPERATURE AND RPM AND ALTERNATOR POWER DATA FOR N2-30%HE. TEST DATE WAS 06-03-23. 38

FIGURE 4.1: CAPSTONE C-30 COMPRESSOR AND TURBINE WHEELS INCLUDE THE GAS THRUST AND JOURNAL BEARINGS. THE COMPRESSOR IS ON THE LEFT SIDE AND IS RELATIVELY COOL, (GREEN COLORS) AND THE TURBINE IS ON THE RIGHT (RED COLORS FOR THE HOUSING AND BEARINGS,COURTESY OF NASA)....................43
FIGURE 4.2: FACE OR FRONT VIEWS OF THE CAPSTONE C-30 COMPRESSOR (LEFT) AND TURBINE (RIGHT). NOTE THAT THE COMPRESSOR WHEEL BLADES ARE BACK SWEPT WHILE THE TURBINE INLET BLADES ARE NOT. ALSO NOTE THAT THE TURBINE BASE IS SCALLOPED, THIS IS LIKELY DONE TO HELP ACCOMMODATE THE GAS FLOW FROM THE INLET NOZZLE AND PRESUMABLY TO HELP BALANCE THE THRUST LOADS. 44
FIGURE 4.3: COMPRESSOR WHEEL AND EXIT DIFFUSER (LEFT) AND TURBINE INLET NOZZLE (RIGHT). 44
FIGURE 5.1: SCHEMATIC OF THE UNMODIFIED C-30 WITH ARROWS ILLUSTRATING THE GAS FLOW PATH AND PROPOSED HOUSING MODIFICATIONS. 50
FIGURE 5.2: "HOT END" OF THE CAPSTONE C-30 MICRO-TURBINE SHOWING THE TURBINE WHEEL, THE COMBUSTOR ANNULUS, AND THE GAS INJECTOR PASSAGES. 51
FIGURE 5.3: PHOTO OF THE 14 TURBINE EXIT BLADES, THE TURBINE INLET ANNULUS, AND THE HIGH PRESSURE RECUPERATOR EXIT. AN ANNULAR SHAPED "COMBUSTOR CAN" IS SLIPPED INTO THE TURBINE INLET ANNULUS TO DIRECT THE GAS EXITING THE RECUPERATOR THROUGH THE INJECTOR PORTS TO THE HEATER. 52
FIGURE 5.4: "HOT" END OF THE CONNECTION FLOW PATHS BETWEEN THE INJECTOR PORTS AND THE HEAT INLET DUCT MANIFOLD FOR THE C-30 CAPSTONE MICRO-TURBINE ASSEMBLY. 53
FIGURE 5.5: CAPSTONE C-30 TURBO-ALTERNATOR-COMPRESSOR CUTAWAY WITH HIGH-PRESSURE ZONE HIGHLIGHTED..53
FIGURE 5.6: SIX TUBES PENETRATING THROUGH THE TURBINE EXIT DOME, THROUGH THE COMBUSTOR DOME SHAPED ANNULUS (MIDDLE "DOME"), AND THROUGH THE TURBINE INLET DOME (SMALLER BOTTOM DOME SHAPED ANNULUS). 54
FIGURE 5.7: CAPSTONE C-30 TURBO-ALTERNATOR-COMPRESSOR ENGINEERING DRAWING CUTAWAY SHOWING THE GAS FLOW PATH. ORANGE LINES SHOW THE FLOW PATH THROUGH THE COMPRESSOR AND RECUPERATOR, RED LINES SHOW THE FLOW PATH THROUGH THE TURBINE AND RECUPERATOR. 54
FIGURE 5.8: "COLD END" OF THE CAPSTONE C-30 MICRO-TURBINE ILLUSTRATING THE SPIRAL RECUPERATOR, THE ALTERNATOR, AND THE INLET COOLING PASSAGES ALONG THE ALTERNATOR. 55
FIGURE 5.9: ASSEMBLY DRAWING OF THE SANDIA CLOSED-BRAYTON-CYCLE TEST-LOOP (SBL-30). 56
FIGURE 5.10: FULLY MODIFIED AND ASSEMBLED CAPSTONE C-30 CLOSED-BRAYTON LOOP AS ASSEMBLED AT THE MANUFACTURES (BARBER-NICHOLS INC.) IS ILLUSTRATED. THE GAS CHILLER IS IN THE FORE GROUND AND THE HEATER IS ON THE LEFT SIDE OF THE IMAGE..56
FIGURE 5.11: SANDIA BRAYTON LOOP AS INSTALLED AT SANDIA. THE LOOP IS UN-INSULATED IN THIS FIGURE. THE HEATER IS ON THE LEFT, THE GAS CHILLER ON THE RIGHT, AND THE TAC IN THE MIDDLE. 57
FIGURE 5.12 OVERVIEW OF THE SANDIA BRAYTON LOOP AS VIEWED FROM THE COMPRESSOR INLET.........................57
FIGURE 5.13: FULLY INSTALLED AND INSULATED SANDIA BRAYTON LOOP. 58
FIGURE 5.14: WATLOW 80 KW BRAYTON LOOP GAS HEATER AND CONTROLLER. 59
FIGURE 5.15: "U" SHAPED HEATER ELEMENTS USED IN THE WATLOW HEATER. THE PHOTO SHOWS THE HEATER ELEMENTS, THE GRID SPACER WIRES, THE BAFFLE, AND THE GAS EXIT THERMOCOUPLE (VERTICAL ROD). 60
FIGURE 5.16 WATLOW 80 KW GAS HEATER ELEMENT DESIGN DRAWINGS AND SPECIFICATIONS.................................64
FIGURE 5.17: ELECTRICAL CONNECTION AND COOLING WATER SUPPLY FOR THE SBL-30 AS LOCATED IN BUILDING 6585 ROOM 2504. ALL POWER IS SUPPLIED BY THE 480 3PHASE 100 AMP SERVICE FROM THE WALL. THE COOLING WATER IS PROVIDED BY THE BUILDING FACILITIES MANAGER...66
FIGURE 5.18: ELECTRICAL POWER CIRCUIT FOR THE HEATER PROVIDED BY WATLOW..67
FIGURE 5.19: IMAGE OF THE BASCO/WHITLOCK SHELL AND TUBE GAS CHILLER. INLET WATER FLOWS FROM THE UPPER RIGHT SIDE OF THE IMAGE TO THE LOWER LEFT, WHILE GAS FLOWS IN THE OPPOSITE DIRECTION. 68
FIGURE 5.20: VIEW OF THE BASCO/WHITLOCK SHELL AND TUBE HEAT EXCHANGER GAS INLET FLANGE, SHOWING THE STAINLESS STEEL TUBES...69
FIGURE 5.21: GAS COOLER SPECIFICATIONS (1)...70
FIGURE 5.22: GAS COOLER DESIGN SPECIFICATIONS..71
FIGURE 5.23: TOP VIEW SCHEMATIC OF SANDIA BRAYTON LOOP AND LOCATION OF MAJOR TEMPERATURE AND PRESSURE SENSORS, AND THE CONTROLLERS...72
FIGURE 5.24: TURBINE INLET TEMPERATURE AND PRESSURE SENSORS AND THEIR FEED THROUGH PORTS. NOTE THAT THESE INSTRUMENTS MEASURE THE GAS TEMPERATURE AND PRESSURE IN ONE OF THE SIX HEATER EXIT TUBES. 74
FIGURE 5.25: COMPRESSOR INLET TEMPERATURE AND PRESSURE FEED THROUGH PORT AND SENSORS.......................75

List of Tables

TABLE 1-1: INITIAL PROPOSED TEST MATRIX 10
TABLE 2-1: LIST OF RECORDED DATA CHANNELS, PROVIDING THE CHANNEL NUMBER, NAME, DISPLAY NAME AND A BRIEF DESCRIPTION OF EACH RECORDED CHANNEL. 16
TABLE 3-1: TEST MATRIX OF TESTS COMPLETED IN THE FIRST PHASE OF TESTING. EACH TEST OR TEST PORTION PROVIDES DATA FOR FLOW CHARACTERIZATION INFORMATION, FOR TRANSIENT MODELING, FOR STATIC LOOP PERFORMANCE OR FOR INVENTORY CONTROL TESTS. 18
TABLE 3-2: LIST OF PURE GASES AND GAS PROPERTIES USED IN THE SANDIA BRAYTON LOOP. TESTS OF PURE N2 AND CO2 HAVE BEEN COMPLETED. PURE HE HAS NOT BEEN PERFORMED AND PROBABLY WILL NOT BE BECAUSE OF ITS LOW MOLECULAR WEIGHT. 26
TABLE 3-3: LIST OF GAS MIXES AND THEIR GAS PROPERTIES TESTED IN THE SANDIA BRAYTON LOOP. 27
TABLE 3-4: FILE NAMES CONTAINING THE COMPLETE SANDIA BRAYTON LOOP OPERATIONS. 35
TABLE 4-1: MEASURED DATE FOR PURE NITROGEN AT TIT=700 K, TEST DATE OF 06-01-19. 39
TABLE 4-2: MEASURED DATE FOR PURE NITROGEN, 9.4% ARGON AT TIT=700 K, TEST DATE OF 06-01-11. 39
TABLE 4-3: MEASURED DATE FOR PURE ARGON AT TIT=800 K, TEST DATE OF 06-03-16. 40
TABLE 4-4: MEASURED DATE FOR PURE ARGON/ 20% HELIUM AT TIT=870 K, TEST DATE OF 06-03-16. 40
TABLE 4-5: MEASURED DATE FOR PURE NITROGEN / 30% HELIUM AT TIT=750 K, TEST DATE OF 06-03-23. 40
TABLE 4-6: MEASURED DATE FOR NITROGEN / 30% HELIUM AT TIT=900 K, TEST DATE OF 06-03-23. 40
TABLE 4-7: MEASURED DATE FOR NITROGEN / 30% HELIUM AT TIT=850 K, TEST DATE OF 06-03-23. 41
TABLE 4-8: MEASURED DATE FOR PURE NITROGEN AT TIT=870 K, TEST DATE OF 05-09-13. 41
TABLE 4-9: MEASURED DATA FOR PURE CO2 AT TIT=700 K, TEST DATE OF 06-05-25. 41
TABLE 4-10: MEASURED DATA FOR THE INVENTORY CONTROL TESTS. 42
TABLE 4-11: ESTIMATE OF CAPSTONE C-30 TURBINE DIMENSIONS 45
TABLE 4-12: ESTIMATE OF CAPSTONE C-30 COMPRESSOR DIMENSIONS 45
TABLE 4-13: VOLUMES OF THE DUCTING AND PIPING COMPONENTS IN THE SANDIA BRAYTON LOOP. 46
TABLE 4-14: TOTAL VOLUME GAS LOOP. 46
TABLE 4-15: DUCT AND COMPONENT VOLUMES, MASS, LENGTH, AND HYDRAULIC DIAMETER. 47
TABLE 4-16: WATLOW HEATER DESCRIPTION. 47
TABLE 4-17: BASCO/WHITLOCK GAS CHILLER HYDRAULIC AND HEAT TRANSFER PROPERTIES USED IN THE RPCSIM MODEL FOR THE SANDIA BRAYTON LOOP 48
TABLE 5-1: WATLOW 80 KW GAS HEATER VESSEL PRODUCT SPECIFICATIONS. 61
TABLE 5-2: WATLOW GAS HEAT PRODUCT SPECIFICATIONS FOR THE IMMERSION HEATERS AND THEIR MATERIAL SPECIFICATIONS. 62
TABLE 5-3: FLUID HYDRAULIC AND HEAT TRANSFER PROPERTIES USED IN THE RPCSIM FOR THE SANDIA BRAYTON LOOP SBL-30. 62
TABLE 5-4 WATLOW GAS HEATER VESSEL DESIGN DRAWINGS AND SPECIFICATIONS. 63
TABLE 5-5: MAXIMUM AND TYPICAL POWER DRAWS/ SUPPLY FORM CAPSTONE POWER MANAGEMENT CIRCUITRY 65
TABLE 5-6: BASCO/WHITLOCK GAS CHILLER HYDRAULIC AND HEAT TRANSFER PROPERTIES USED IN THE RPCSIM MODEL FOR THE SANDIA BRAYTON LOOP 68
TABLE 5-7: DESCRIPTION OF INSTRUMENTATION, FEEDTHROUGHS, AND CONNECTORS AT EACH STATION IDENTIFIED IN FIGURE 5.23. 73
TABLE 5-8: VOLUMES ON THE COMPONENTS IN THE GAS LOOP. 76
TABLE 5-9: TOTAL VOLUME GAS LOOP. 76
TABLE 5-10: DUCT AND COMPONENT VOLUMES, MASS, LENGTH, AND HYDRAULIC DIAMETER. 77

1 Introduction

The Generation IV Program is developing advanced reactors and power conversion cycles for next generation nuclear power plants. The advanced reactor systems being investigated include liquid metal and gas cooled systems that have the potential for higher outlet temperatures than current light water reactors. The Sodium Fast Reactor (SFR) , Lead Fast Reactor (LFR), Gas Fast Reactor (GFR) and the Very High Temperature Reactor (VHTR) cover an outlet temperature range of 500 to 950 C (~770 to 1220 K). Brayton cycles using inert or other gas working fluids have the potential for operation at these higher temperatures and can potentially provide higher efficiency and more compact power conversion systems than current steam cycles.

Although open Brayton cycle are in use for many applications (combined cycle power plants, aircraft engines), only a few closed Brayton cycles have been tested (Suid, 1990). Experience with closed Brayton cycles coupled to nuclear reactors is even more limited (Frutschi, 2005). Current projections of Brayton cycle performance are based on analytic models developed in at the National Labs, Universities or NASA. There is relatively limited experimental data to use for model comparisons or validation. This report describes the results of a series of test performed using the recently constructed Sandia Brayton Loop (SBL-30) to develop steady state data, transient data, flow data and control information data for a closed loop gas Brayton cycle (Wright, 2005 and 2006). This data provides a basis for comparing and validating aspects of the various steady state and dynamic models being used to design Brayton cycles for next generation reactors.

1.1 Supercritical CO2 Brayton Cycles

Of particular interest is the super-critical carbon-dioxide (S-CO2) Brayton cycle which uses CO2 as the working fluid. The super-critical CO2 Brayton cycle is considered promising because it can achieve very high efficiencies (40-50%) at relatively low temperatures (< 1000 K) and with very compact turbo-machinery. It is expected that the low temperatures required by S-CO2 Brayton loops will allow the use of standard metals such as stainless steels to fabricate both the reactor and the Brayton cycle components, with the potential for reduced costs. Likewise the very compact turbomachinery is expected to result in reduced costs as well. The high efficiency occurs because the very little work is required by the compressor to pump the supercritical fluid. In addition the cycle also takes advantage of other non-ideal gas behavior near the critical point (such as increased heat capacity) to improve efficiency because heat rejection occurs more nearly at constant temperature. (An ideal cycle (Carnot) rejects heat at constant temperature.)

No supercritical CO2 test loop has been developed, though small (<1 MWe) and medium scale (10-30 MWe) systems are planned. Even though the Sandia Brayton Loop is not operated with CO2 near the critical point, the loop and test data will provide relevant data for a variety of gases including inert gases, nitrogen, CO2 and gas mixtures from an operating Brayton loop. To the extent possible the existing Sandia Brayton Cycle test loop will be used to help develop and validate the current DOE Program dynamic and steady state models.

The goal of this experimental task focuses on providing data to verify simulation models in four technical areas. The technical issues that will be covered include:

1. the prediction of portions of the characteristic flow curves for the turbine and the compressor,
2. the prediction of the static/steady-state behavior of a complete loop (including the expected operational curves that predict power generation as a function of shaft speed for various fixed turbine inlet temperatures),
3. the ability of the dynamic systems models to predict simple transients (10% step changes in shaft speed or other more complex transients such as startup and shutdown), and
4. the prediction of selected operational aspects of various control strategies.

The Sandia Brayton loop is capable of operating with ideal gases or gas mixtures include helium and argon as well as with mixtures of helium, nitrogen and carbon dioxide. (far from the critical point). The data from the non-CO2 tests are presented in this report, and a subsequent report will be provided that includes the CO2 Brayton data and analysis. The mix of gases used in the experiments reported here was selected to span the range of gas properties from ideal gases to non-ideal gases such as CO2.

1.2 Closed Brayton Cycle Test matrix

Table 1-1 illustrates a summary of the initially proposed test matrix. The test matrix was envisioned to use various working fluids that ranged from ideal (Helium and Argon) to very non-ideal such as CO_2. In addition various binary gas mixtures were also proposed. Four types of tests were planned, these include the four types just described (characteristic flow curve determination, static CBC loop operational behavior tests, dynamic tests, and some control tests. Because of the amount of data that would be collected from each test and to simplify the analysis we limited the test matrix to these four tests and we focused on tests that could be performed largely within the existing safety documentation. No hardware modifications to the loop were made; however, the safety documentation was upgraded to include CO2 and CO2 gas mixture testing.

Table 1-1: Initial proposed test matrix

Test Description / Gas Type	Nitrogen	Argon	Helium	CO2	Gas Mixtures
Flow Curve Validation Test	X	X		X	X
Static Closed Loop Test	X	X		X	X
Dynamic Test	X	X		X	X
Control Test (Inventory)	X	X			X

1.3 Report Contents

Chapter 2 of this report describes the Sandia Brayton loop including photos and engineering drawings of the actual hardware. Chapter 3 provides a description of the test matrix, the rationale for using this test matrix, and the results of the testing. The tests results are grouped into sub-sections which describe the four main types of tests that were performed. These include data to help validate the turbo-compressor flow characteristics, static loop data that shows the dependency between generated power versus shaft speed, a summary data of the transient test, and summary results of the inventory control tests. Chapter 4 provides a condensed version of the details of the test conditions, and it also provides sufficient information, generally in tabular form, to allow steady state and transient analysis of the CBC data. Chapter 5 provides additional details of the Sandia Brayton loop - the test loop and the turbo compressor flow characteristics. Chapter 6 provides the summary and some initial conclusions obtained from this data and also introduces potential future work.

Numerous operations of the Brayton loop were performed but the time history data for only three operations are described in this report. Steady state data was obtained from over six operations of the loop. For each operation of the loop two figures are presented that summarize the transient data and the steady state flow, static power curve, and inventory control data. The third chapter of the report collates that data and presents it according to four types of tests outlined in the test matrix. Thus the report has one section each for the flow curve validation tests, the static closed loop test, the dynamic test, and the control test. Following the test results, is a section that provides information including test data and loop data that is needed to model each test. Generally, the steady state test results require less information to model, while the dynamic model testing requires a complete description of the loop.

2 Sandia Brayton Test Loop

Few reactors have ever been coupled to closed Brayton-cycle systems. As a consequence of this lack of experience, the mechanisms for control and the system behavior under dynamically varying loads, during startup and shut down conditions, coupled to the requirements for safe and near autonomous operation are uncertain or unfamiliar to the nuclear community. As a consequence of this lack of experience Sandia National Laboratories sponsored a Laboratory Directed Research and Development effort (LDRD) to study the coupling of nuclear reactors to gas dynamic Brayton power conversion systems. *(Advanced High Efficiency Direct Cycle Gas Power Conversion Systems for Small Special Purpose Nuclear Power Reactors", reference SAND 2006-2518.)* The research focused on three areas:

1. developing an integrated dynamic system model,
2. fabricating a 10-30 kWe closed Brayton cycle test loop (call the SBL-30, for the Sandia Brayton Loop 30 kWe), and
3. validating these models by operating the Brayton test-loop.

Operation of the test-loop and developing the system models has allowed Sandia to develop a set of tools and models that can be used to determine how nuclear reactors operate with gas turbine power conversion systems. These tools are proving useful for evaluating control strategies, and for modeling larger reactor systems, such as High Temperature Gas reactors and other Next Generation Systems.

2.1 Sandia Brayton Loop Summary Design Description

Sandia contracted Barber-Nichols Inc. to design, fabricate, and assemble an electrically heated CBC system (Barber-Nichols Inc, 2006). The system design is based on a commercially available Capstone micro-turbine power plant (Wright 2005). This approach was taken because it was the most cost effective among a number of approaches considered. All of the rotating components, the recuperator, the gas bearings, and the control components could be used in the closed system. The Capstone open cycle gas turbine system was selected largely because it only required modifying the housing to permit the attachment of an electric heater and a water cooled gas chiller. This approach utilized all of the other components including the alternator and associated rectification electronics and control hardware. The Sandia Brayton test loop uses a 30 kWe Capstone C-30 gas-micro-turbine generator that normally operates at 1144 K turbine inlet temperature (TIT) with a shaft speed of 96,000 rpm (Capstone, 2005).

The CBC test-loop hardware is currently configured with a heater that is designed to ~80 kW_t with an outlet temperature of 1000 K. Improved heater systems that better simulate the thermal hydraulics of nuclear reactors and that are capable of providing higher temperatures and more power can be used in the future. At the present time the heater is limited to 63 kW and 900 K outlet temperatures. The chiller is capable of rejecting up to 90 kW_t and has a water flow rate of 68 liters/min of chilled water at 285 K=56 F. The Sandia house water supply is at 56 F. Figure 2.1 shows a block diagram of the loop and some measured gas temperatures and pressures for the operation that used a gas mixture of 70% Nitrogen and 30% Helium. For these conditions the heater power was 50 kW and the generated electrical power was 8 kWe which results in an efficiency of 16%. The heater power is controlled by a 4-20 mA current source by a Sandia provided National Instruments controller. The water flow rate is not directly controlled at this time. Some minor modifications to the Sandia facilities were required to provide 122 kW of electrical power at 480 V 3 phase, and the chilled water.

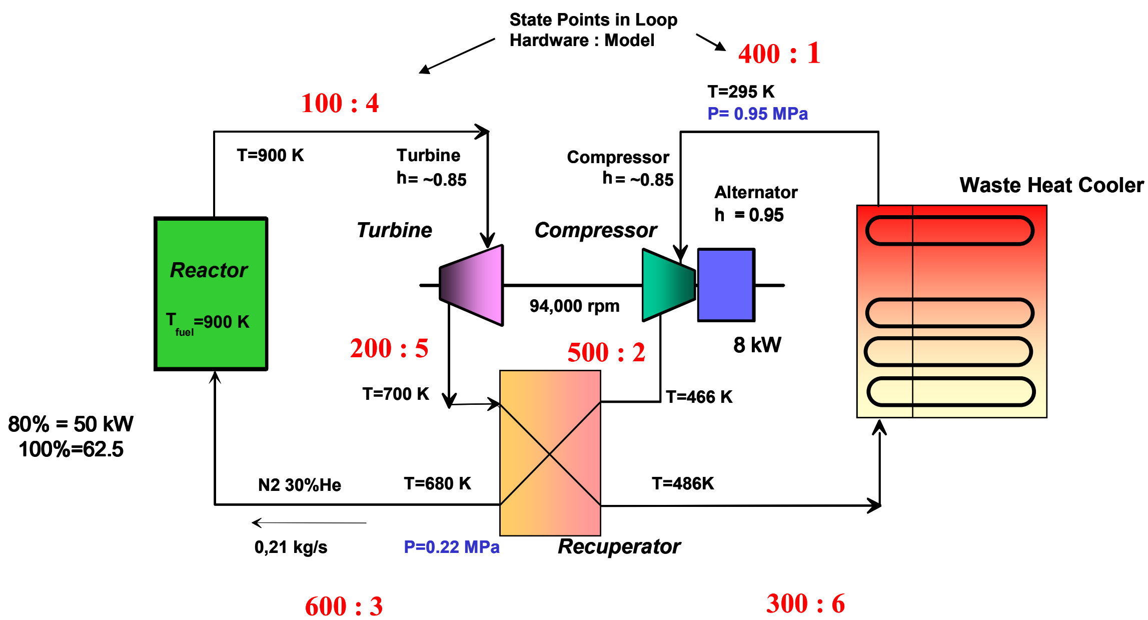

Figure 2.1: Schematic Block Diagram of Sandia Brayton Loop. The measured gas temperature, pressure and power levels for a test that used N2 30%He as the working fluid is illustrated. Red numbers indicate coolant state point identifiers for the hardware:models.

Figure 2.2 shows an engineering drawing of the Brayton loop as developed. Figure 2.3 shows an actual photo of the test loop as installed at Sandia and without the insulation added to the loop.

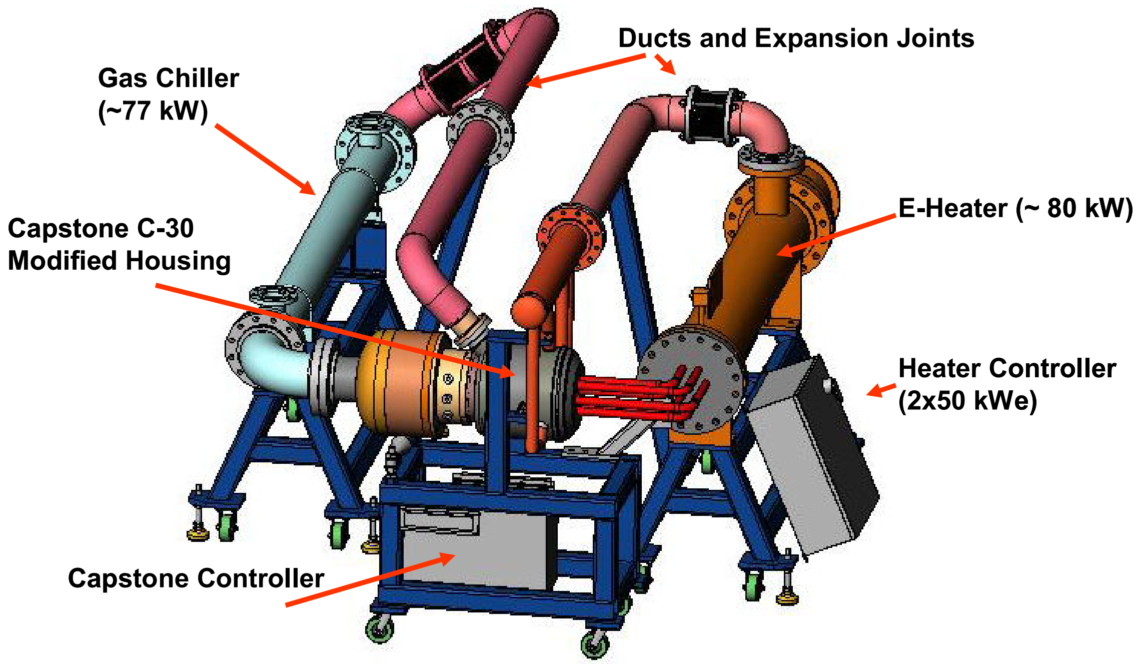

Figure 2.2: Assembly drawing of the Sandia closed-Brayton-cycle test-Loop (SBL-30).

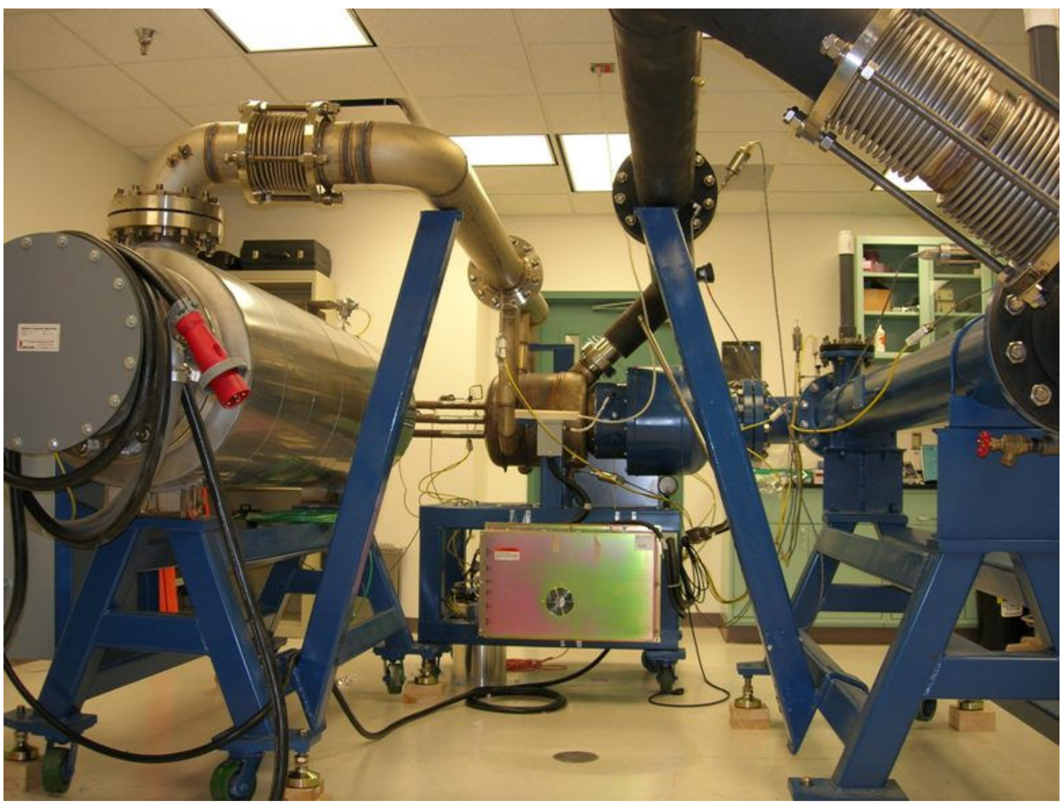

Figure 2.3: Sandia Brayton Loop as installed at Sandia. The loop is un-insulated in this figure. The heater is on the left, the gas chiller on the right, and the TAC in the middle.

Figure 2.4 shows a photo of the loop after the thermal insulation was added to the loop. The initial tests at Sandia indicated that without the insulation the heat losses to the room were large (10-20 kW) at the higher operating temperatures. With the insulation, heat losses are now minimal (~ < 1-2 kW) even for TIT of 900 K. The loop operates quietly, requiring no hearing protection, although it is available for use.

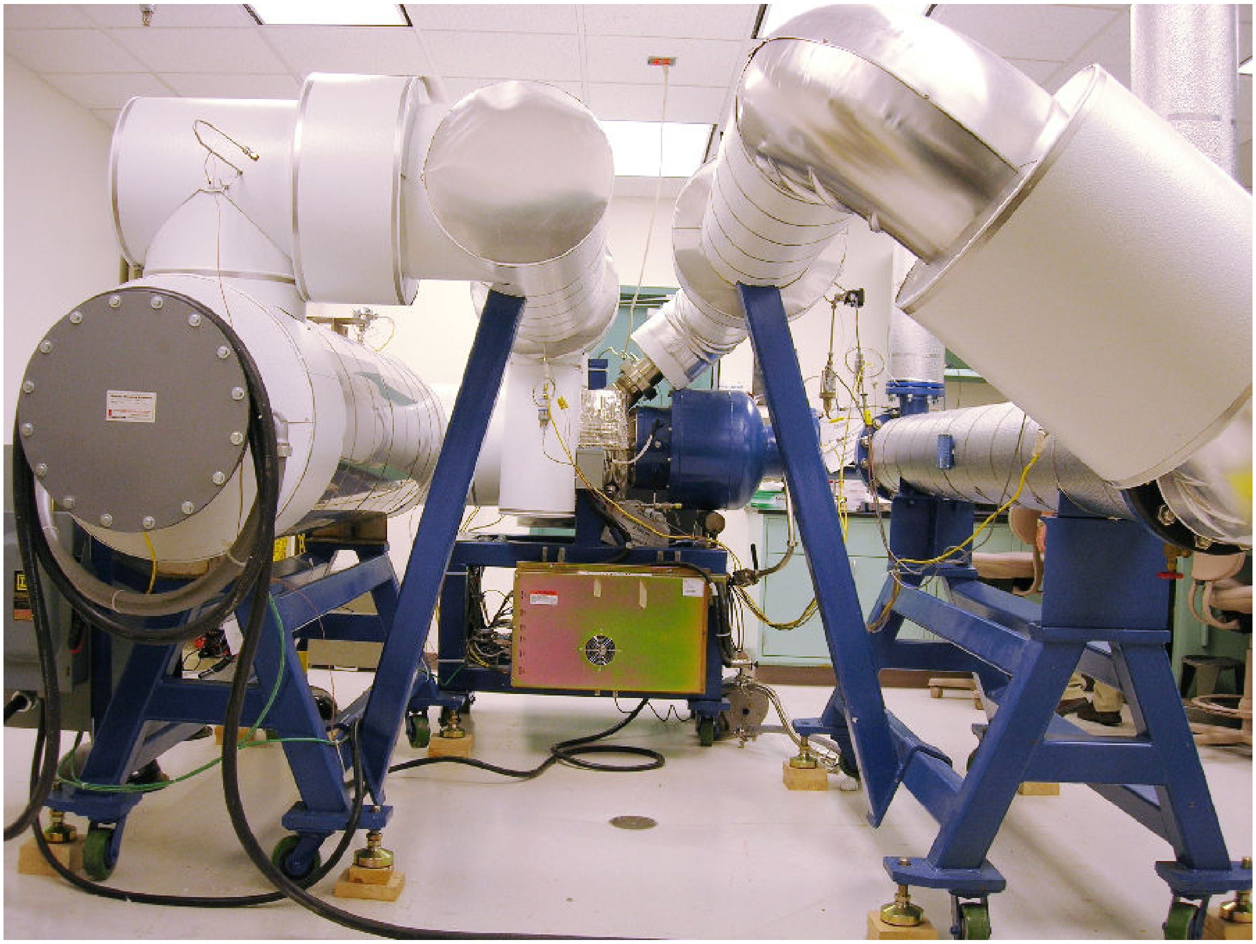

Figure 2.4: Fully installed and insulated Sandia Brayton Loop.

2.2 Ducting and Instrumentation Description

A schematic of the Sandia Brayton Loop is shown in Figure 2.5. This figure shows the location of the pressure and temperature sensors used in the loop. The major sensors consist of temperature and pressure measurements at either the entrance or exit of every major component. The stations are labeled 1-6 starting at the compressor inlet. (The manufacturer used a different numbering scheme when installing the instrumentation). This nomenclature starts with 100 (at the turbine inlet) and then progresses around the loop in increments of 100. The loop also contains a flow orifice at station 6B. The orifice is has a diameter of ½ the ducting inside diameter and the pressure taps are at ½ and 1 times the diameter of the ducting. The ½ diameter tap is located down stream of the orifice. For the gas temperature we use the temperature sensor located at station 6. The flow is calculated using the methods described in ASME MFC-3M-1989. In all cases type K thermocouples are used. For the gas temperature measurements the thermocouples are 1/8" diameter ungrounded sheathed thermocouples. Other pressure tapes not shown in the diagram are located on the inlet and outlet flange of the Watlow heater. Similarly a number of thermocouples were added to provide measurements of hot duct wall temperatures.

Pressure Taps, Temperature Taps, and other Hardware

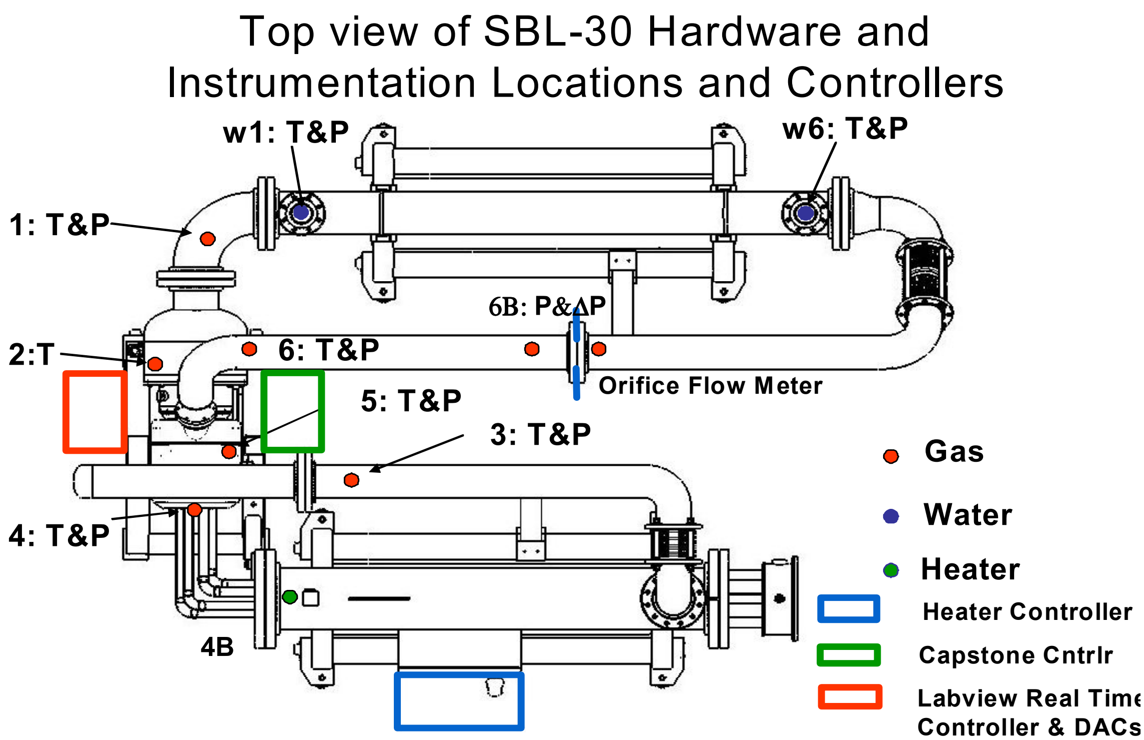

Figure 2.5: Top view schematic of Sandia Brayton Loop and location of major temperature and pressure sensors, and the controllers.

Table 2-1: List of recorded data channels, providing the channel number, name, display name and a brief description of each recorded channel.

Channel Number	Channel Name	Display Name	Description
1	T 100	T 100 Turb In	Turbine Inlet Temperature
2	T 200	T 200 Turb Out	Turbine Exit Temperature
3	T 300	T 300 GCool In	Recuperator Hot Leg Exit Temperature or Gas Chiller Inlet Temperature
4	T 400	T 400 Comp In	Compressor Inlet Temperature
5	T 601	T 601 Htr In	Heater Inlet Duct Gas Temperature after Manifold
6	T 700	T 700	Water Coolant Inlet Temperature
7	T 701	T 701	Water Coolant Outlet Temperature
8	T 500	T 500 Comp Out	Not Available
9	CJ Temp 1	CJ Temp 1	Cold Junction Temperature in FP NI hardware-1st module
10	T 602	T602 Htr Man Pipe	Heater Inlet Duct Manifold Wall Temperature
11	T 603	T603 Htr In Pipe	Heater Inlet Duct Wall Temperature
12	T 302	T302 Chlr InDuct1	Gas Chiller Inlet Duct Wall Temperature 1
13	T 303	T303 Chlr InDuct2	Gas Chiller Inlet Duct Wall Temperature 2
14	T 101	T 101 Htr Out	Heater Gas Outlet Temperature
15	T 102	T 102 Htr Flng	Heater Outlet Flange Temperature
16	T 604	T 604 Htr In	Heater Gas Inlet Temperature
17	T 103	T 103 Htr Elmt	Heater Element Surface Temperature
18	CJ Temp 2	CJ Temp 2	Cold Junction Temperature in FP NI hardware-2nd module
19	P 100	P 100	Turbine Gas Inlet Pressure
20	P 200	P 200	Turbine Gas Outlet Pressure
21	P 300	P 300	Hot Leg Recuperator Gas Outlet Pressure or Gas Chiller Inlet Pressure near Recuperator
22	P 400	P 400	Compressor Gas Inlet Pressure
23	P 500	P 500	Compressor Gas Outlet Pressure
24	P 600	P 600	Ambient Pressure Measured in NEMA box
25	P 601	P 601	Recuperator Cold Leg Outlet Pressure Heater Inlet Duct Pressure and Recuperator Exit
26	P 700	P 700	Water Inlet Pressure
27	P 701	P 701	Water Outlet Pressure
28	FLOW 1	P301 FLOW P	Orifice Pressure (upstream of Orifice)
29	FLOW 2	P302 FLOW dP	Orifice Pressure Drop (1D 0.5 D)
30	Water Flow	Water Flow (gpm)	Water flow rate Gallons per Minute
31	P 101	P 101	Heater Outlet Pressure at Flange
32	P 604	P 604	Heater Inlet Pressure at Heater Entrance
33	Ambient Pressure	Ambient Pressure	Ambient Pressure Measured in NEMA box (=P600)
34	Mass Flow	FLOW	Mass flow rated based on Orifice Measurements
35	RPM	RPM	Shaft speed (revolutions per minute)
36	POWER	POWER	Alternator Power
37	T Aux 1	INVERTER POWER	Inverter Power
38	T Aux 2	T Aux 2	Auxilliary Data Reported From Capstone Controller
39	T Aux 3	T Aux 3	Auxilliary Data Reported From Capstone Controller
40	T Aux 4	T Aux 4	Auxilliary Data Reported From Capstone Controller
41	T Aux 5	T Aux 5	Auxilliary Data Reported From Capstone Controller
42	T Aux 6	T Aux 6	Auxilliary Data Reported From Capstone Controller
43	T Aux 7	T Aux 7	Auxilliary Data Reported From Capstone Controller
44	T Aux 8	T Aux 8	Auxilliary Data Reported From Capstone Controller
45	CBC State	CBC State	Capstone Controller Error State
46	Sweep Mode	Sweep Mode	Sweep Mode Flag (for power sweeps)
47	Heater Delta T	Heater Delta T	Heater dT (T101-T604)
48	Target Inlet Temp	Target Inlet Temp	Target T100 Temperature
49	Target RPM	Target RPM	Target RPM
50	Heater Power %	Heater Power %	Heater Power in percent (100 % = 62.3 kWe, Nov 9, 2005)
51	OverTemp	OverTemp	Over temperature flag reported by Capstone Controller (?)
52	Sweep Time	Sweep Time	Time within sweep
53	On Time	On Time	Data Time (absolute time)
54	Spare A	Spare A	Spare A
55	Spare B	Spare B	Spare B
56	Spare C	Spare C	Spare C
57	Spare D	Spare D	Spare D

3 Measured Test Data from the Sandia Closed Brayton Loop

The Sandia Brayton loop was operated over six times to generate the data presented here. Each operation consisted of up to 12 hours of operation and often began the previous day with filling and purging of the system. The major tests were performed on 9/13/2005, 10/17, 2005, 1/11/2006, 3/16,2006 and 3/25/2006., Each test began with a fill and purge process, which reduced the residual gases in the loop (air) to less than 2%. The fill and purge process lasts about 3 hours. After the system was filled with the correct gas and to the desired fill pressure the Brayton loop operations began. Each operation generally lasted 6-12 hours and the 57 channels of data was collected every second. The collected data is listed in Table 2-1 above. The full data files are available in excel file formats on the DOE Next Generation Server. Truncated transient data files are also available for dynamic simulation studies. The truncated files only provide the required input data such as the heater power, the coolant flow rate and water temperature, and the turbomachinery shaft speed.

3.1 Test Matrix

Test matrix options were discussed at the Gen IV Energy Conversion December 12, 2005 meeting at ANL and documented in a program letter dated, January 10, 2006 “NGen CBC Test Matrix.doc”. This document identifies the high priority tests that could be performed in the near term using the SNL closed Brayton test loop without modifications. The intent is to provide a range of test data that can be used to evaluate features of current models. The proposed experiments involve performing tests in 4 technical areas of interest:

1. **Characteristic flow curve tests** to allow predicting the portions of the characteristic flow curves for small high speed radial turbines and compressors and the turbo-compressor operating curve,
2. **Static Power Generation Brayton tests** – to allow modeling of the static/steady-state behavior of a complete loop (including the expected operational curves that predict power generation as a function of shaft speed for various fixed turbine inlet temperatures)
3. - **Dynamic tests** – to provide basic dynamic response data including startup shutdown and step changes in shaft speed.
4. – **Gas inventory control tests** - to provide preliminary data for modeling inventory control strategies for Closed Brayton Loops.

Table 3-1 illustrates the test matrix completed in the first phase of testing. The top of the table summarizes the gas properties for each of the various working fluids. The test matrix is arranged to test both ideal gases (Ar), non-ideal gases such as N_2 and CO_2, and gas mixtures. The check boxes indicate the type of data that was obtained for each gas and can be categorized into one of the four groups of tests listed above. The gas types and mixtures were purposely varied to study a range of conditions. The ratio of Cp/Cv= γ varied from 1.407 (nitrogen) to 1.67 (Ar or Ar /He). The molecular weight was varied from a low of 21 gm/mole to 44.01 gm/mole. Similarly the gas conductivity was varied from 18 mW/m-K in Ar at 300 K to a high of 46 mW/m-K in a Nitrogen 30% Helium. These gases and gas mixtures were selected to see if the methods used by the modelers were capable of predicting the observed integral effects on flow, pressure ratio, or power level as well as differential data such as temperature differences or pressure drop.

Table 3-1: Test matrix of tests completed in the first phase of testing. Each test or test portion provides data for flow characterization information, for transient modeling, for static loop performance or for inventory control tests.

SNL CBC Testing For Gen IV		Pure Gases				Gas Mixtures			
	Test Date	1/11/2006 10/17/2006	3/16/2006	5/25/2006		1/11/2006	3/16/2005	3/16/2005	3/23/2006
Gas Type	Description	N2	Ar	CO2	He	90N2-10Ar	90Ar-10He	80Ar-20He	70N2-30He
	Cp J/kg*K	1026	→ 518	844	5378	941.4	571	634	1221
	k(300K) mW/m*K	26	18	16	154	26	24	33.1	46
	k(1000K) mW/m*K	60	42	54	336	59	56	72	105
	Ro (J/kg*K)	297	208	188.9	2079	284	229	254	399
	MW (gm/mole)	28	39.9	44.01	4	29	36.4	32.7	21
	Gamma	1.407	→ 1.66	1.316	1.66	1.433	1.66	1.66	1.486
SS	Inventory Test	x	x		Mix				x
SS	Temperature Increase	x	x	x	Mix				x
SS	Flow and RPM Op-Curves	x		x	Mix	x		x	x
SS	Operating Pwr Curve	x		x	Mix	x		x	x
SS	Operating Pressure Ratio	x		x	Mix	x		x	x
Transient	RPM Step Decrease (5000 rpm)	x			Mix	x		x	x
Transient	RPM Step Increase (1000 rpm)	x	x	x	Mix		x	x	x
Transient	Startup	x	x	x	Mix				x
Transient	Shutdown	x		x	Mix	x			x
SS	MW Increase	x							
SS	MW Decrease		x				x		

A brief description of each test type is summarized below.

3.1.1 Characteristic Flow Test

These tests measured the pressure ratio and temperature ratio (or alternatively the efficiency of the turbine and compressor) as a function of dimensionless flow at 40,000, 60,000, 80,000 and 90,000 rpm. Table 3-1 illustrates the results of this type of test for an actual test sequence. Table 3-1 compares the pressure ratio based on the flow data used in the Sandia RPCSIM dynamic model with the measured data. The solid lines show the predicted pressure ratio flow curves for the compressor and turbine, while the blue triangles show the operating points. Multiple operating points can be obtained as a function of mass flow rate by simply changing the fill pressure. However, changing the pressure will not affect the dimensionless flow, so there should be no significant pressure ratio changes as a function of dimensionless flow for fixed shaft speed. Still this test, as shown in the figure below, provides sufficient information to verify whether the characteristic flow curves that are being used are accurately predicted and implemented, at least for the operating range of a real machine.

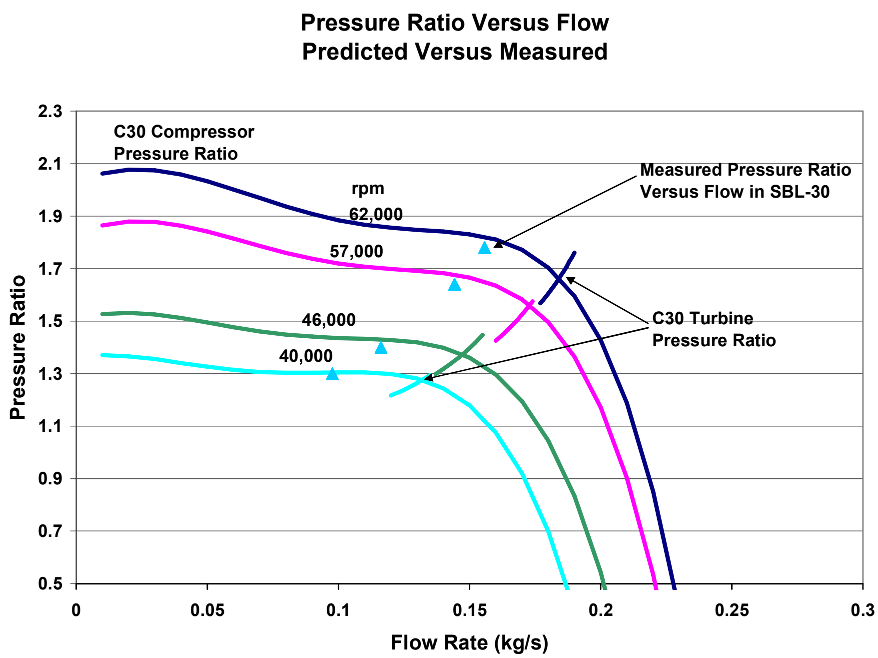

Figure 3.1: Comparison of the measure operating curve (pressure ratio versus flow measured from test TT4) for the Capstone C30 turbine and compressor versus predicted curves (solid lines) based on the mean line flow analysis off-design performance models for a 285 K compressor inlet temperature and a 700 K turbine inlet temperature. The measured data (blue triangles) corresponds to a shaft speed of 40, 46, 57, and 62 krpm

3.1.2 Static Operating Power Curve Test

The objective of these tests was to compare the results of a complete static or steady state closed Brayton loop model with the real behavior. In these tests the power generation capability of the whole loop is compared with the measured data. This report provides a complete description of the CBC test loop to enable modelers to obtain this static or steady state information of generated power as a function of rpm. The geometric and loop data needed includes the flow volumes, heat transfer areas, hydraulic diameter and flow lengths. These data allow prediction of electrical power generated and heater power versus rpm at various turbine inlet temperatures such as 880 K, 800 K, 700 K, 600 K, 500 K for rpm values varying from 40,000-90000 rpm. These curves (see Figure 3.2) are the power operating curves and provide a lot of insight into how the complete system will behave over a variety of operating conditions that range from low power operations, motoring, self-sustaining, and non-linear behavior of the system model.

The Sandia Brayton loop uses load or rpm control to control the power and rpm. This control function was provided by the Capstone Controller. This mode of control uses a feedback loop to continuously adjust the load (which is equivalent to the alternator electrical power) to match the setpoint shaft speed. Because of this feature, the rpm and flow can be controlled at will. Higher shaft speeds mean higher flow rates. For sufficiently high turbine inlet temperature (TIT), an increase in shaft speed results in an increase in power, but only up to a point. Above a certain well defined shaft speed, the shape of the power curve decreases for increasing rpm. Extensive modeling of the closed Brayton loop indicates if the system were operated at a fixed load and without the feedback loop then the shaft speed would only operate on the negative sloped regions of the power curve as these portions are dynamically stable (Wright 2003, 2005, and 2006).

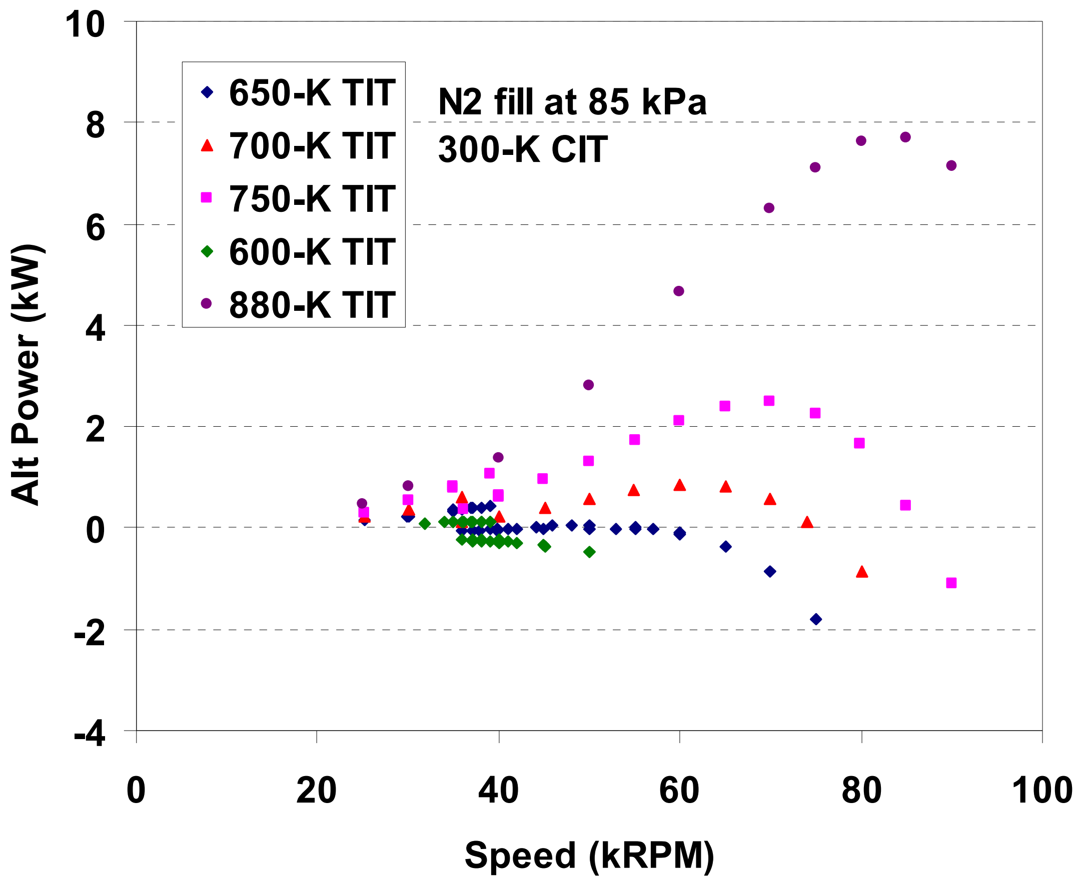

Figure 3.2: Operational curve of Sandia Brayton Loop showing power produced by the alternator versus shaft speed for turbine inlet temperatures of 600 K, 650 K, through 880 K. Note the turbine inlet temperature must be above 650 K before self sustaining operations can be maintained at any turbine inlet temperature.

3.1.3 Dynamic Tests

Measure power transients and operating conditions for the loop are provided to enable analysis of the transient data of any tests including startup and shut down. This report provides additional data for thermal mass, volumes of ducting, and rotating inertia to enable transient modeling. The required Brayton loop data description is provided in section 4.

3.1.4 Inventory Control Tests

Generally two control methods are proposed for the super critical CO2 loop. One involves inventory control and the other involves bypass flow. In the recent set of tests only the inventory control tests were performed. In these tests the Brayton loop was operated at steady state turbine inlet temperature and shaft speed, then the fill gas pressure was reduced or increased, generally by 10 kPa. The new steady state power levels generated by the alternator power level were recorded as well as the transient behavior of the loop. The observed transient effects were small but some thermal and pressure fluctuations were observed after detailed examination of the measured data. This data was most frequently performed at low power levels where the power produced by the turbine was nearly balanced by the power consumed by the compressor. This location was selected as it determines the self-running conditions and also the motor power requirements for startup. Future control tests may incorporate a bypass valve if funding is available.

3.2 Test Conduct

The conduct of each test consists of a number of sequences. The loop is first filled with the desired working fluid, a system checkout and initialization process is then performed to assure that the system components, data acquisition and controls are working, and that the proper valves, pumps, electrical connections are all made. This initialization process is followed by system startup followed by a sequence of power, rpm, pressure, gas type, and thermal maneuvering tests that are designed to study some behavior. After the sequence of tests, the shutdown sequence is initiated, followed by data storage and control systems shutdown. The following paragraphs briefly describe the various sequences used to conduct the Brayton cycle test loop operation.

3.2.1 Fill and Purge Sequence

For each test it is necessary to fill the loop with the desired gas. For each fill sequence the loop was evacuated to 6 psia, and pressurized to 22 psia with the desired coolant. This purge process was repeated 3 times, thus after three purge and fill processes the residual fraction of the original gas in the loop (assumed to be 100% air) was reduced to 2%. Often the fill and purge process was performed the day before the transient test and the whole process typically lasts 3-4 hours. When the system was left filled over night, the loop volume was left pressurized above ambient pressures so that gas leakage was always out of the loop. Because the loop contains about 20 ft^3, the pressure changes over night were low but measurable. Typical leak rates were measured to be about 1-1.7scc/s. We believe that these leaks are through the numerous and large grafoil closure rings located between the flanges of the ducting. The leak rates are larger than desired but don't appear to strongly affect the results of the test over the time period of the tests.

3.2.2 Startup Sequence

Figure 3.3 and Figure 3.4 show actual recorded data made during a test that was performed on January 11, 2006. It will be used to illustrate roughly how all tests were performed. These figures contain markers indicating key events in a run. These events consist of startup (spinning the shaft and starting the turbomachinery), inventory control (pressure reductions or increases), thermal power level changes (results in gas temperature increases), gas filling with a different gas or addition of the same gas, shaft speed changes at constant turbine inlet temperature, and shut down.

All tests were started by first "motoring" the turbo-machinery for a few minutes prior to starting the heater. The startup of the turbomachinery easily seen as increased rpm at 10,000 s in the illustration, see Figure 3.3 and Figure 3.4. Typically the rpm was first increased to 25,000 rpm for a few minutes then increased to 40,000 – 50,000 rpm. In all cases the shaft speed was limited to keep the motor power to less than 2.5 kW as this is near the upper capability of the Capstone motor control circuitry.

Once the turbomachinery begins to spin, the low pressure leg of the loop decreases and the high pressure leg increases in pressure. Increases in shaft speed always result in reductions in the low pressure leg and increases in the high pressure leg of the loop. During startup the compression and expansion processes causes some minor changes in gas temperature which can easily be observed in the test however they are not readily visible in the illustration due to the scale used in the plots.

Once the turbo-compressor begins spinning and the mass flow rates are checked to see that they are in the correct range then the heater power is turned on. This occurs at about 10,300 seconds in the illustration, and results in an increase in gas temperature. Also observe that as the gas heats the overall pressure in the system increases. Once heating starts and the gas temperature appear correct then the controller is switched to automatic thermal control. In this mode the controller uses a feedback loop to adjust the thermal power level to produce a setpoint temperature for the turbine inlet temperature. Because of the thermal inertia of the heater and other loop components it can take up 20 minutes or more to reach a desired set point temperature. Typically the auto-control feature is used to keep the turbine inlet temperature at the desired set point and then the shaft speed or gas pressure is changed to observe the new state points of the loop. This has the effect of producing near steady state temperatures within about twenty minutes, but the power level slowly fluctuates as thermal energy is transferred into the heater walls and bulkhead.

3.2.3 Inventory Control

The inventory control tests were performed once the steady-state turbine inlet was achieved. In the illustration this started at about 15,000 s into the run and lasted until almost 18,000 s. During these inventory reductions the turbine inlet temperature (TIT) was kept at 650 K. The test was performed by reducing the compressor inlet pressure in increments of 10 kPa while the shaft speed was kept constant at 50,000 rpm. Note that reductions in compressor inlet pressure also resulted in a reductions in the high pressure leg of the loop. The test consists of recording the changes in measured alternator power, and compressor pressure ratio as a function of compressor inlet pressure or fill gas inventory. This test was performed for three gases, N_2, Ar, and N_2-30%He.

The current models assume that there is approximately 0.529 m^3 or about 18.7 ft^3 of volume in the loop which when filled with 115 kPa of Nitrogen consists of about 0.705 kg of gas in the loop. Typically this phase of the test reduces the system pressure by 40-50 kPa. This represents up to 30 percent of the fill gas inventory or about 0.23 kg of gas.

3.2.4 Turbine Inlet Temperature Changes, (Transient and Steady State Data)

Shortly after the inventory test phase some transient heating was performed. Here the feedback controller was used to increase the TIT in two steps of 50 K. This data is viewed as transient data and resulted in step increases in generated electrical power, hot leg gas temperatures and gas pressures. The rate of change of these temperatures and pressures were controlled primarily by the power level but also by the thermal inertia of the system.

Text files are available that give the actual time history of the measure data. These data have been filtered over a 30 second interval and the data in the file is reported every 15 seconds. The data include the time, the raw gas flow rate (kg/s), the electrical power in percent, the shaft speed (rpm), the inlet coolant water temperature, and the water flow rate (gallons per minute).

3.2.5 Fill Gas Change

In most operations the fill gas type and pressure were changed during the run. In the examples shown in Figure 3.3 and Figure 3.4 this occurred at 22000 s. Initially in this example the gas was filled with nitrogen at 120 kPa. At 22,000 s the compressor inlet pressure was 115 kPa, and an additional 10 kPa of Argon gas was added to the system. This change resulted in not only a change in pressure but also an increase in the molecular weight, and specific heat ratio, and reductions in the gas conductivity. The data in Table 3-1 shows a list of these changes.

3.2.6 RPM Changes at Constant TIT (Static Power Operating Curve Tests and Pressure Operating Lines or Flow Curves)

The static power operating curve portion of the test was made by changing the turbo-compressor shaft speed while keeping the TIT constant at 750 K. In the example shown in Figure 3.3 and Figure 3.4 this phase of testing began at 22,500s and ended at 25,500s. Again note that as the rpm increases the low pressure leg values decrease while the high pressure leg values increase. This is a consequence of the pressure ratio changes due to higher shaft speeds in a closed system. During this portion of the run both generated electrical power and pressure ratio data were recorded and plotted as a function of rpm or mass flow rate. Plots of the electrical power as a function of shaft speed provide the static loop dependent measurement of the power operating curve. Plots of the pressure ratio versus flow rate produce the operating line of the characteristic flow curve for that specific gas type and TIT. The Steady-State operating pressure curves versus mass flow rate are shown in Section 3.3, and the operating power generation curves are shown in Section 3.4.

3.2.7 Transient effects of rpm level changes

Many of the operations include a transient measurement that consisted of a rapid shaft speed reduction. In effect speed control is one method of controlling the electrical power generated. Rapid power maneuvers are one example of this method of control. In the example operation shown in a fast reduction in rpm occurred at 26,000s. The rpm was reduced from 75,000 rpm to 60,000 in a few seconds. The resulting power transient (which consists of a spike) is shown in Figure 3.4. Note that in this example the heater power has already been turned off so in effect this phase of the run is really part of the shutdown sequence. The raw data files capture this transient at 1 second intervals and will be provided on the project server.

3.2.8 System Shutdown

The last operational sequence is shut down. In examples shown in Figure 3.3 and Figure 3.4 this process began at about 26,000 seconds. The real time controller first turns the heater power off (25,500s in this example) while the rpm level is kept constant. As the system cools the TIT drops and the generated power decreases. When the motor power required to keep the shaft speed at the set point value exceeds 2.5 kWe, then the rpm speed command is reduced first to 60,000 rpm and then in increments of 5,000 rpm. This results in near stepwise reductions in rpm which always correspond with a resulting power spike. Again the transient data files can be used to model this data. In some runs the shaft speed reductions were manually controlled to keep the alternator power level positive but near zero for as long as possible. These tests are often referred to as decay heat removal tests as they show that it is possible to remove the sensible heat from the reactor for over 1 hour while still producing positive and usable power.

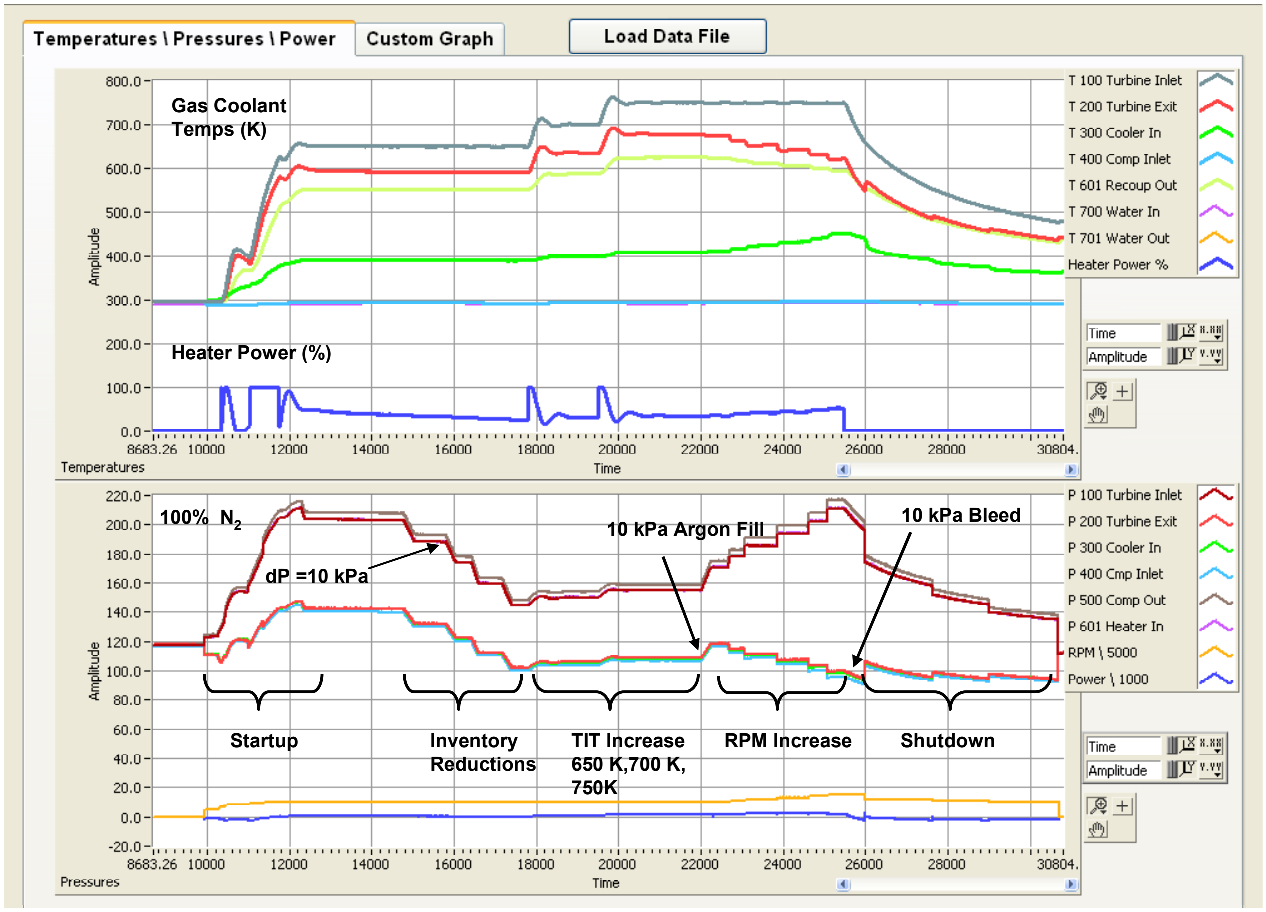

Figure 3.3: Typical operational transient of the Sandia Brayton Loop. The top image shows the recorded gas temperature data (degrees K) along with the heater power (shown as the blue line in percent thermal power). Based on resistance measurements 100% power is 62.5 kW of heater power. The lower set of curves shows the pressure data for all pressure taps on the high and low pressure legs of the loop.

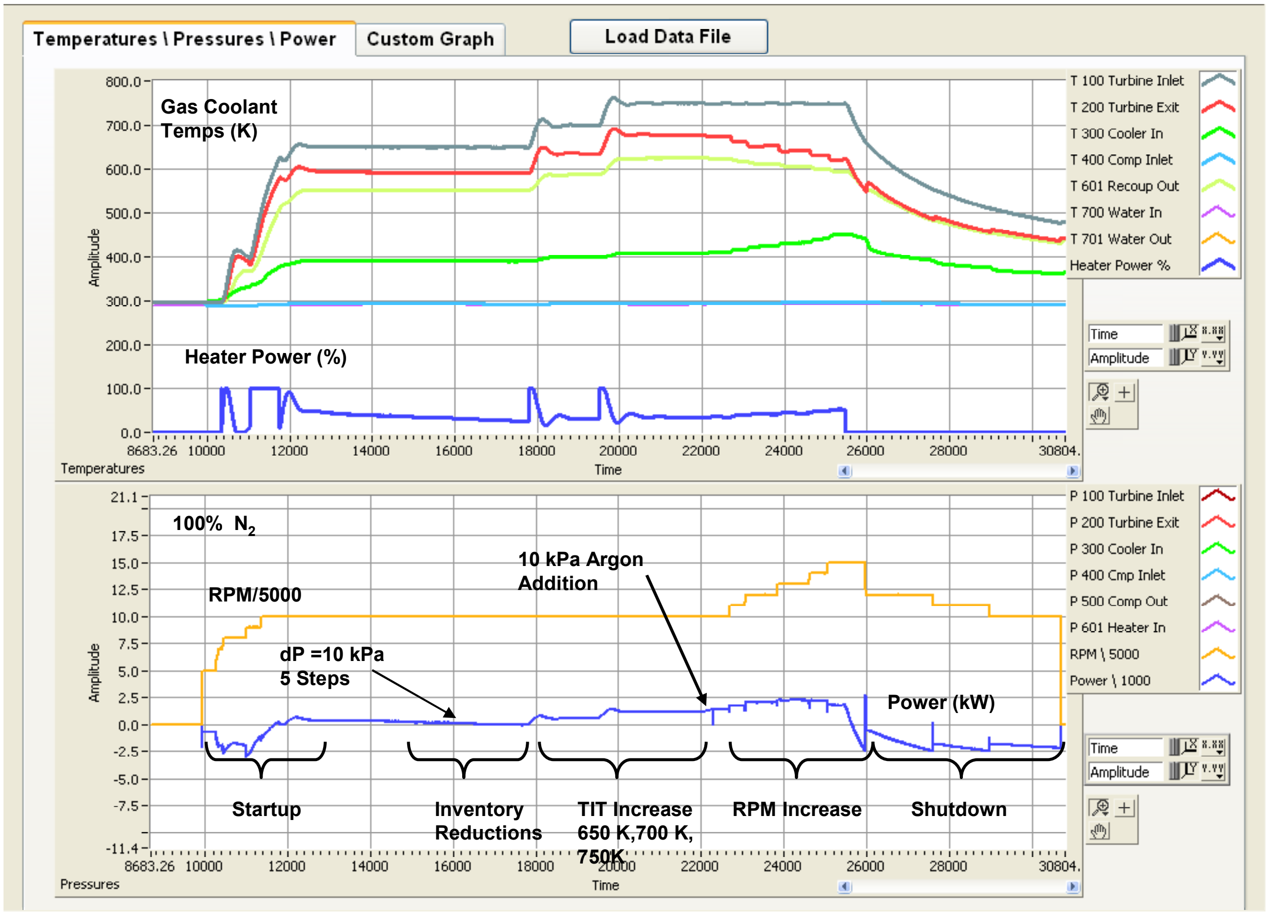

Figure 3.4: Typical measured data with a blow up of the turbomachinery shaft speed and the measured alternator power. This is the same data as shown in the previous figure except that the lower plot is expanded to show the shaft speed and alternator power.

3.3 Steady State Flow Curve Validation Test Results

The steady-state flow characterization data is shown in Figure 3.5. This data was generated by the sequence of test operations describe above in Section 3.2.6. This figure plots the measured compressor and turbine pressure ratios as a function of mass flow rate for various gases and gas mixtures. These curves represent the intersections of the compressor and turbine pressure ratio as shown in Figure 3.1. In general these are curves are nearly straight lines with positive slope and small but positive curvature. In this figure both the compressor and turbine pressure ratios are plotted as a function of rpm. Frictional pressure drops and pressure drops due to form losses in the components must be made up by the compressor, thus the compressor pressure ratio is always larger than the turbine pressure ratio. At low flow rates the fractional pressure drop is on the order of 1.5% while at the higher flow rates the fractional pressure drop is about 3%.

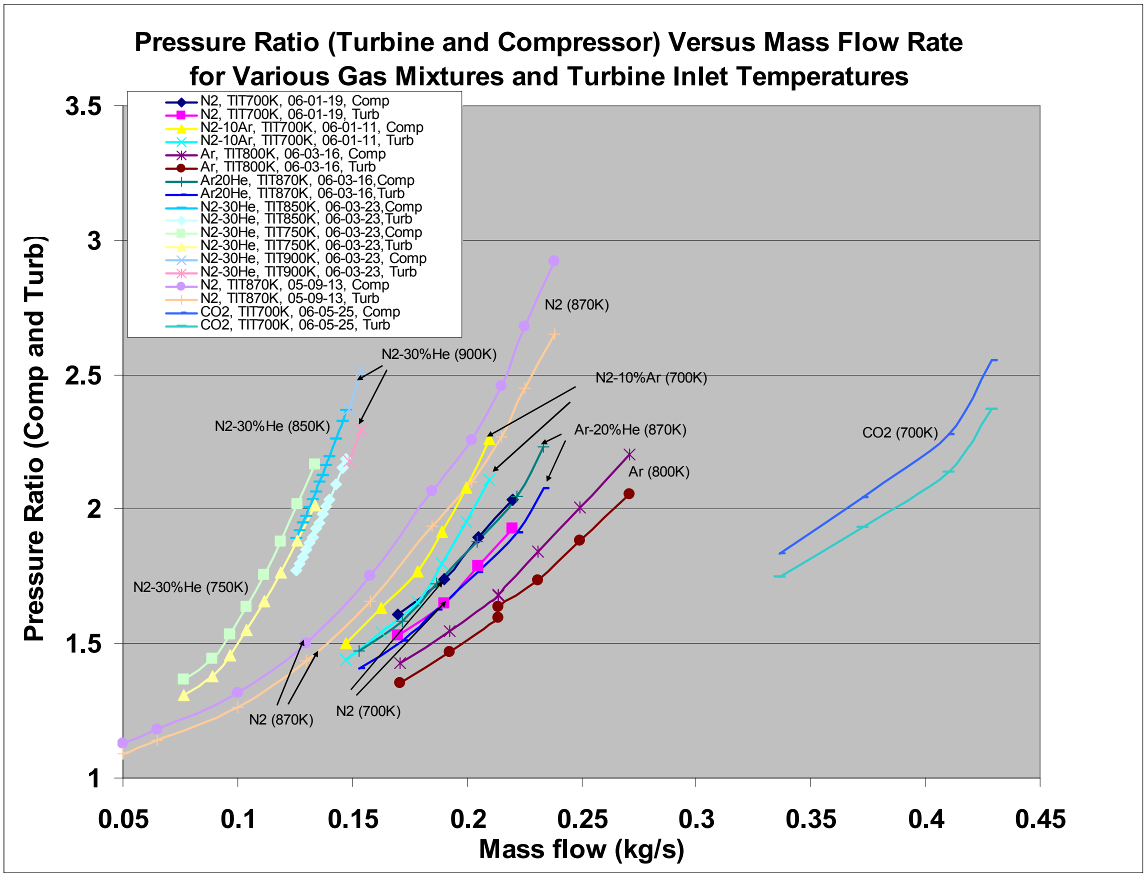

Figure 3.5: Measured compressor and turbine pressure ratio as function of mass flow rate. Mass flow rate is in kg/s of fluid being tests.

The pressure ratio operating curve tests were performed for a variety of gases. Pure gases of N2, Argon and CO2 were used, as were mixed gases. Table 3-2 lists the pure gases used and their gas properties. The gas mixtures that were used include 90%N2-10%Ar, 90%Ar-10%He, 80%Ar-20%He, and 70%N2 -30%He. Table 3-3 shows the gas mixtures and gas properties for these gases.

Table 3-2: List of pure gases and gas properties used in the Sandia Brayton loop. Tests of pure N2 and CO2 have been completed. Pure He has not been performed and probably will not be because of its low molecular weight.

SNL CBC Testing For Gen IV		Pure Gases			
	Test Date	1/11/2006 10/17/2006	3/16/2006	tbd	
Gas Type	Description	N2	Ar	CO2	He
	Cp J/kg*K	1026	518	844	5378
	k(300K) mW/m*K	26	18	16	154
	k(1000K) mW/m*K	60	42	54	336
	Ro (J/kg*K)	297	208	188.9	2079
	MW (gm/mole)	28	39.9	44.01	4
	Gamma	1.407	1.66	1.316	1.66

Table 3-3: List of gas mixes and their gas properties tested in the Sandia Brayton Loop.

SNL CBC Testing For Gen IV		Gas Mixtures			
	Test Date	1/11/2006	3/16/2005	3/16/2005	3/23/2006
Gas Type	Description	90N2-10Ar	90Ar-10He	80Ar-20He	70N2-30He
	Cp J/kg*K	941.4	→ 571	634	1221
	k(300K) mW/m*K	26	24	33.1	46
	k(1000K) mW/m*K	59	56	72	105
	Ro (J/kg*K)	284	229	254	399
	MW (gm/mole)	29	36.4	32.7	21
	Gamma	1.433	→ 1.66	1.66	1.486

The general trend shown in the data shown in Figure 3.5 is that gases with lower molecular weights are located more to the left side of the plot while those with the larger molecular weights are located more to the right hand side of the plot. This is to be expected because higher molecular weight gases have higher densities and lower heat capacities. Therefore, for similar shaft speeds (similar volumetric flow rates) more mass is being pumped around the loop for the higher density gases which causes the plots of the pressure ratio operating curves to move to the right in the plot for higher molecular weights. Other properties such as ratio of Cp/Cv and perhaps gas conductivity may be important parameters as well. To help display this sensitivity to the gas properties we have also plotted (see Figure 3.6) the same pressure ratio data as a function of dimensionless flow. Dimensionless flow is defined as:

$$w` = \frac{w\sqrt{T_{in}\,{R_{ugc}}/{MW}}}{D_{in}^{\;2}\;p_{in}\sqrt{\gamma}}.$$

Where w is the mass flow rate (kg/s), R_{ugc} is the universal gas constant, T_{in} is the inlet compressor gas temperature, D_{in} is the inlet wheel diameter, p_{in} is the inlet gas pressure, and γ is the ratio of Cp/Cv. In Figure 3.6 and in Figure 3.7 this definition for dimensionless flow was used to make the plot, but the inlet diameter was assumed to be 1 because the turbine and compressor wheel sizes aren't changing. Note that the data tends to line up more on a single line than in Figure 3.5. Even though the data is better behaved using the dimensionless plot form, the curves for each gas type are still far enough apart to indicate that these are truly different pressure operating lines. This is most clearly seen in Figure 3.7 where the compressor pressure ratio working line is included in the plot. Most likely, this means that a single curve or family of curves cannot be used to represent the characteristic curves for all gases.

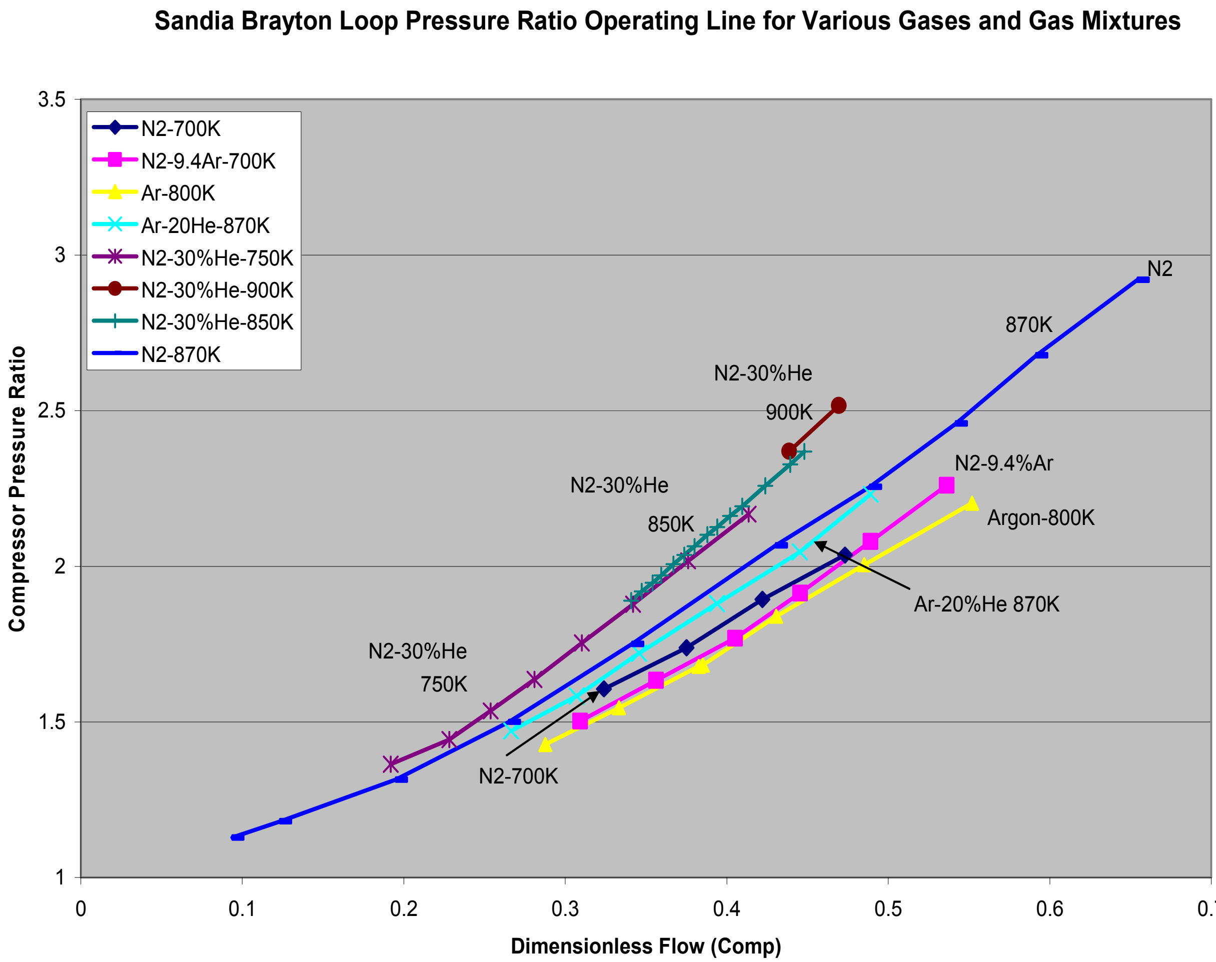

Figure 3.6: Operating compressor pressure ratio lines plotted as a function of dimensionless flow.

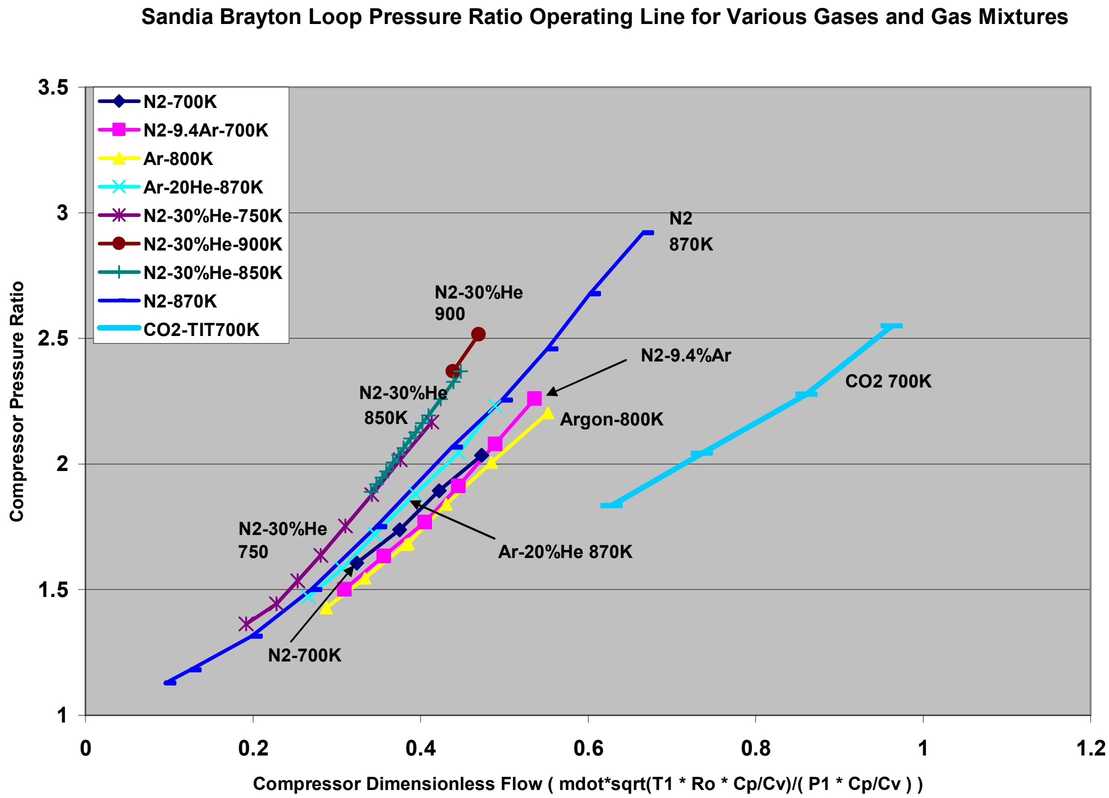

Figure 3.7: Operating compressor pressure ratio lines plotted as a function of dimensionless flow with data for CO2 included and on an expanded scale.

3.4 Static Closed Loop Test

The static Closed Brayton Cycle power operation curve is shown in Figure 3.6. This data was generated by the sequence of rpm shaft speed changes described above in Section 3.2.6. This figure plots the measured alternator power as a function of shaft speed. Each curve represents the alternator power for a fixed turbine inlet temperature and for a fixed gas type. At Sandia we call these curves the power operating curves. In general the curves show an increase in generated power as the shaft speed increases. However the curves always exhibit a maximum and begin to decrease above a certain rpm. Our simple lumped parameter model for these systems predicts this type of behavior.

Earlier tests at Sandia using the Brayton loop were used to generate the family power operating curves. This data is shown in Figure 3.2. Note that at low TIT temperatures the slope of the power operating curve is always negative, but at high TIT the curves start off with a positive slope, reach a maximum and then begin to decrease. This family of operating power curves for specific gas is very useful. It can be used to illustrate some of the non-linear behavior of the closed Brayton loop because the steady state solution has two solutions for each generator power level. One of these solutions is at low rpm and the other at higher rpm. The curves can also be used to predict the break-even or self-sustaining operating conditions of the loop at low rpm and low turbine inlet temperatures. If the curves are extrapolated to zero on the left hand side of the plot, the rpm crossing value at zero power is the self-sustaining shaft speed. This means that the power generated in the turbine just equals the power used by the compressor (plus other losses) for fixed turbine inlet temperature and for each gas type.

The zero crossing at the highest shaft speeds also provides valuable data. The power operating curves at zero alternator power at the higher rpm regions of the plot provide the "loss of load" shaft speed. This is approximately the shaft speed that would be reached if the load were suddenly lost. Whether the turbo-alternator-compressor stays together at this speed depends on the design of the turbine, compressor, and alternator. Of course one should also be very careful in using extrapolated values for this point as we have observed more complex behavior at shaft speeds that are 50-100% greater than the designed shaft speed. At very high shaft speeds our models indicate a reverse temperature gradient in the recuperator. This temperature reversal occurs because the high speed causes a high pressure ratio in both the turbine and compressor, which also means a high temperature ratio. In a reactor driven system the turbine inlet temperature stays nearly constant for fixed reactivity insertion. Thus at high shaft speeds we find that the exit temperature of the turbine is below the exit temperature of the compressor. This results in an inverted temperature gradient within the recuperator. To date, this phenomenon has only been observed in the models and not in the hardware because we can't spin the turbo-compressor fast enough in the hardware.

Other modeling and data analysis has shown that the closed Brayton system is "dynamically stable" on the negative slope portion of the family of operating power curves and "dynamically unstable" for the positive sloped portion of the operating power curve. The Sandia Brayton loop can be operated at any location because the Capstone controller is continually adjusting the load to keep the power at the desired set point. Thus, it uses a dynamic feedback system to achieve stability on the positive sloped portion of the curve.

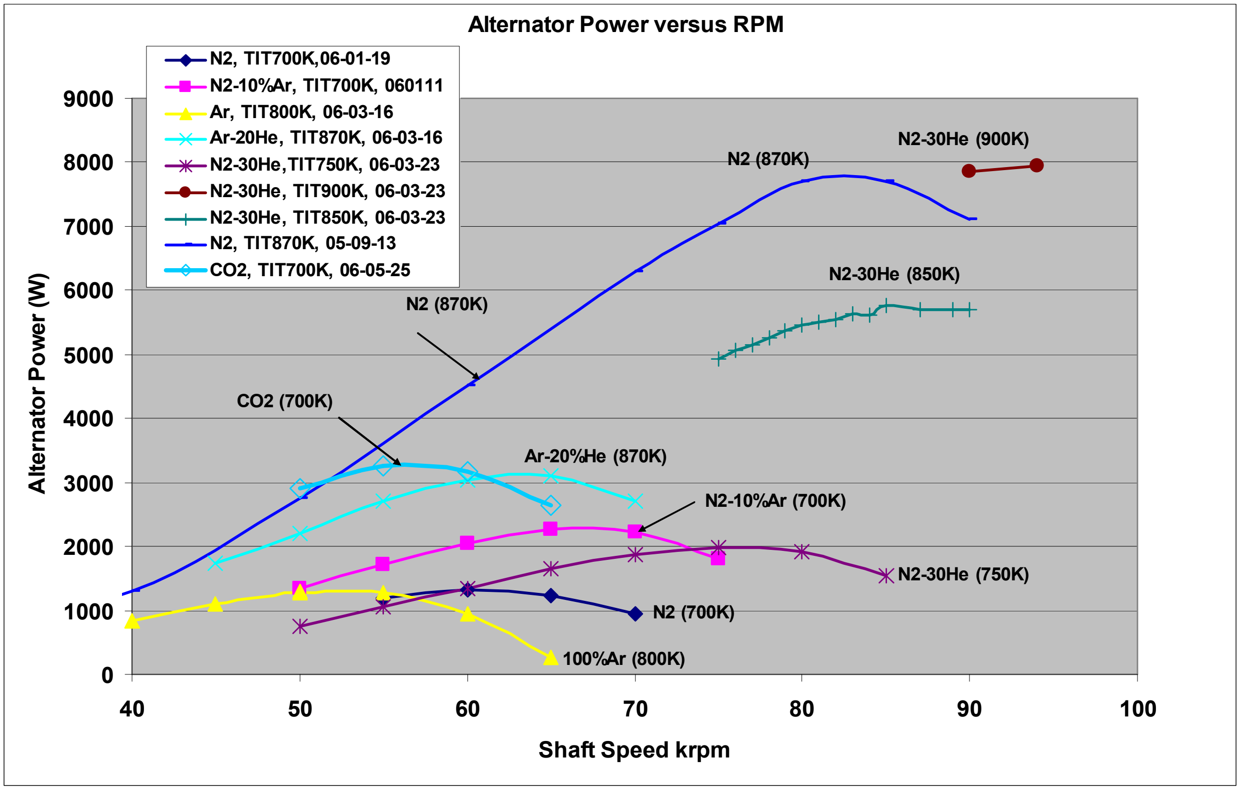

Figure 3.8: Power operating curve for various gases and for fixed turbine inlet temperatures plotted as a function of shaft speed.

A larger scale plot of the measured power operating curve is shown in Figure 3.9. This data was taken at TIT and shaft speeds that produced lower electrical power levels. These limitations were used in part to not over stress the CBC unit for these first tests, and also to provide better data near lower power, lower rpm and lower temperature regions of operation.

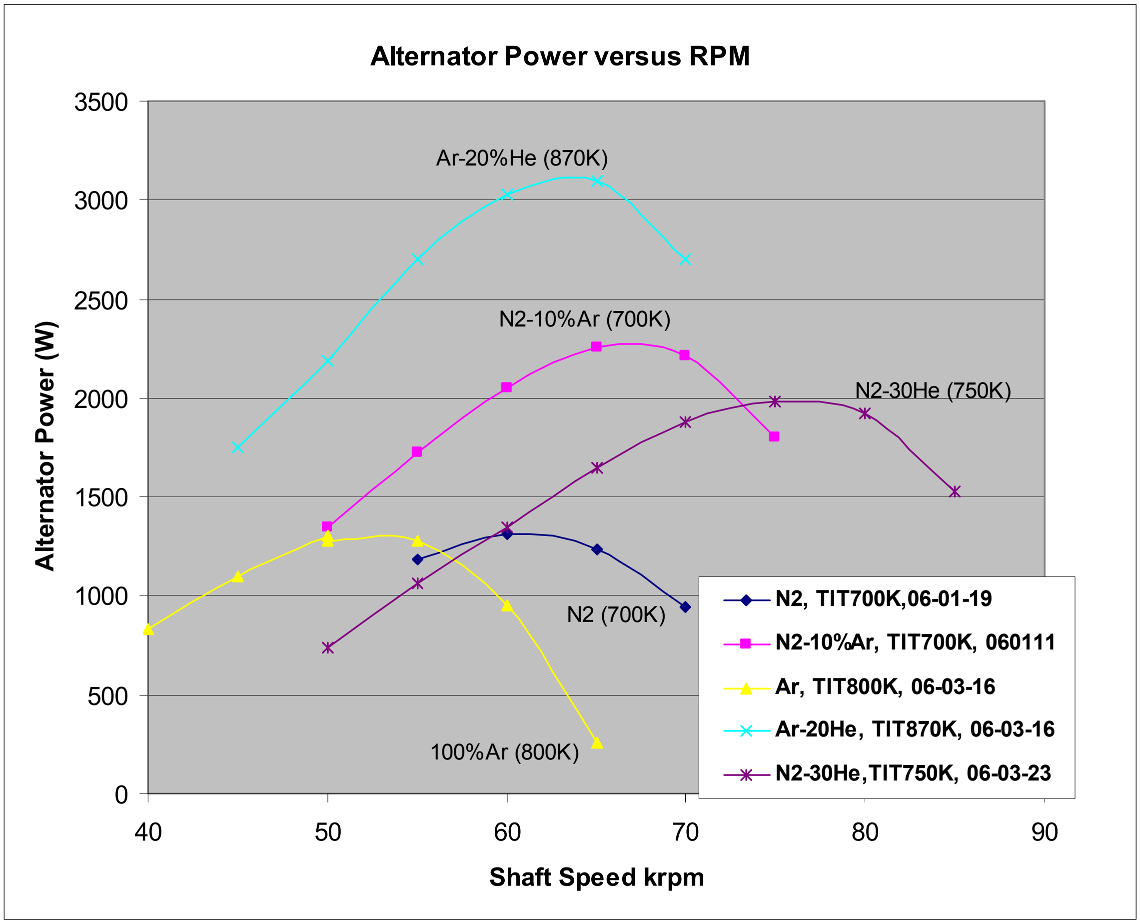

Figure 3.9: Larger scale plot of the operating power curve for various gases and for fixed turbine inlet temperatures.

3.5 Steady State Inventory Control Test Data

Control of reactor systems coupled to closed Brayton cycle systems is an issue for high temperature helium Brayton systems and for super-critical CO_2 systems. For simple recuperated Brayton systems major control approaches include turbine inlet temperature control, rpm or load control, inventory control, bypass control, and throttle control. Supercritical Brayton systems can use all of these approaches in addition to compressor inlet temperature control, and split flow control approaches as well. For large power plants the turbine and alternator will be required to rotate at 3600 rpm, which means that for conventional system designs the compressor (or pump) will also rotate at this constant speed. Because of the constant speed compressor the flow through the reactor or the primary heat exchanger will also be fixed. Under these conditions the option of using rpm/load control is not available. Because the flow rate is essentially fixed due to the fixed shaft speed, other mechanisms are needed to provide ways of shifting power, or adjusting to transients that may be either rapid or slow. Changes in reactor core temperature can be used to change the power level, but in general this method of control is undesirable because of the large thermal mass of the core and for materials and thermal cycling reasons as well.

Inventory control (changes in the average pressure or fluid density within Brayton cycle loop) is one way to change the mass flow rate through the Brayton loop even when the compressor speed is fixed. This approach has the advantage that system efficiency is not strongly affected but for large systems it may be slow as additional pumps are required to increase or lower the working fluid pressure (inventory). Section 3.2.3 described the method that we used to perform the inventory control tests, where the turbine inlet temperature and shaft speed were kept constant and the compressor inlet pressure was reduced in 10 kPa increments. The results of the tests are illustrated in Figure 3.10. This plot compares the alternator power (as reported by the Capstone controller) as a function of compressor inlet pressure for a fixed TIT and for three gases. Based on current understanding of loop operation, it is clear that this reported value is not just the pure alternator power. One explanation is that it is the power output after the rectification and after the buck boost voltage regulation. As such, there are electronic losses included in this data which may be a function of power or rpm. Current loss models are not sophisticated enough to account for these effects at this time.

The three gases that were used included N2, Ar, and 70%N2 – 30%He (mole fraction). The TIT was kept at 650 K for the nitrogen and helium nitrogen mixture. For argon the TIT had to be increased to 700 K to get some of the data to fall in the positive net power production level.

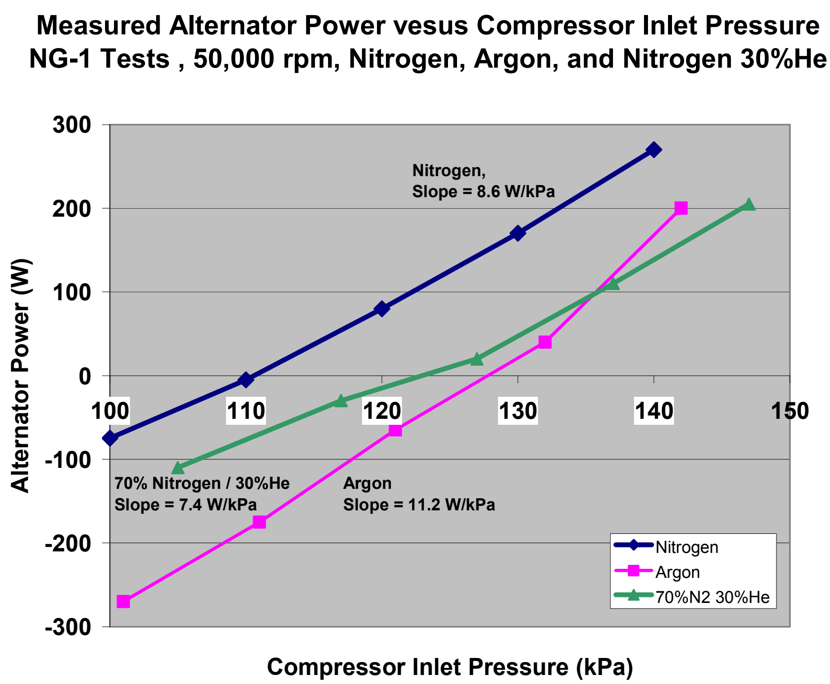

Figure 3.10: Measured results of inventory control tests showing the alternator power as a function of fill gas pressure. These data were taken at state points near zero net power generation as the power levels are small (a few hundred watts) compared to maximum power levels attainable of 10-30 kWe.

First it is observed that the generated electrical power is proportional to compressor inlet pressure. This is what would be expected. Also, pure nitrogen produces the highest power values of the three gases. This is probably because the Capstone turbine and compressor were designed to operate with air which is 80% nitrogen and has similar gas properties as air. This is an indication that for the turbine and compressor the head coefficient (ratio of adiabatic head to tip velocity squared) or the velocity ratio are closer to their optimum values and thus result in the highest efficiencies. These curves are all similar and in the range of 10 W/kPa, but slight differences do exist. It is expected that at higher power levels (nearer to 10 kWe) the magnitude of the inventory slope value (W/kPa) would be proportional to power. It is suggested that some of these tests be repeated at higher power levels.

The inventory power coefficient = electrical power per kPa coefficient (slope of the curve) was also plotted as function of molecular weight in Figure 3.11. This curve shows a trend that increases in magnitude in proportion to molecular weight, but further data is required to confirm this apparent effect.

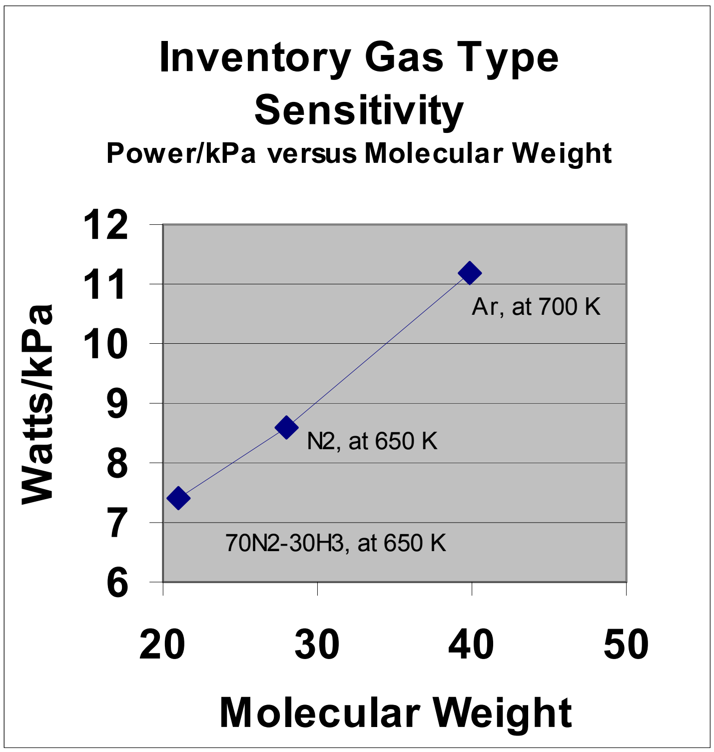

Figure 3.11: Plot of inventory coefficient (electrical power per kPa) when measured over the range of -250 - + 250 We and plotted as a function of molecular weight. Note that the Argon data is at 700 K not at 650 K.

3.6 Transient Test Data

Transient data for three CBC loop operations are provided. Figure 3.12 through Figure 3.17 illustrates the recorded data in a graphical form. These files are contained on the file server. In addition, filtered and sample data are also provided. These files are much shorter and used the complete data set but are
filtered using a time average 30 second window. The data is recorded in the file every 15 seconds. The file names for the filtered data are also provided in the table. The filtered data only contains the input data required to run a dynamic simulation. The data is in the comma separated file format. The data is in columns representing time, electric power (%), rpm (rev/s) mass flow

rate of gas (kg/s), water inlet temperature. Note that the data control and acquisition system are set to work with nitrogen. Because of this, the mass conversion coefficient for the gas mass flow rate is incorrect. However, even though gas mass flow rate is provided it is not needed by the modeling effort because it is calculated by the characteristic flow curves knowing the rpm and the inlet gas temperatures. **Note, the flow must be corrected by the ratio of the MW of the actual gas used divided by the MW of Nitrogen to obtain a real value for the mass flow rate.** The flow rate is probably only good to 5-10%.

The transient data for all channels is provided on the Next Generation file server and as an accompanying CD. The CD also contains a very large excel file that has all the measured data taken for all channels at approximately one second intervals. These data sets consist of raw data and have their own sheet names that use the date of the test as the sheet name. All data are in MKS (meters, kilograms, seconds and degress Kelvin) units except for water flow which is in gallons per minute, and power which is in percent of full power. Full power is 62.5 kW.

The transient data files are provided to allow modeling of an entire transient if desired. Portions of the data can also be used to perform dynamic analysis on specific parameters. Significant portions to model include startup, shutdown and rapid changes in rpm.

Table 3-4: File names containing the complete Sandia Brayton loop operations.

Complete Data Set File name	Filtered Data Set File Name	Gas Mixtures
CBC_060111_1320.csv	F_CBC_060111_1320.csv	Nitrogen , Nitrogen + 9.4%Ar
CBC_060316_0858.csv	F_CBC_060316_0858.csv	Argon, Argon+20%He
CBC_060111_1320.csv	F_CBC_060111_1320.csv	Nitrogen – 30% Helium

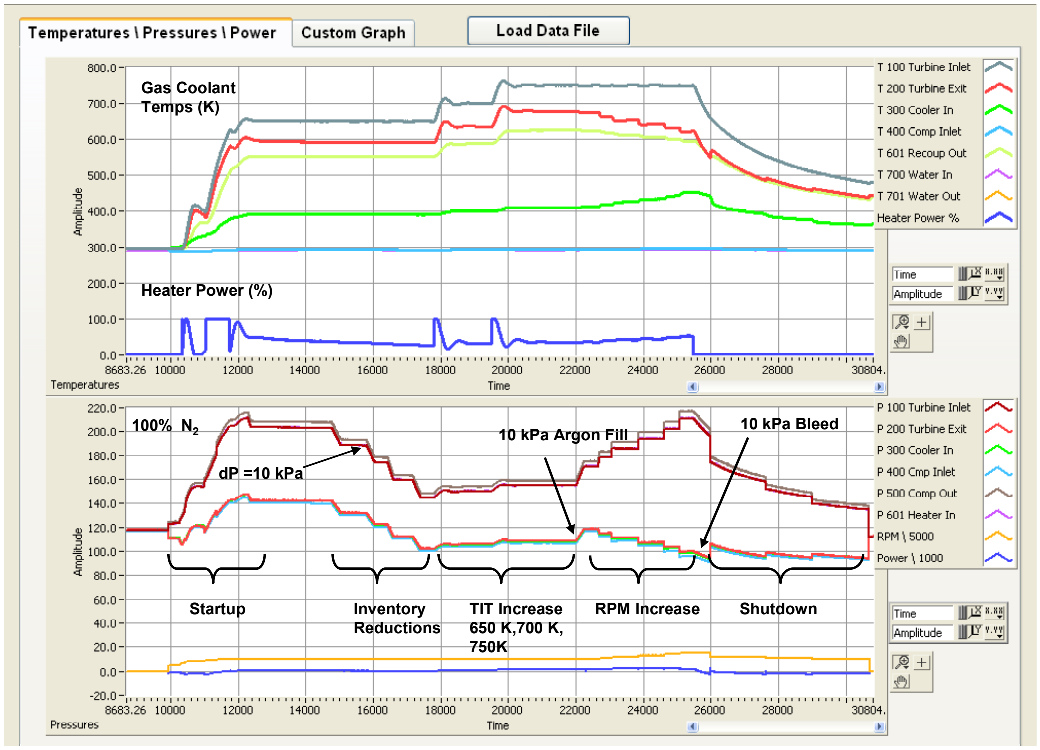

Figure 3.12: Screen images of measured temperature and pressure data for N2 and N2-10%Ar. Test date was 06-01-11.

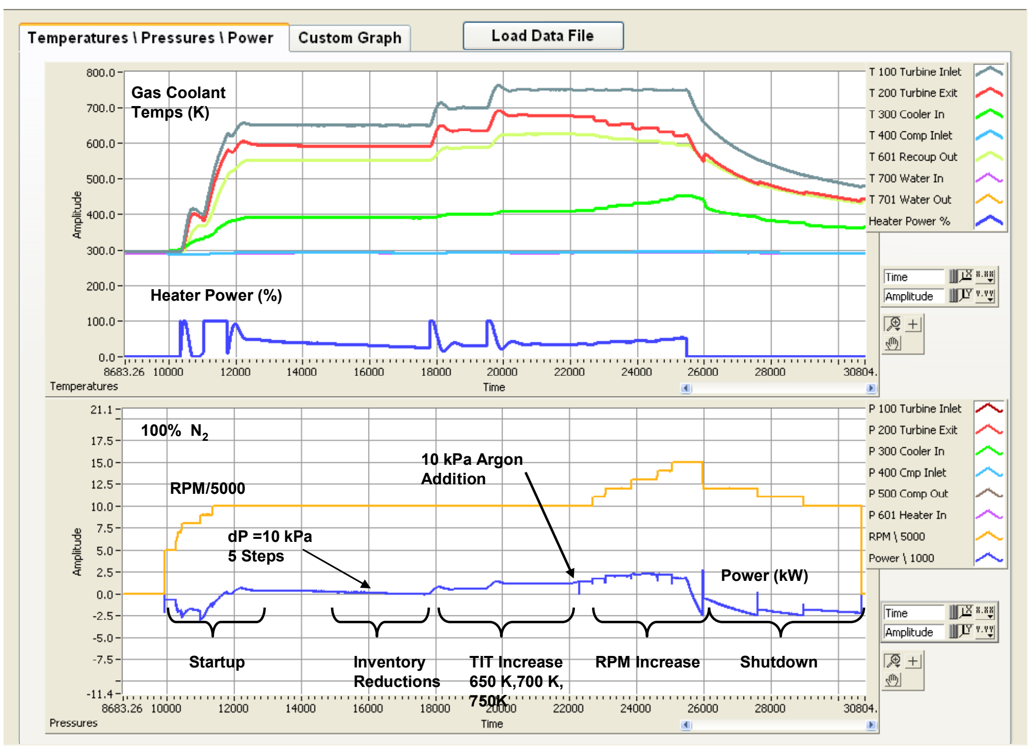

Figure 3.13: Screen images of measured temperature and rpm and alternator power data for N2 and N2-10%Ar. Test date was 06-01-11.

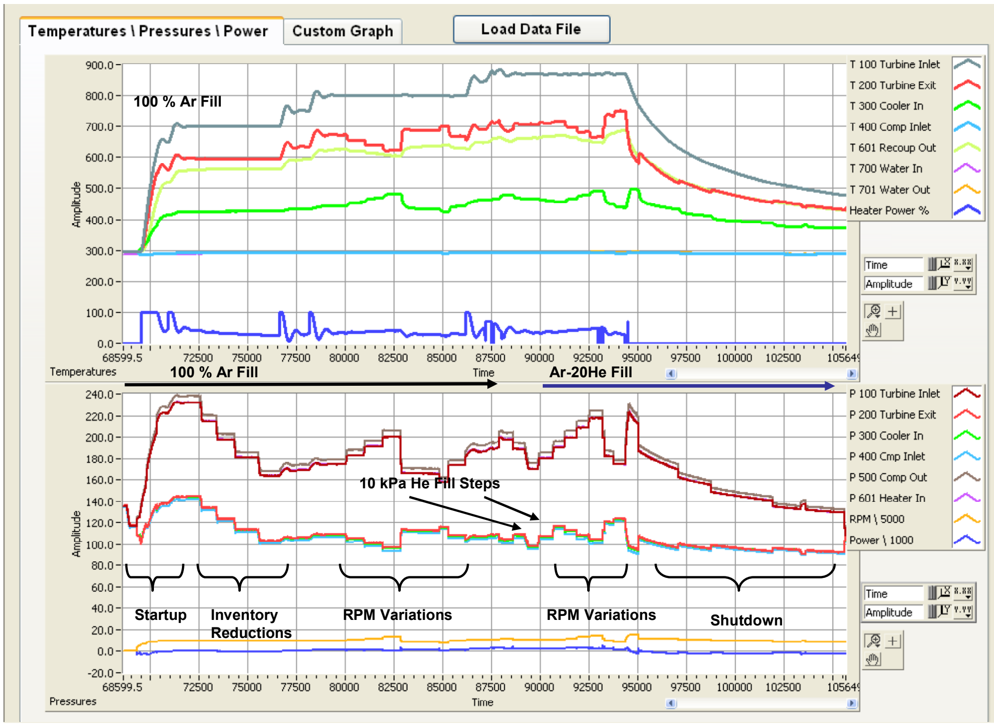

Figure 3.14: Screen images of measured temperature and pressure data forArgon and Argon 10%He. Test date was 06-03-16.

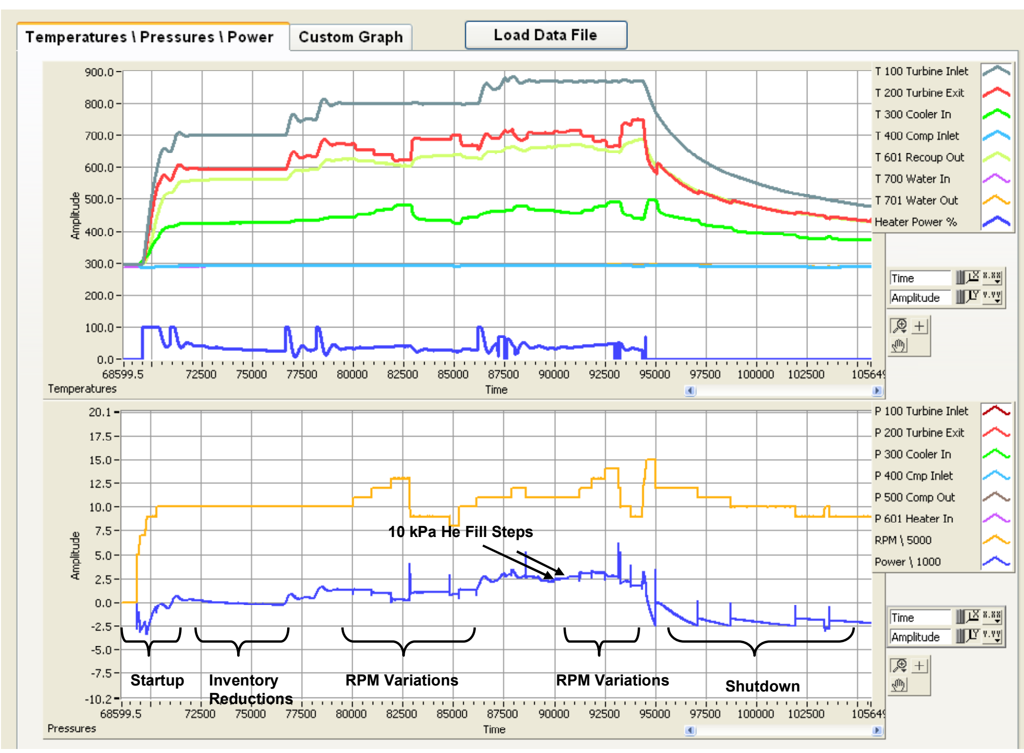

Figure 3.15: Screen images of measured temperature and rpm and alternator power data for Argon and Ar-20%He. Test date was 06-03-16.

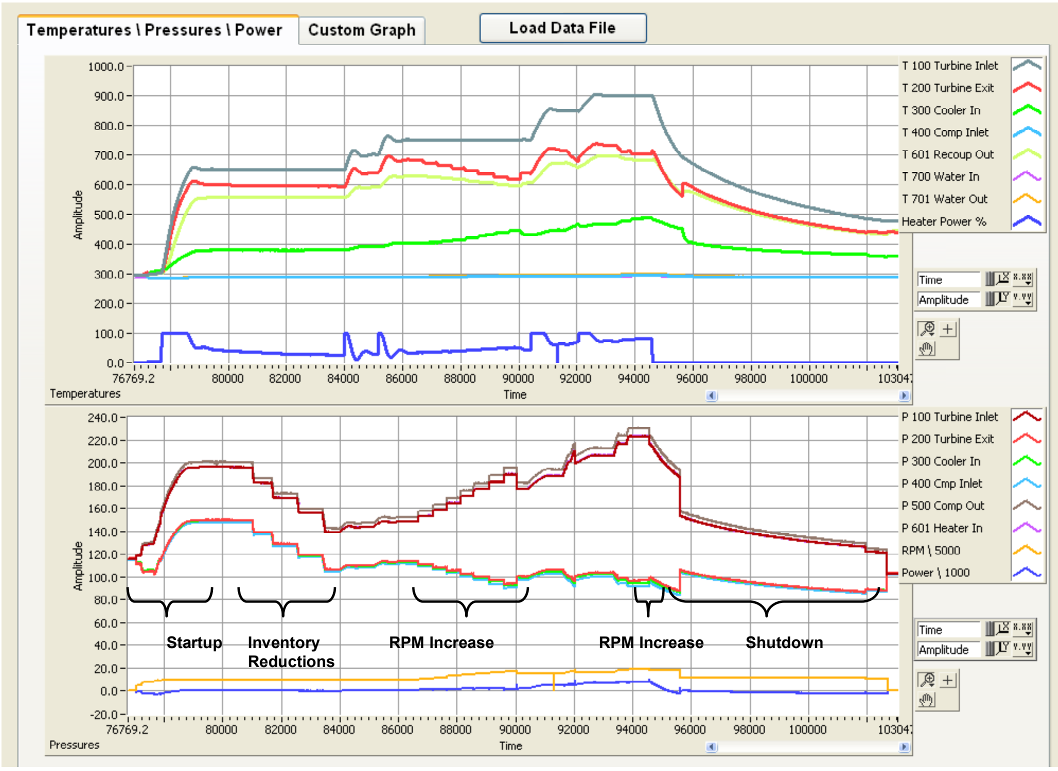

Figure 3.16: Screen images of measured temperature and pressure data for N2-30%He Test date was 06-03-23.

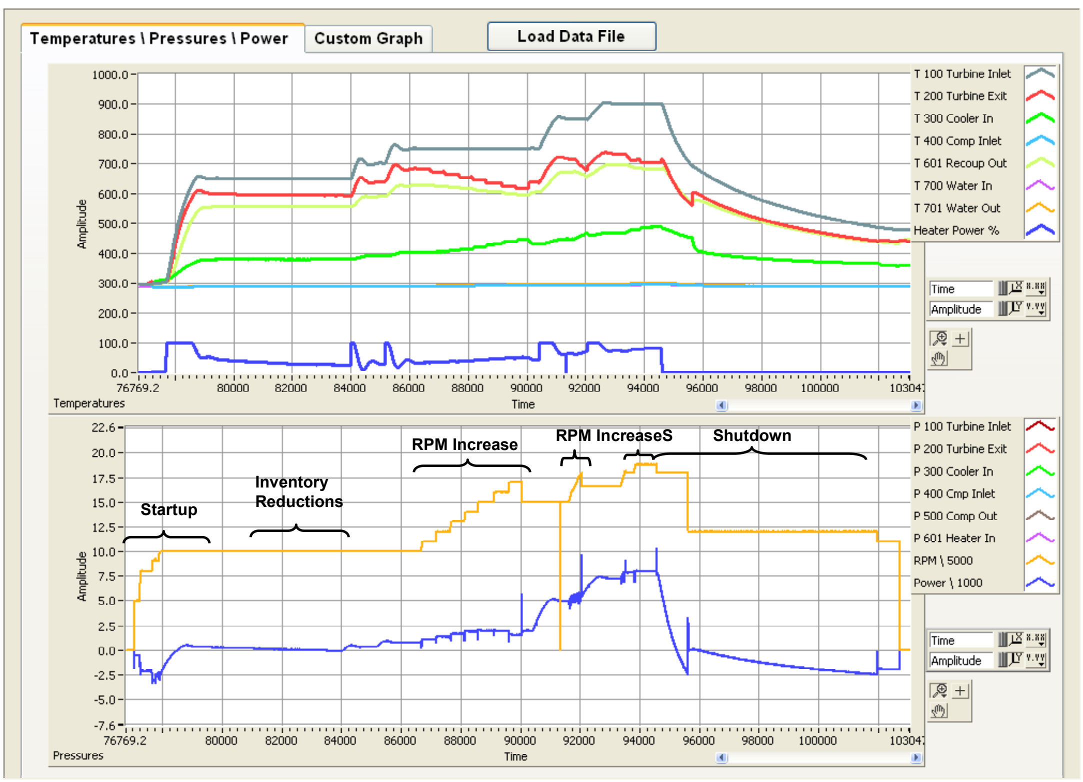

Figure 3.17: Screen images of measured temperature and rpm and alternator power data for N2-30%He. Test date was 06-03-23.

4 Summary Description of Geometry, Dimensions and Test Conditions

This section of the report collects all the data provided in the data result plots described in the previous section. This section also provides other information such as the turbine inlet temperature (TIT), the gas type that was used for each test, and the compressor inlet temperature.

4.1 Geometry and Test Conditions for Steady State Flow Data

This section of the report presents the conditions of the tests and the recorded data used to make the plots described in sections 3.3 and 3.4. Additional test conditions are provided in these tables for turbine and compressor inlet temperature. The method of performing these tests was described in sections 3.1.1 and 3.1.2. The data presented here was taken from complete transient data, finding the sequence of time where these measurements were made and then pulling the data out and putting it in to excel for plotting. In some cases the data was pulled off of plots, in others it was obtained from the raw data files. There is always a possibility that some of the data was incorrectly recorded. Typical uncertainty values for temperature are 1 K, for pressure they are 1 kPa, for mass flow rate the uncertainty is estimated to be about .01 kg/s, for rpm the uncertainty is 30-50 rpm, and for alternator power (P.e) the uncertainty is about 30-50 W.

Table 4-1: Measured date for pure nitrogen at TIT=700 K, test date of 06-01-19.

60119										
N2	TIT	CIT	MW	R.o	Cp/Cv					
TIT=700K	700	290	28.01	284	1.407					
krpm	raw mdot	mdot	p_CIT	P_COT	p_TIT	p_TOT	r.c	r.t	P.e	P.htr
55	0.17		127	204	199	130	1.606299	1.530769	1180	41.5
60	0.19		122.5	213	207.5	126	1.738776	1.646825	1311	45.5
65	0.205		117.5	222.5	216.5	121	1.893617	1.789256	1238	49
70	0.22		112.5	229	225.5	117	2.035556	1.92735	944	52.6

Table 4-2: Measured date for pure nitrogen, 9.4% argon at TIT=700 K, test date of 06-01-11.

60111										
N2-9.4%Ar	TIT	CIT	MW	R.o	Cp/Cv					
TIT=700K	700	290	29	297	1.433					
krpm	raw mdot	mdot	p_CIT	P_COT	p_TIT	p_TOT	r.c	r.t	P.e	P.htr
50	0.14	0.147	116.5	175	170.6	118.4	1.502146	1.440878	1346	35.2
55	0.155	0.16275	112	183	177.5	115	1.633929	1.543478	1727	39.1
60	0.17	0.1785	108	191	185	112	1.768519	1.651786	2053	41.8
65	0.18	0.189	104	199	194	108	1.913462	1.796296	2259	44.6
70	0.19	0.1995	100	208	202	103.5	2.08	1.951691	2213	49.4
75	0.2	0.21	96	217	211	100	2.260417	2.11	1799	52.6

Table 4-3: Measured date for pure argon at TIT=800 K, test date of 06-03-16.

60316										
Ar (100%)	TIT	CIT	MW	R.o	Cp/Cv					
TIT=800K	800	290	39.9	208	1.66					
krpm	raw mdot	mdot	p_CIT	P_COT	p_TIT	p_TOT	r.c	r.t	P.e	P.htr
40	0.12	0.170982	113.3	161.7	156.7	115.8	1.427184	1.353195	830	24
45	0.135	0.192355	110	170	165.3	112.5	1.545455	1.469333	1100	28
50	0.15	0.213727	106.5	178.8	174	109.2	1.678873	1.593407	1300	33
50	0.15	0.213727	105.8	178	173.2	105.8	1.68242	1.637051	1280	30
55	0.162	0.230825	102.2	188	182	105	1.83953	1.733333	1280	36.2
60	0.175	0.249348	98	196.5	190.8	101.3	2.005102	1.883514	950	38
65	0.19	0.270721	93.5	206	200	97.4	2.203209	2.053388	260	40.5

Table 4-4: Measured date for pure argon/ 20% helium at TIT=870 K, test date of 06-03-16.

60316										
Ar 20%He	TIT	CIT	MW	R.o	Cp/Cv					
TIT=870K	870	290	32.7	254	1.66					
krpm	raw mdot	mdot	p_CIT	P_COT	p_TIT	p_TOT	r.c	r.t	P.e	P.htr
45	0.131	0.153028	121	178	174	123.8	1.471074	1.405493	1749	30.14
50	0.147	0.171719	117.8	186.5	181.7	120.4	1.583192	1.509136	2190	33.7
55	0.16	0.186905	113.9	196	190	117	1.720808	1.623932	2705	38.9
60	0.175	0.204427	109.3	205.5	199.5	113	1.880146	1.765487	3030	41.7
65	0.19	0.221949	105	214.8	208.3	109	2.045714	1.911009	3096	43.9
70	0.2	0.233631	100.6	224.5	217.5	104.8	2.23161	2.075382	2703	50.7

Table 4-5: Measured date for pure nitrogen / 30% Helium at TIT=750 K, test date of 06-03-23.

60323										
N2-30%He	TIT	CIT	MW	R.o	Cp/Cv					
TIT=750K	750	290	21	399	1.486					
krpm	raw mdot	mdot	p_CIT	P_COT	p_TIT	p_TOT	r.c	r.t	P.e	P.htr
50	0.103	0.077	111.3	151.8	148	113.2	1.363881	1.30742	740	33.6
55	0.12	0.089	109	157.3	153	111.2	1.443119	1.375899	1060	34.7
60	0.13	0.097	106.2	163	158.5	108.8	1.53484	1.456801	1350	37.2
65	0.14	0.104	103.3	169	164.3	106	1.636012	1.55	1650	39.6
70	0.15	0.111	100.2	175.7	170.5	103	1.753493	1.65534	1880	42.2
75	0.16	0.119	97	182.2	176.5	100	1.878351	1.765	1980	44.8
80	0.17	0.126	93.7	189	183	97.3	2.017076	1.880781	1920	48
85	0.18	0.134	90.2	195.5	189.4	94	2.167406	2.014894	1530	51.3

Table 4-6: Measured date for nitrogen / 30% Helium at TIT=900 K, test date of 06-03-23.

60323										
N2-30%He	TIT	CIT	MW	R.o	Cp/Cv					
TIT=900K	900	290	21	399	1.486					
krpm	raw mdot	mdot	p_CIT	P_COT	p_TIT	p_TOT	r.c	r.t	P.e	P.htr
90	0.2	0.149	94.5	223.9	216.2	99.2	2.369312	2.179435	7850	78
94	0.207	0.154	91.4	230	223	97	2.516411	2.298969	7940	80.5

Table 4-7: Measured date for nitrogen / 30% Helium at TIT=850 K, test date of 06-03-23.

60323										
N2-30%He	TIT	CIT	MW	R.o	Cp/Cv					
TIT=850K	850	290	21	399	1.486					
krpm	raw mdot	mdot	p_CIT	P_COT	p_TIT	p_TOT	r.c	r.t	P.e	P.htr
75	0.169	0.126	102.8	194.2	188.2	106.1	1.889105	1.773798	4940	62
76	0.171	0.127	102.0	195.8	189.5	105.5	1.919608	1.796209	5060	63
77	0.173	0.128	101.2	197	191.2	105	1.94664	1.820952	5150	63
78	0.175	0.130	100.8	198.7	192.7	104.2	1.97123	1.849328	5270	64
79	0.177	0.131	99.8	200.2	194.1	103.5	2.006012	1.875362	5370	64
80	0.179	0.133	99.1	201.8	195.3	103	2.036327	1.896117	5450	65
81	0.181	0.134	98.5	203.3	197	102.1	2.063959	1.929481	5510	66
82	0.183	0.136	97.5	204.9	198.1	101.7	2.101538	1.947886	5550	66
83	0.184	0.137	97	206.2	200	101	2.125773	1.980198	5630	67
84	0.186	0.138	96.1	207.8	201.2	100.2	2.162331	2.007984	5610	67
85	0.188	0.140	95.3	209	202.6	99.5	2.193075	2.036181	5760	68
87	0.192	0.143	94	212.3	205.7	98.3	2.258511	2.092574	5690	69
89	0.196	0.146	92.5	215.3	208.5	96.8	2.327568	2.153926	5710	90
90	0.198	0.147	91.6	217	210.2	96.1	2.368996	2.187305	5690	83

Table 4-8: Measured date for pure nitrogen at TIT=870 K, test date of 05-09-13.

50913										
N2	TIT	CIT	MW	R.o	Cp/Cv					
TIT=870K	750	290	28.01	399	1.486					
krpm	raw mdot	mdot	p_CIT	P_COT	p_TIT	p_TOT	r.c	r.t	P.e	P.htr
25	0.05	0.05	129	145.5	143	131	1.127907	1.091603	500	27
30	0.065	0.065	127.5	150.5	148	130	1.180392	1.138462	800	33
40	0.1	0.1	124	163	159.3	126	1.314516	1.264286	1300	43
50	0.13	0.13	118.7	178	174	121.3	1.499579	1.43446	2750	53
60	0.158	0.158	112	196	190.3	115	1.75	1.654783	4520	63
70	0.185	0.185	104	215	209	108	2.067308	1.935185	6300	70
75	0.202	0.202	100	225.5	218.7	104.2	2.255	2.098848	7050	77
80	0.215	0.215	96	236	229	101	2.458333	2.267327	7700	83
85	0.225	0.225	92	246.3	239	97.6	2.677174	2.44877	7700	90
90	0.238	0.238	88	257	249	94	2.920455	2.648936	7100	100

Table 4-9: Measured data for pure CO2 at TIT=700 K, test date of 06-05-25.

60525										
CO2	TIT	CIT	MW	R.o	Cp/Cv					
TIT=700K	750	300	44.01	188.9	1.316					
krpm	raw mdot	mdot	p_CIT	P_COT	p_TIT	p_TOT	r.c	r.t	P.e	P.htr
50	0.214	0.336194	131.7	241.5	235.9	135.1	1.833713	1.746114	2910	62.2
55	0.237	0.372327	124.5	254.2	247.7	128.3	2.041767	1.930631	3250	63.7
60	0.261	0.410031	117.2	266.9	260.2	121.8	2.277304	2.136289	3165	67
65	0.273	0.428883	109.7	279.7	272.6	115	2.549681	2.370435	2645	71

4.2 Test Conditions for Steady State Inventory Control Data

The test procedures for collecting the inventory control data were described in section 3.1.4 and the results of the data were collected and plotted in section 3.5. The actual recorded data and other information is provided in Table 4-10.

Table 4-10: Measured data for the inventory control tests.

TIT = 650 K	TIT = 650 K	TIT=700K	TIT=700K	TIT=650 K	TIT=650 K
N2	N2	Argon	Argon	N2_30He	N2_30He
CIP (kPa)	Alt Pwr	CIP (kPa)	Alt Pwr	CIP (kPa)	Alt Pwr
140	270	142	200	147	205
130	170	132	40	137	110
120	80	121	-65	127	20
110	-5	111	-175	117	-30
100	-75	101	-270	105	-110

4.3 Geometry and Test Conditions for all Tests

4.3.1 Detailed Description of the Capstone C30 Radial Turbine and Compressors

This section of the report presents a detailed description and photos of the Capstone C-30 compressor and turbine. This description is necessary because it provides the wheel sizing and dimensions needed to generate the characteristic flow curves for the turbine and compressor. The data is also needed for dynamic modeling. In addition, this design information also provides short descriptions of the technology used in the turbo-machinery such as gas foil bearings and other information regarding flow paths, thrust bearing load balancing and thermal control of the bearings. Most of this data is collected in tables and presented in hopefully a very usable form.

4.3.1.1 Capstone C-30 Compressor and Turbine

A photo of the complete compressor and turbine for the Capstone C-30 (30 kWe) wheel set, including gas bearings, is shown in Figure 4.1 (Photos courtesy of NASA Glenn Research Center). The entire wheel set for this 30 kWe system is less than 6 inches long and the wheel diameters are around 4 inches. The reader should note that the dimensions for a 132 kWe turbo-compressor set that is designed for He/Xe at 2 MPa are about the same. The small dimensions of the turbine and compressor and the high flow velocities through the turbine and compressor (about 70% the speed of sound) mean that the gas flow can achieve equilibrium conditions very rapidly (on the order of 0.3 – 0.4 ms). Thus pressure changes caused by speed changes or temperature or pressure changes will result in new equilibrium flow rates within about 1 ms or faster. A quasi-steady state approach to estimating the pressure changes and flow rates through the rotating machinery, such as used in the mean-line flow analysis methods is therefore justified. Because the flow and pressures reach their equilibrium flow conditions so rapidly (within the turbo-compressor wheel set), the time rate of change in flow through the system will be governed mainly by the rate of change of rpm which is in turn controlled by the moment of inertia of the shaft, wheels, and alternator as well as by the misbalance in the torque/power in the turbine, alternator, and compressor. The inertia due to the mass of gas within the entire ducting network is currently ignored in the models. By way of comparison, we estimate the mass of the rotating turbomachinery components including alternator to be approximately 20-30 kg, while the mass of the coolant in the loop is only about 5 kg. In fact, one way to account for the mass of the coolant is to add its inertia to the rotating components.

Radial Compressor and Turbine

(Capstone C -30, Courtesy of NASA Glenn)

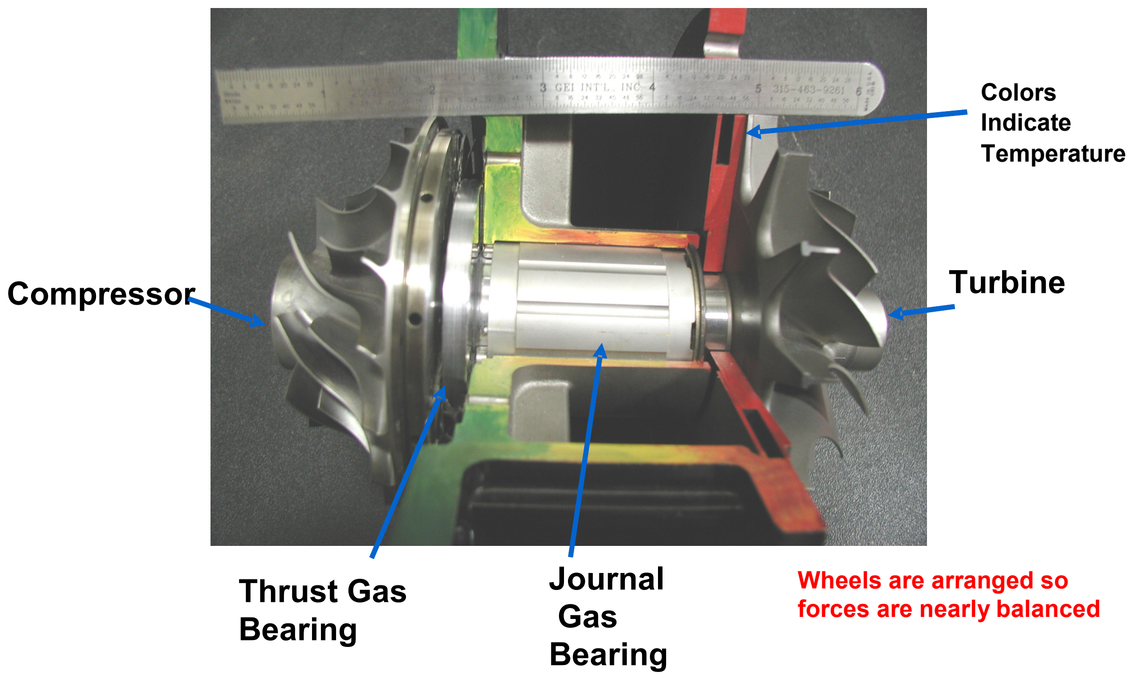

Figure 4.1: Capstone C-30 compressor and turbine wheels include the gas thrust and journal bearings. The compressor is on the left side and is relatively cool, (green colors) and the turbine is on the right (red colors for the housing and bearings,courtesy of NASA).

Figure 4.1 also shows the gas journal bearing and the gas thrust bearing of the turbo-compressor. The face side of the compressor and turbine are shown in Figure 4.2, and Figure 4.3 shows the compressor outlet diffuser and the turbine inlet nozzle. The bearings and turbo-compressor wheels are arranged so that the pressure difference across the face of the compressor wheel is balanced by the pressure difference across the turbine wheel. Also note that the bearings and shaft materials are cooler closer to the compressor than on the turbine side. Gas flow in the bearings is from the compressor side to the turbine side (from cold to hot) because the turbine inlet pressure is less than the compressor exit pressure.

The permanent magnet alternator shaft (not shown) is connected to the compressor and turbine shaft via a small rod or pencil-like shaft. The compressor inlet gas is the coldest gas in the entire CBC loop thus it is used to cool the alternator. The gas flows from the left side of Figure 4.1 into the compressor inlet and then is flung radially outward where it goes to the recuperator and then ultimately to the reactor. The hot gas from the reactor/heater enters in a narrow annulus in the right side of Figure 4.1, through the nozzle and then radially inward where it impacts and expands against the turbine blades and then flows axially out of the turbine face.

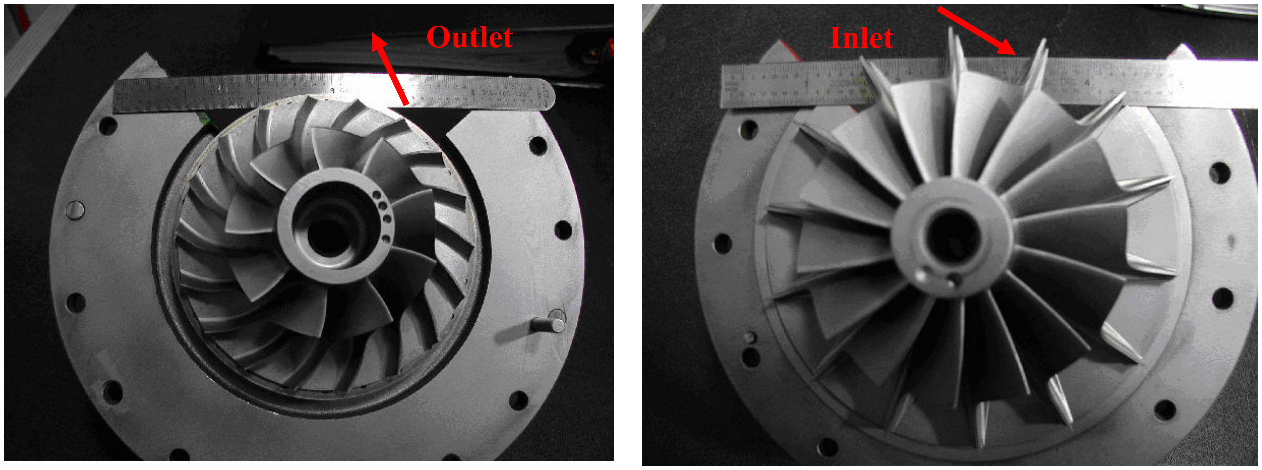

Figure 4.2: Face or front views of the Capstone C-30 compressor (left) and turbine (right). Note that the compressor wheel blades are back swept while the turbine inlet blades are not. Also note that the turbine base is scalloped, this is likely done to help accommodate the gas flow from the inlet nozzle and presumably to help balance the thrust loads.

Based on these images and on others made during fabrication by Barber-Nichols Inc. (manufacturer of the Sandia Brayton Loop), we have been able to estimate most of the dimensions required to determine the characteristic flow curves. Table 4-11 and Table 4-12 summarize the approximate dimensions for the Capstone C-30 turbine and compressor.

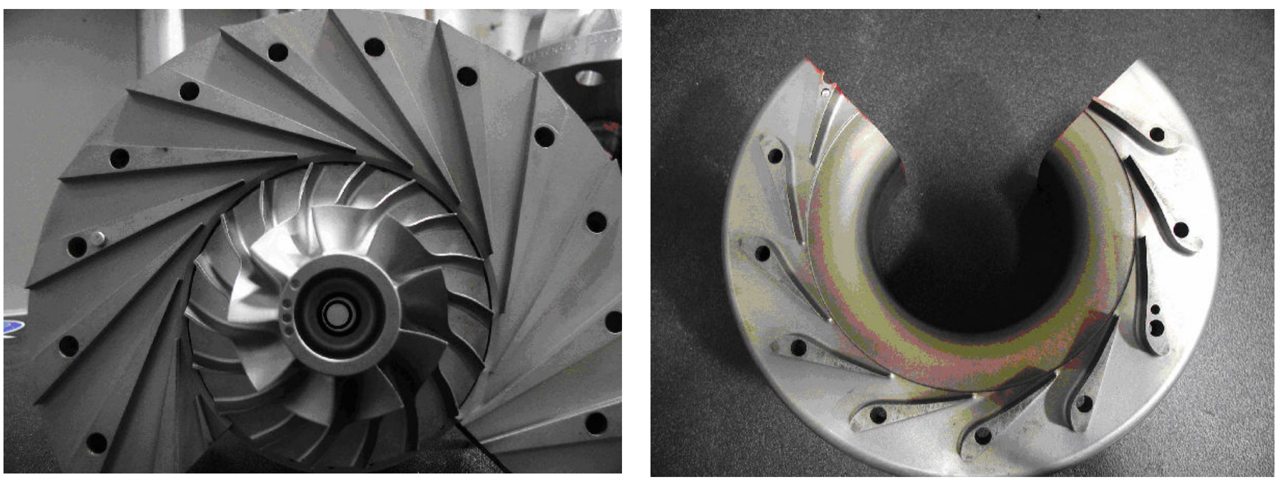

Figure 4.3: Compressor wheel and exit diffuser (left) and turbine inlet nozzle (right).

Table 4-11: Estimate of Capstone C-30 Turbine Dimensions

Capstone C-30 Turbine Dimensions (approximate)		
Description	**Variable Name**	**Value**
Tip Radius	r_{tip}	54.61 mm
Hub Radius	r_{h1}	11.73mm
Shroud Radius	r_{s1}	37.82 mm
Blade Height	b_2	7 mm
Blade Exit Angle	β_{2b}	-55 degrees
Blade Thickness	t_b	0.7 mm
Number of Blades	Z_r	18/9 (split + full / full)
Design rpm	N_{rpm}	96,000 rpm
Design Pressure Ratio p_{o2}/p_{o1}	r_c	3.7

Table 4-12: Estimate of Capstone C-30 Compressor Dimensions

Capstone C-30 Compressor Dimensions (approximate)		
Description	**Variable Name**	**Value**
Tip Radius	r_{tip}	50.81 mm
Hub Radius	r_{h1}	12.83 mm
Shroud Radius	r_{s1}	27.95 mm
Blade Height	b_2	3.6 mm
Blade Exit Angle	β_{2b}	-45 degrees
Blade Thickness	t_b	1.8 mm
Number of Blades	Z_r	18/9 (split + full / full)
Design rpm	N_{rpm}	96,300 rpm
Design Pressure Ratio p_{o2}/p_{o1}	r_c	3.7

4.3.2 Summary Description of the Sandia Brayton Loop Geometry and Dimensions

This section of the report provides a summary description of the Brayton loop and provides lengths, flow diameters, diameters, volumes, wall thickness and other parameters that are required to develop a complete dynamic model for the loop. A more complete description of the loop is provided in the Sandia final LDRD report (Wright, 2006), which is provided on the CD. Also the initialization file used by the Sandia model is also included on the CD. This input file provides all the data used by Sandia for its modeling effort.

4.3.2.1 Description of ducting and piping

The dimensions and properties of the ducting and piping are provided in Table 4-13, Table 4-14, and in Table 4-15. The duct materials from the cold exit from the recuperator through the compressor inlet were all made of carbon steel. All other ducts were 304 or 316 stainless steel.

Table 4-13: Volumes of the ducting and piping components in the Sandia Brayton loop.

Component: Pipes & Ducts	Inner Diam	Inner Diam	Length	Vol
	(in)	(m)	(m)	(m3)
Low-Pressure Leg				
Turbine Housing	17.760	0.451	0.480	0.077
Recup-to-Gas-Cooler Small Pipe	4.760	0.121	0.130	0.001
Gas-Cooler Inlet First Elbow	6.352	0.161	0.380	0.008
Gas-Cooler Inlet Line	6.352	0.161	3.250	0.066
Gas-Cooler Inlet Second Elbow	6.352	0.161	0.380	0.008
Cooler Inlet Bellows	6.625	0.168	0.410	0.009
Gas-Cooler Inlet Elbow	6.352	0.161	0.740	0.015
Gas Cooler Tubes	0.527	0.013	189.0	0.027
Compressor Inlet Elbow	7.9810	0.203	0.5100	0.016
Compressor Inlet Pipe	7.9810	0.203	0.2000	0.006
Filter Housing	20.000	0.508	0.470	0.095
Generator Housing	13.500	0.343	0.200	0.018
High-Pressure Leg				
Recup-to-Heater Small Pipes	2.635	0.067	2.500	0.009
Recup-to-Heater Manifold	5.761	0.146	1.120	0.019
Heater Inlet Large Pipe	6.060	0.154	1.500	0.028
Heater Inlet First Elbow	6.060	0.154	0.380	0.007
Heater Inlet Bellows	6.625	0.168	0.230	0.005
Heater Inlet Second Elbow	6.060	0.154	0.300	0.006
Gas Heater Inlet Pipe	6.352	0.161	0.180	0.004
Gas Heater Shell	11.380	0.289	2.300	0.151
Gas Heater Element Tubes	0.430	0.011	-124.2	-0.012
Turbine Inlet Pipes	1.402	0.036	4.860	0.005
Turbine Inlet Elbows	1.402	0.036	0.120	0.000

Table 4-14: Total volume gas loop.

Low-Pressure Leg Total Vol (m3)	0.348
Low-Pressure Leg Pressure (MPa_g)	0.206
Low-Pressure Leg Energy (MJ)	0.036
High-Pressure Leg Total Vol (m3)	0.221
High-Pressure Leg Pressure (MPag)	0.413
High-Pressure Leg Energy (MJ)	0.046
Total loop volume (m3)	0.569

Table 4-15: Duct and component volumes, mass, length, and hydraulic diameter.

Duct or Component ID		Volume (liter)	Length (m)	Hydraulic Diameter (m)	Mass (kg)
V_{11}	Compressor Inlet Duct	127 liter	0.662 m	..4048 m	60.748
V_{22}	Compressor Outlet Duct	3 liter	0.10 m	0.4 m	0.252
V_{23}	High Pressure leg of Recuperator	20 liter	0.25 m	rcp	250
V_{33}	Heater Inlet Duct	77 liter	4,239 m	0.307 m	121.78
V_{34}	Reactor Coolant Volume or Length	139 liter	2.235 m	rx	---
V_{44}	Heater Outlet Duct Volume	5 liter	1.067	..0696 m	9.6769
V_{55}	Turbine Outlet Duct	3 liter	0.1 m	.4 m	0.25196
V_{56}	Low Pressure leg of Recuperator	20 liter	0.25 m	rcp	250
V_{66}	Gas Chiller Inlet Duct	108 liter	5.004 m	0.3226 m	70.425
V_{61}	Gas Chiller	27 liter	2.5 m	gcx	114

4.3.2.2 Watlow heater description

Table 4-16 lists the thermal hydraulic properties used to model the Watlow heater that is used in the Sandia dynamic model. The wall material of the heater was 316 ss, and the heater elements were clad with Inconel 600. Chapter 5 provides an in depth description of the heater.

Table 4-16: Watlow heater description.

Heat Transfer to Coolant from Heater Elements		**Heat Transfer from Coolant Vessel Wall**	
Radius of element	4.953 mm	Wall inner radius	0.1492 m
L of element	1.727 m	Wall Length	2.235 m
Element Heat transfer Area	6.3988m^2	Wall heat transfer Area	2.0952
Flow Area	0.598 m^2		
Hydraulic Diameter	5.15 mm		
Element Inverse Thermal Capacitance (κ, kappa)	0.0016 K/J	Mass of Wall	221 kg
Number of effective pin or elements	108		

4.3.2.3 Precooler or waste heat gas chiller description

Table 4-17 describes the thermal hydraulic properties used to model the precooler or the gas chiller heat exchanger. The heat exchanger is a tube and shell heat exchanger with gas flowing in the tubes and water flowing in the surrounding space. Chapter 5 provides a more in depth description of the gas chiller.

Table 4-17: Basco/Whitlock gas chiller hydraulic and heat transfer properties used in the RPCSIM model for the Sandia Brayton Loop

Hydraulic and Heat Transfer Properties of the Gas Cooler Heat Exchanger	
Mass of Heat Exchanger	114 kg
Area of Water Flow Leg in Heat Exchanger	10.109 m^2
Area of Gas leg in Heat Exchanger	8.0870 m^2
Length of Wtr leg in Heat Exchanger	2.896 m
Length of Gas Leg in Heat Exchanger	2.896 m
Effective Wall thickness of Heat Exchanger	1.587 mm
Hydraulic Diameter of Water Leg	21.3 mm
Hydraulic Diameter of Gas Heat Exchanger leg	25.4 cm
Flow area in HP Heat Exchanger Leg	.019 m^2
Flow area in LP Heat Exchanger Leg	.008867 m^2

5 Detailed Description of the Sandia Brayton Test Loop Description

Because of the limited experience in operating reactor driven closed Brayton cycle systems (and indeed operating just closed Brayton systems) we decided that the best way to validate the models was to build an electrically heated closed Brayton loop. We would then use a reactor simulator controller to operate the electrical heater as a reactor using air or nitrogen as the working fluid. Our goal was to manufacture a closed Brayton loop by modifying available commercial turbo-machinery. To accomplish this task, Sandia issued a Request for Quote to evaluate the possibilities of manufacturing an inexpensive closed Brayton loop. Barber-Nichols Incorporated (Barber-Nichols, 2005,) responded to the request and developed an approach that could be accomplished within the time constraints and budget available to this project. The result is the 30 kWe Sandia Brayton Loop (SBL-30) that it described here.

We provide a detailed description of the Sandia Brayton Loop in this section of the report. We first describe the Capstone C-30 open cycle gas turbine upon which the Sandia closed Brayton loop is based. The modifications to the Capstone C-30 system are described next, and some time is spent describing the modifications to the turbo-alternator compressor and the flow path through it, because it is quite complicated, and it impacted the design modifications that were required. The flow path is difficult to follow because is consists of flow through a series of nested annular “cans”. A number of photos of the modifications are provided, along with photos of the assembled unit at the Barber-Nichols site and now at Sandia. These sections are then followed by a description of the electrical heater, the gas chiller, and then an overview of the ducting and instrumentation are described. Within these sections, information regarding size, mass, flow volume, heat transfer areas, and hydraulic diameters of the various components is provided to support other modeling efforts. In addition, a brief description of the pressure safety issues is summarized.

5.1 Closed Brayton Cycle Test-Loop Description

Sandia contracted Barber-Nichols Inc. to design, fabricate, and assemble an electrically heated CBC system. The system design is based on modifying a commercially available micro-turbine power plant. This approach was taken because it was the most cost effective among a number of approaches considered because all the rotating components, the recuperator, the gas bearings, and the control components could be reused. Other methods of designing and fabrication a closed loop Brayton cycle that were examined included modifying an automobile turbo-charger and possibly using an auxiliary power unit (APU). The modification of the Capstone open cycle gas turbine system was selected largely because it only required modifying the housing to permit the attachment of an electric heater and a water cooled gas chiller. This approach therefore allowed the reuse of all the other components including the alternator and associated rectification electronics and control hardware. The Sandia Brayton test loop uses a 30 kWe Capstone C-30 gas-micro-turbine generator that normally operates at 1144 K turbine inlet temperature (TIT) with a shaft speed of 96,000 rpm (Capstone, 2005).

The CBC test-loop hardware is currently configured with a heater that is designed to ~80 kW_t with an outlet temperature of 1000 K. Other heater systems that better simulate the thermal hydraulics of nuclear reactors and that are capable of providing higher temperatures and more power can be attached in the future. At the present time the heater is limited to 63 kW and 900 K outlet temperatures. The chiller is capable of rejecting up to 90 kW_t and has a water flow rate of 68 liters/min of chilled water at 285 K=56 F. The Sandia house water supply is at 56 F. The heater power is controlled by a 4-20 mA current source by a Sandia provided National Instruments controller. The water flow rate is not directly controlled at this time. Some minor modifications to the Sandia facilities were required to provide 122 kW of electrical power at 480 V 3 phase, and the chilled water.

5.2 Capstone Turbo-Alternator-Compressor Modifications

A schematic drawing of the unmodified C-30 micro-turbine unit as an open air gas turbine is shown in Figure 5.1. In this configuration the C-30 micro-turbine uses natural gas fuel to heat the ?. The original path of the gases and temperatures is indicated by the arrows and colors. The flow path is quite convoluted and flows through several annular regions. The blue lines show that the gas inlet passes along the alternator housing to directly cool it. This gas then flows through the compressor and passes into the recuperator (the gas is colored yellow at this point). After exiting the recuperator (orange) it flows axially and radial around an internal annulus and then flows into the combustor region from both sides of a baffle. The combusted gases (red) then flow (to the left in the drawing) into the radial turbine and then exit the turbine axially (orange). The turbine exit gases then reverse direction while flowing around the combustor region and then flow axially (to the left) back into the recuperator. The gas exiting the recuperator (yellow) then flows into a plenum and exits to the atmosphere.

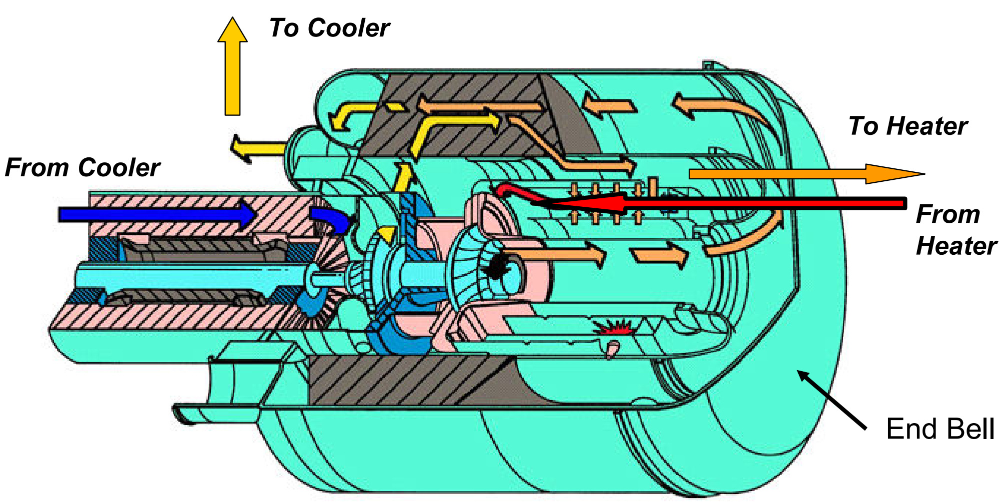

Figure 5.1: Schematic of the unmodified C-30 with arrows illustrating the gas flow path and proposed housing modifications.

On the hot end of the unit, (illustrated in Figure 5.1) the two long straight arrows indicate the modified flow paths that are required to connect the gas from the recuperator to the heater (orange) and from the heater to the turbine (red). The arrow that points to the left shows the flow path of the gas from the heater to the turbine inlet. . The design modifications used the six tubes to transport the hot gas from the heater into the “combustor” annulus. Photos of the interior of the hot head of the unit are shown in Figure 5.2 with the top “End Bell” removed. A close up view of the recuperator exit and the turbine exit are shown in Figure 5.3. The gas injector and igniter passages were used to connect to a heater inlet manifold as shown in Figure 5.3 and Figure 5.4.

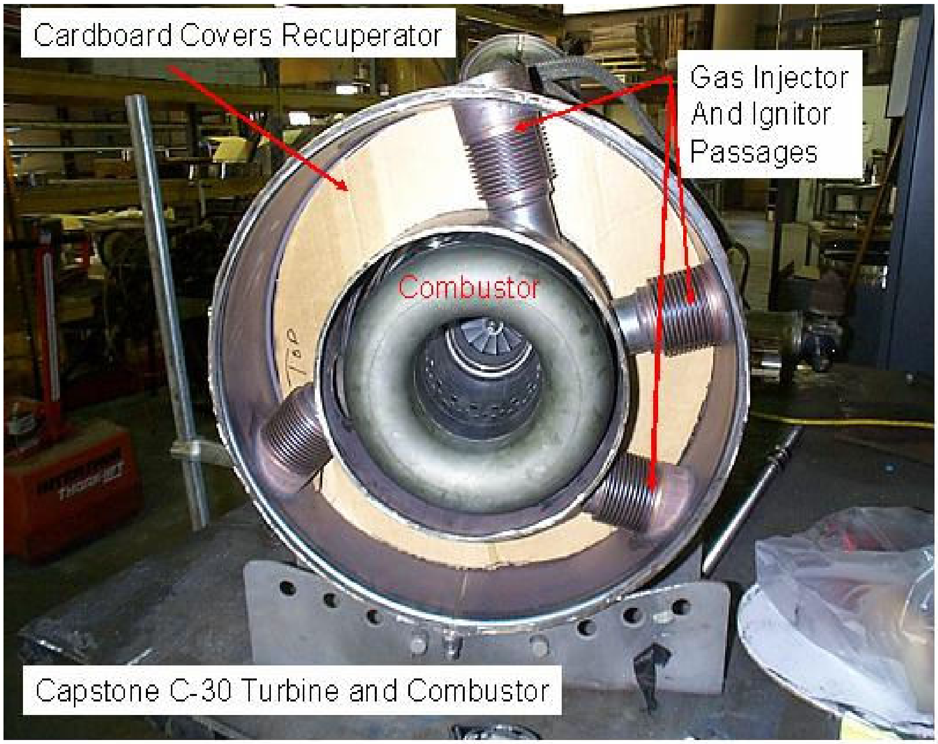

Figure 5.2: "Hot End" of the Capstone C-30 micro-turbine showing the turbine wheel, the combustor annulus, and the gas injector passages.

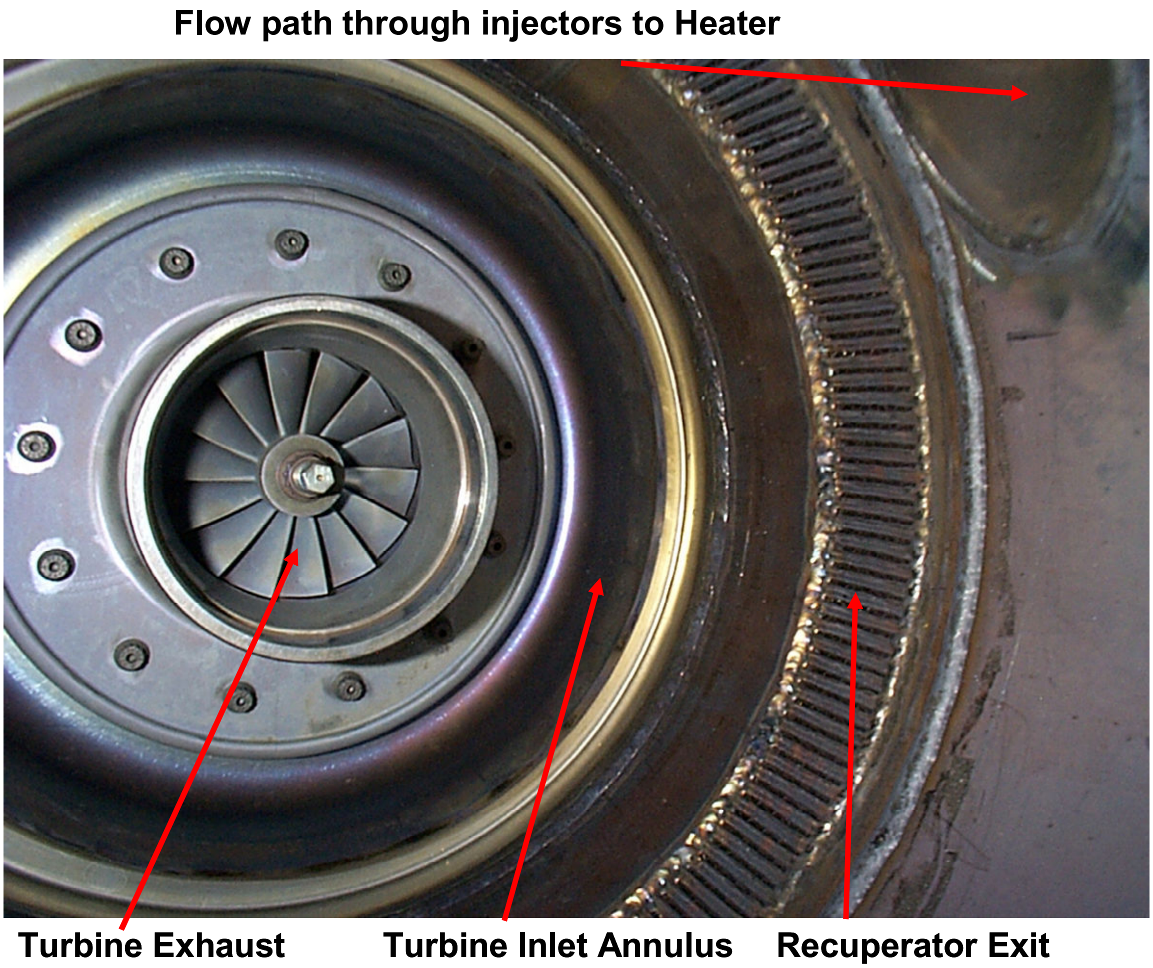

Figure 5.3: Photo of the 14 turbine exit blades, the turbine inlet annulus, and the high pressure recuperator exit. An annular shaped "combustor can" is slipped into the turbine inlet annulus to direct the gas exiting the recuperator through the injector ports to the heater.

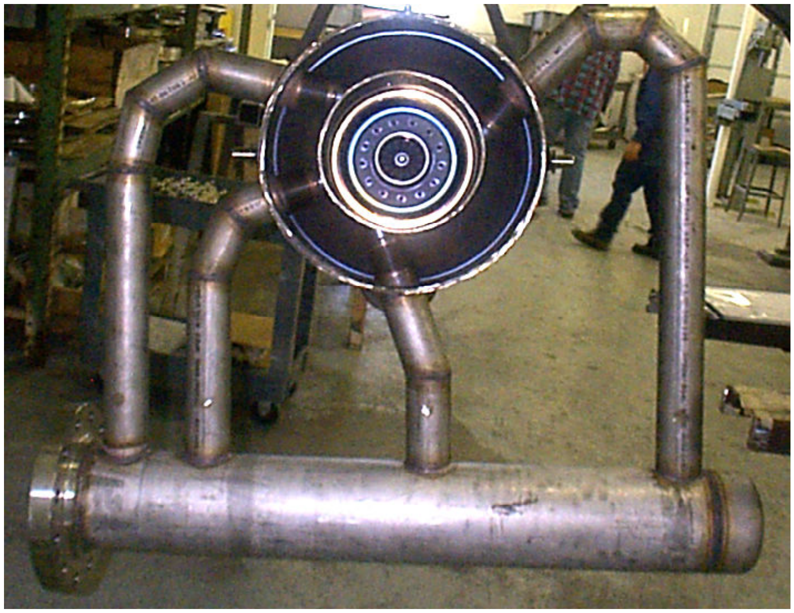

Figure 5.4: "Hot" end of the connection flow paths between the injector ports and the heat inlet duct manifold for the C-30 Capstone Micro-Turbine assembly.

To connect the heater outlet gas to the turbine inlet passage, six tubes were used to penetrate the three cover domes or housings as shown in design drawing of Figure 5.5 and in the photo of the hardware illustrated in Figure 5.6. The tubes first penetrate the turbine exit bell housing, next they penetrate through the combustor outer housing annulus and also through the turbine exit inner housing dome shaped annulus. These design modifications use the six tubes to transport the hot gas from the heater into the "combustor" annulus. Figure 5.7 provides further details from a cut-away drawing of the turbo-compressor unit illustrating how the injector and igniter passages are connected to a common manifold that supplies gas to the heater. The flow passages are also shown as well.

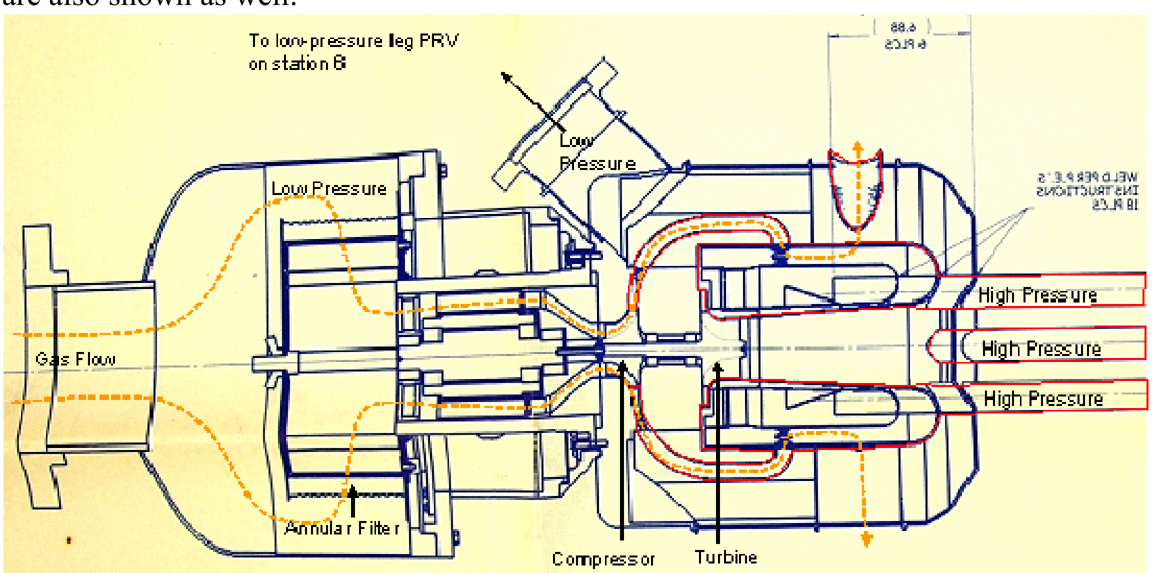

Figure 5.5: Capstone C-30 turbo-alternator-compressor cutaway with high-pressure zone highlighted.

Figure 5.6: Six tubes penetrating through the turbine exit dome, through the combustor dome shaped annulus (middle "dome"), and through the turbine inlet dome (smaller bottom dome shaped annulus).

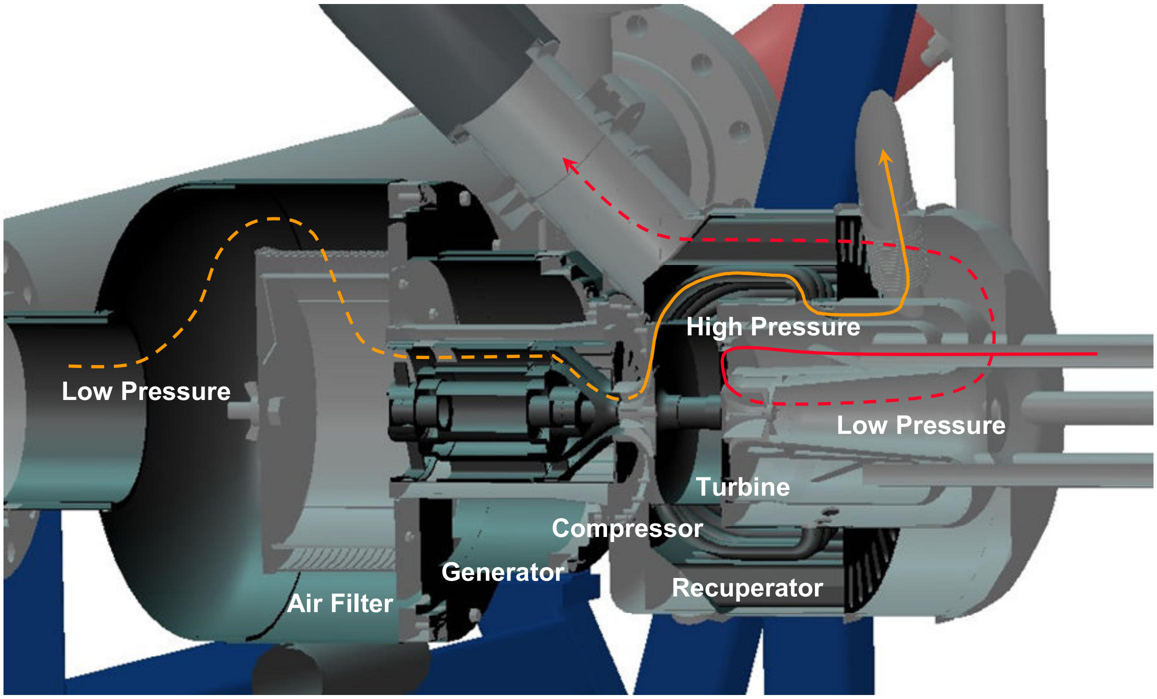

Figure 5.7: Capstone C-30 turbo-alternator-compressor engineering drawing cutaway showing the gas flow path. Orange lines show the flow path through the compressor and recuperator, red lines show the flow path through the turbine and recuperator.

A photo of the cold end of the turbo-alternator-compressor is shown in Figure 5.8. This photo clearly shows the inlet flow passage past the alternator, it also shows the low pressure gas exit leg from the recuperator. The spiral shaped annular flow passages from the recuperator are clearly visible in this image. We have been able to make estimates of the heat transfer areas, and hydraulic diameters for the recuperator based on images like this.

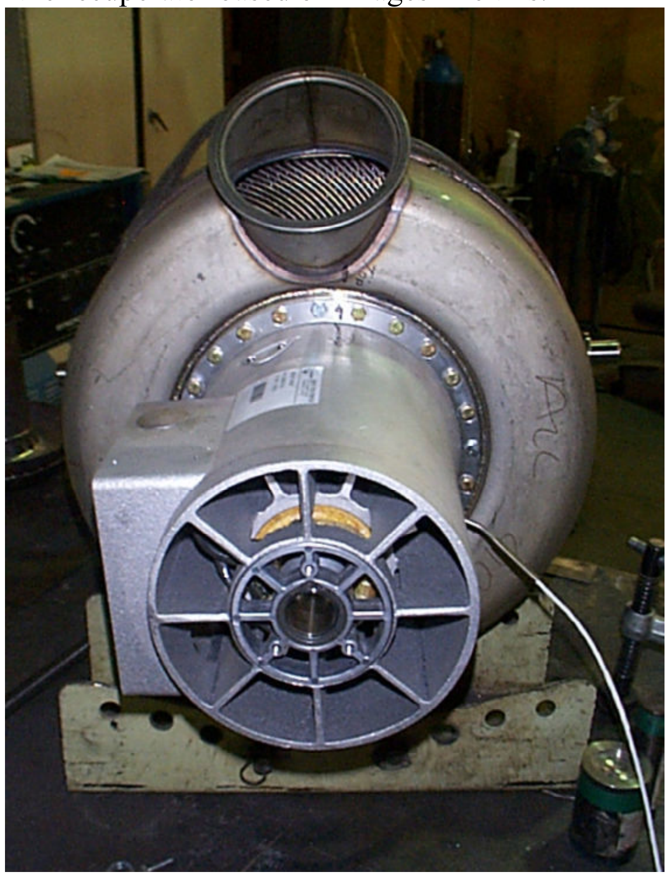

Figure 5.8: "Cold End" of the Capstone C-30 micro-turbine illustrating the spiral recuperator, the alternator, and the inlet cooling passages along the alternator.

The electrical heater and the gas chiller were then connected to the turbo-alternator-compressor as shown in Figure 5.9 which shows a complete assembly drawing of the entire closed Brayton cycle. Note that the system design used a “U” shaped configuration so that it would fit into the laboratory. This configuration easily accommodates thermal expansion by use of the ducting bellows at the ends of the legs. In addition the heater and chiller are mounted on pedestals, while the turbo-alternator compressor set stands on wheels to allow for some motion during heating. The photo in Figure 5.10 shows the fully assembled and operational Brayton loop at Barber Nichols Inc. These photos show the system without thermal insulation, as permanent insulation was only installed on the system after shipping the unit to Sandia.

Photos of the un-insulated Sandia Brayton Loop, as installed at Sandia, are shown in Figure 5.11 and in Figure 5.12. Figure 5.13 shows a photo of the Sandia Brayton Loop with insulation and as installed and operational.

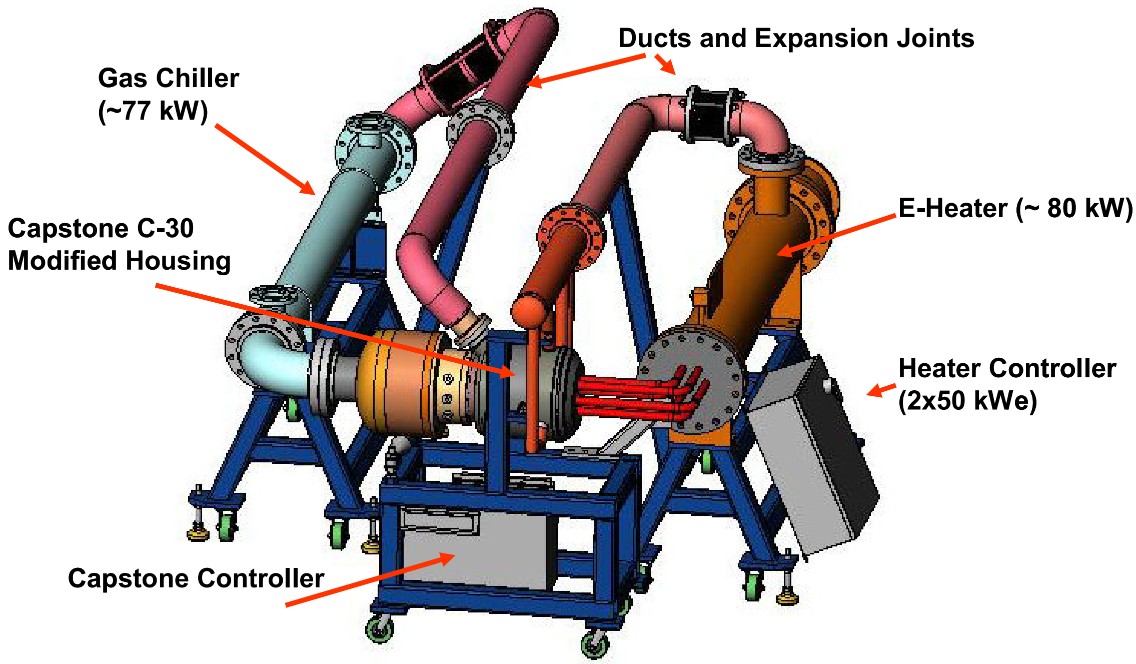

Figure 5.9: Assembly drawing of the Sandia closed-Brayton-cycle test-Loop (SBL-30).

Figure 5.10: Fully modified and assembled Capstone C-30 closed-Brayton loop as assembled at the manufactures (Barber-Nichols Inc.) is illustrated. The gas chiller is in the fore ground and the heater is on the left side of the image.

Figure 5.11: Sandia Brayton Loop as installed at Sandia. The loop is un-insulated in this figure. The heater is on the left, the gas chiller on the right, and the TAC in the middle.

Figure 5.12 Overview of the Sandia Brayton loop as viewed from the compressor inlet.

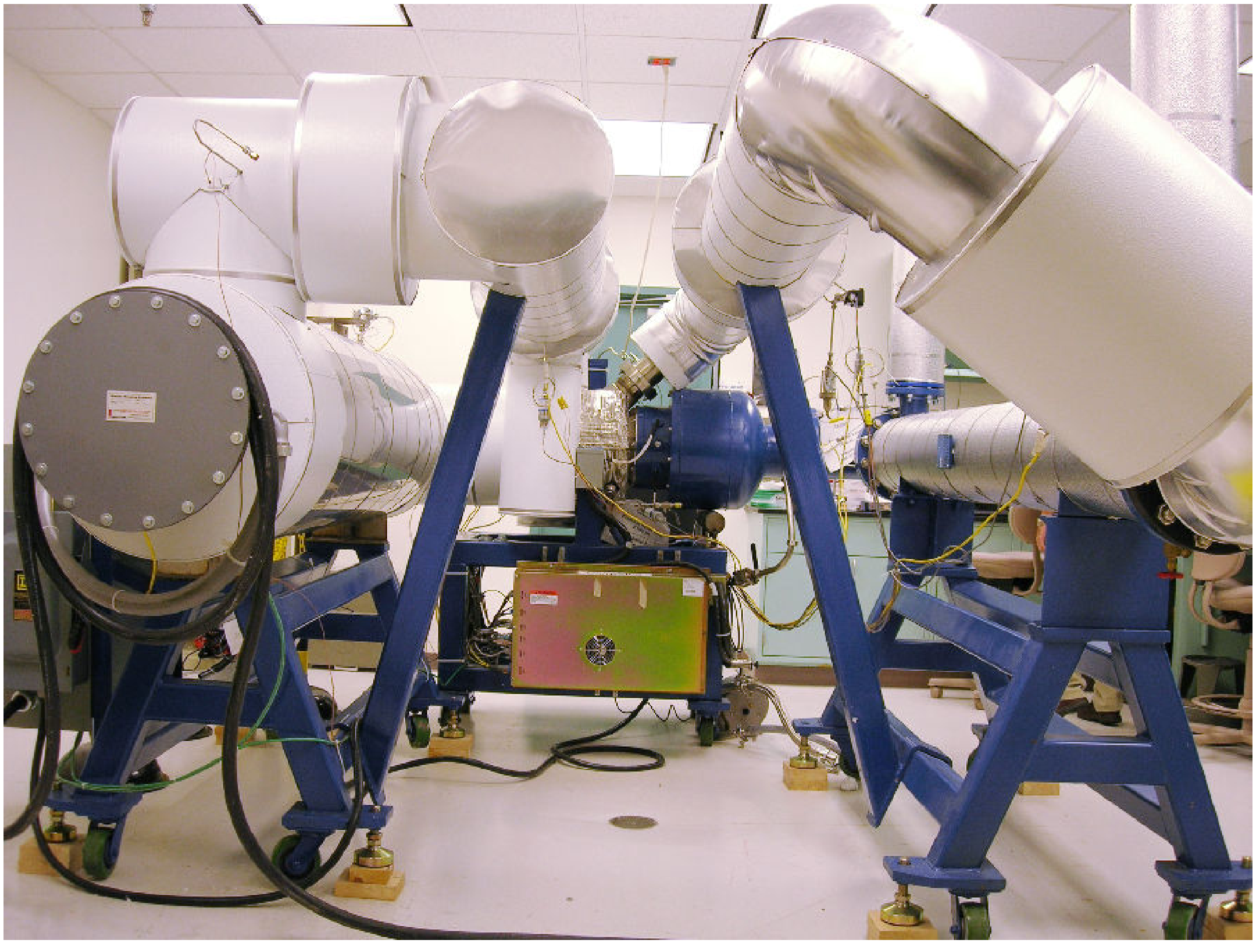

Figure 5.13: Fully installed and insulated Sandia Brayton Loop.

5.3 Gas Heater Description

The Brayton loop gas heater was designed to add about 80 kW of thermal power to the gas which would heat the flowing nitrogen or air to about 1000 K for a flow rate of about 0.25 kg/s. The heater and controller were designed and fabricated by Watlow Inc., Wright City, Mo. A photo of the heater and controller is shown in Figure 5.14 and in many of the other photos already shown. In general the heater consists of a horizontal 12” diameter schedule 300 304 stainless steel vessel through which 54 “U” shaped heater elements are placed. The heater elements are 0.430” inches in diameter and have a leg length of 71” (see Figure 5.15)The gas flows in an “L” shaped fashion through the heater, but 7 baffles force the gas flow into a serpentine path the crosses the heater elements. The inlet flow is downward, and the exit flow is horizontal. The heater element power density is about 5 Watt/in^2 and requires a supply voltage of 480 V 3 phase. The heaters are wired into two banks of three phase resistance bridges with each leg of the resistance bridge having a resistance that varies from 10.55 – 12.22 ohms. The vessel is designed to ASME specifications and it was designed for a fill gas pressure of up to 42 psia at a vessel temperature of 1425 K. The vessel was hydrostatically pressure tested to 474 pisg. Detailed engineering design specifications and drawings for the vessel and for the heater elements are listed in Table 5-1 and in Figure 5.16.

Figure 5.14: Watlow 80 kW Brayton loop gas heater and controller.

Figure 5.15: "U" shaped heater elements used in the Watlow heater. The photo shows the heater elements, the grid spacer wires, the baffle, and the gas exit thermocouple (vertical rod).

The RPCSIM dynamic model for the Sandia Brayton loop uses the reactor model for the electrical heater. However new input parameters are used to simulate the heater elements, the wall, and other design parameters. The RPCSIM core prism model is used for the wall, and the fuel pin model is used for the heater elements. The data that were used to determine the model input parameters were obtained from the tables and figures presented here and summarized in Table 5-3. The heat transfer coefficient uses the Dittus-Boelter model for gas heating. Thirty axial nodes are used along the length of the heater.

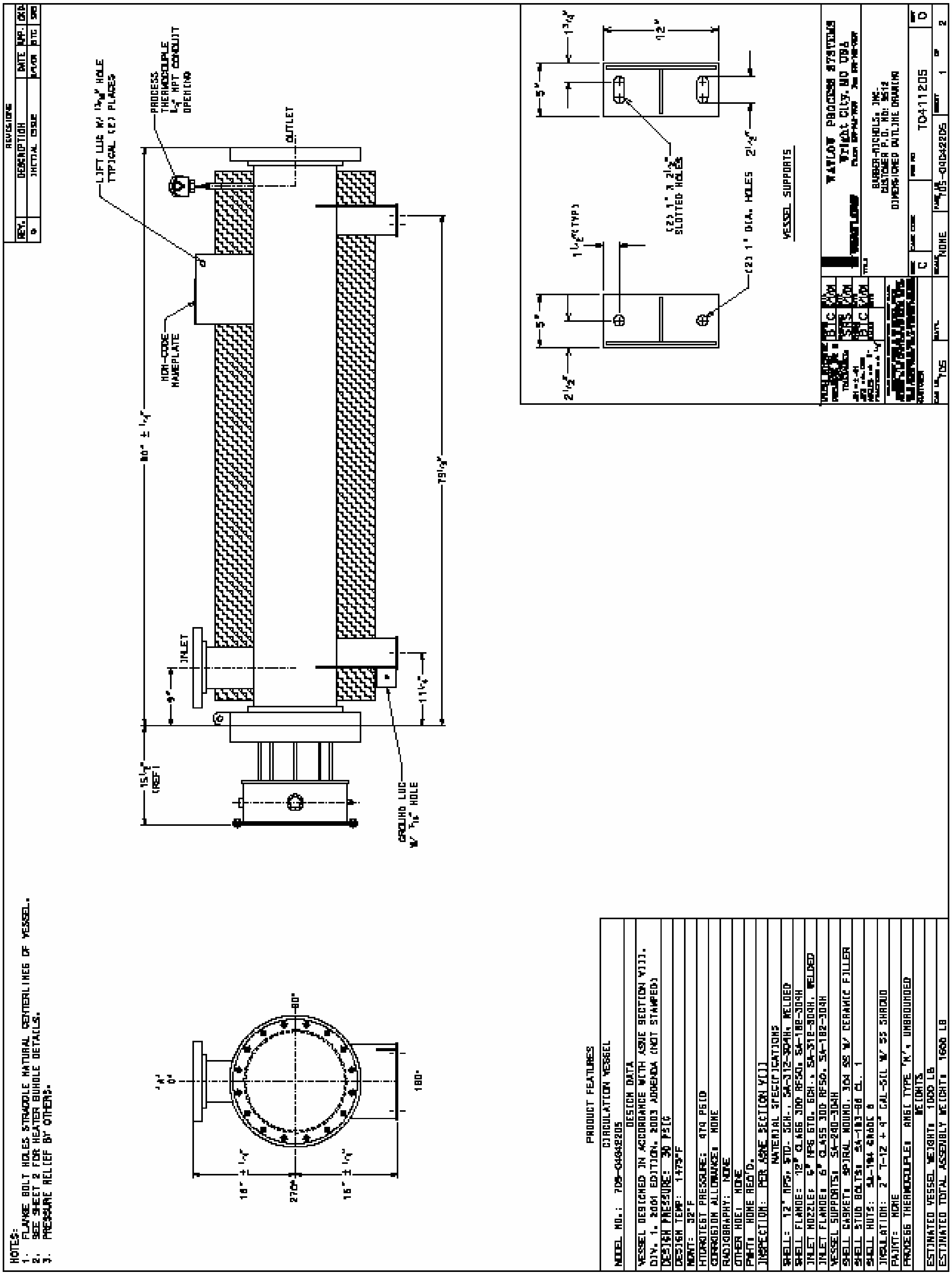

Table 5-1: Watlow 80 kW gas heater vessel product specifications.

Table 5-2: Watlow gas heat product specifications for the immersion heaters and their material specifications.

PRODUCT FEATURES

CIRCULATION VESSEL
MODEL NO.: 705-D4C42205
DESIGN DATA
VESSEL DESIGNED IN ACCORDANCE WITH ASME SECTION VIII, DIV. 1. 2001 EDITION. 2003 ADDENDA (NOT STAMPED)
DESIGN PRESSURE: 30 PSIG
DESIGN TEMP: 1475°F
MDMT: 32°F
HYDROTEST PRESSURE: 474 PSIG
CORROSION ALLOWANCE: NONE
RADIOGRAPHY: NONE
OTHER NDE: NONE
PWHT: NONE REQ'D.
INSPECTION: PER ASME SECTION VIII
MATERIAL SPECIFICATIONS
SHELL: 12" NPS. STD. SCH., SA-312-304H, WELDED
SHELL FLANGE: 12" CLASS 300 RFSO, SA-182-304H
INLET NOZZLE: 6" NPS STD. SCH., SA-312-304H, WELDED
INLET FLANGE: 6" CLASS 300 RFSO, SA-182-304H
VESSEL SUPPORTS: SA-240-304H
SHELL GASKET: SPIRAL WOUND, 304 SS W/ CERAMIC FILLER
SHELL STUD BOLTS: SA-193-B8 CL. 1
SHELL NUTS: SA-194 GRADE 8
INSULATION: 2" T-12 + 4" CAL-SIL W/ SS SHROUD
PAINT: NONE
PROCESS THERMOCOUPLE: ANSI TYPE 'K'. UNGROUNDED
WEIGHTS
ESTIMATED VESSEL WEIGHT: 1000 LB
ESTIMATED TOTAL ASSEMBLY WEIGHT: 1600 LB

Table 5-3: Fluid hydraulic and heat transfer properties used in the RPCSIM for the Sandia Brayton Loop SBL-30.

Heat Transfer to Coolant from Heater Elements		**Heat Transfer from Coolant Vessel Wall**	
Radius of element	4.953 mm	Wall inner radius	0.1492 m
L of element	1.727 m	Wall Length	2.235 m
Element Heat transfer Area	6.3988m^2	Wall heat transfer Area	2.0952
Flow Area	0.598 m^2		
Hydraulic Diameter	5.15 mm		
Element Inverse Thermal Capacitance (κ, kappa)	0.0016 K/J	Mass of Wall	221 kg
Number of effective pin or elements	108		

Table 5-4 Watlow gas heater vessel design drawings and specifications.

PRODUCT FEATURES

IMMERSION HEATER
MODEL NO: T01-04GD2205
ELECTRICAL DATA
DUTY: 79KW, 480 VAC, 3 PH
ELECTRICAL CLASSIFICATION: NON-HAZARDOUS
ELECTRICAL ENCLOSURE: NEMA 12
MAX. ANTICIPATED HOUSING TEMP: 142°F
ELECTRICAL CONNECTION(S): (2) 3 PH CKTS., #2 AWG MAX.
PROCESS DATA
MEDIUM: NITROGEN
NOMINAL FLOW RATE: 2000 LB/HR
OPERATING PRESS: 21 PSIG
INLET TEMP: 960°F
OUTLET TEMP: 1350°F
ESTIMATED SHEATH TEMPERATURE: 1500°F
RECOMMENDED SHEATH LIMIT TEMPERATURE: 1700°F
DESIGN DATA
VESSEL DESIGNED AND MANUFACTURED IN ACCORDANCE WITH ASME SECTION VIII, DIV. 1, 2001 EDITION, 2003 ADDENDA (NOT STAMPED)
DESIGN PRESSURE: 30 PSIG
DESIGN TEMP: 1475°F
MDMT: 32°F
TEST PRESSURE: 474 PSIG
NDE: DYE PENETRANT
POST WELD HEAT TREAT: NONE
CORROSION ALLOWANCE: NONE
MATERIAL SPECIFICATIONS
TUBESHEET: 12" CLASS 300 RF BLIND, SA-182-304H PER ASME B16.5-1996 EXCEPT 2 5/8" THK.
HEATING ELEMENTS: ALLOY 600 OVER STEEL
ELEMENT SUPPORTS/BAFFLES: 304 SS
ELECTRICAL ENCLOSURE: CARBON STEEL
ENCLOSURE HARDWARE: ZINC PLATED
ENCLOSURE PAINT: VENDOR STANDARD GRAY
ELEMENT END SEAL: EPOXY
HEATER SPECIFICATIONS
QTY & SIZE OF ELEMENTS: (54) 0.430" DIAMETER
WATT DENSITY/HEAT FLUX: 8 WPSI
IMMERSED LENGTH (BUNDLE REMOVAL DIST.): 77"
LIMIT SENSOR: (1) ANSI TYPE 'K' THERMOCOUPLE, UNGROUNDED
WEIGHTS
ESTIMATED HEATER BUNDLE WEIGHT: 600 LB

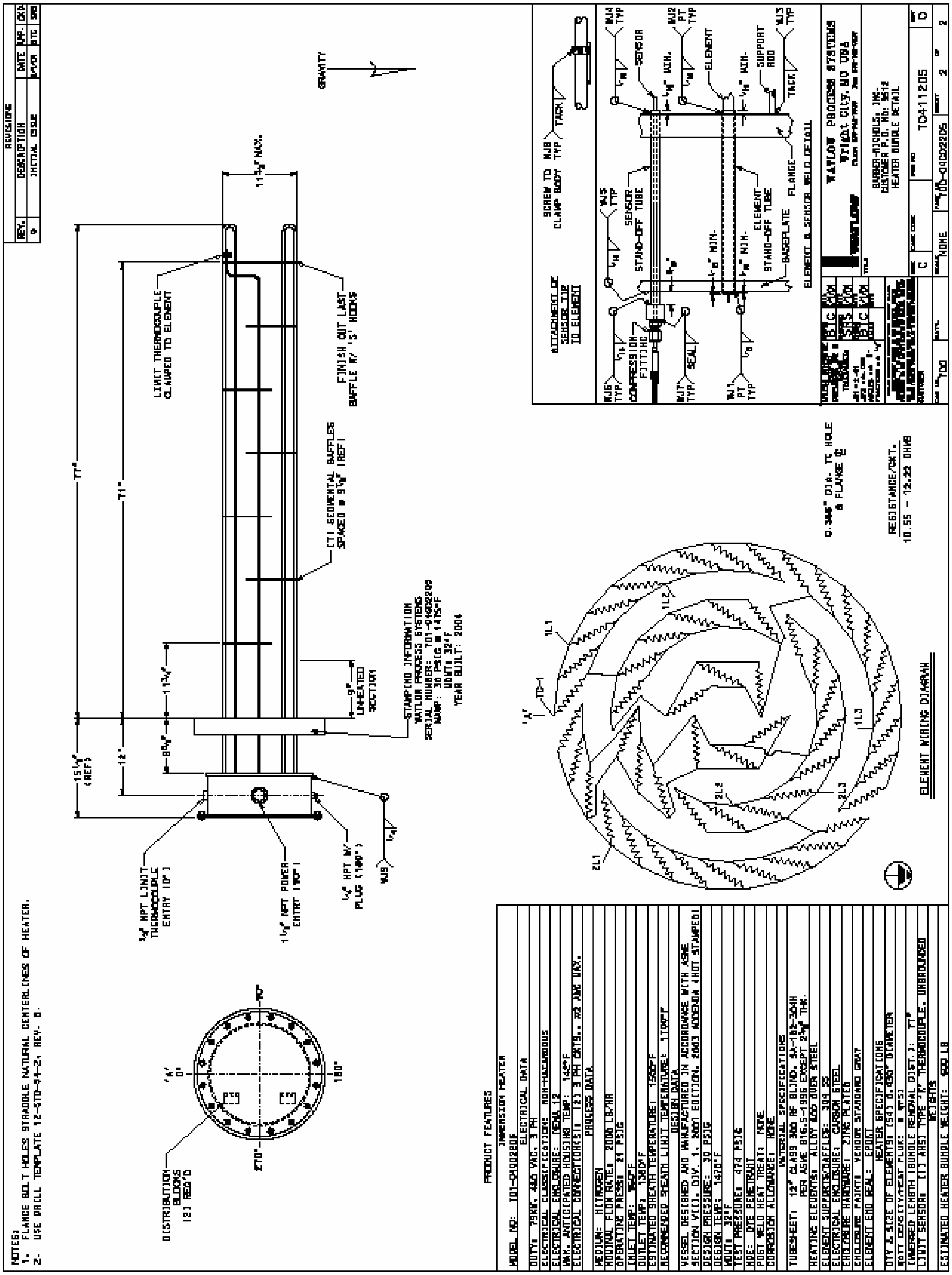

Figure 5.16 Watlow 80 kW gas heater element design drawings and specifications.

5.3.1 Electrical Power Description

Electrical power is required to run both the Watlow heater and the Capstone Power Management Controller. Both circuits require 480 V 3 phase power. The Capstone Power Management Controller is a grid connected controller and is designed to power the electronics in the controller, the inverter circuitry and the motor/alternator. As such, it can draw power from the grid to "motor" the permanent magnet alternator, or it can put power back on the grid which in the Sandia Brayton test loop goes to powering the heater. The Capstone Model 330 electrical output can accommodate 3 phase, 400-480 VAC, and 45-65 Hz. Both voltage and frequency are determined by the grid.

Table 5-5 shows the maximum and typical power draw conditions expected from the Capstone Power Management Controller during various phases of operation. The facility power in the laboratory was increased to 100 amperes from 60 amperes (480 Volt) to accommodate the power draw and the supply to the grid and heater. Figure 5.18 shows the approximate layout of the hardware as located in Sandia building 6585 room 2504. The laboratory was designed to supply these levels power and cooling water, but minor modifications were required to connect the water to fill and drainage system, and to increase the amperage. These modifications were made by Sandia facilities.

Table 5-5: Maximum and Typical Power Draws/ Supply form Capstone Power Management Circuitry

	Max	Typical	Duration
Motor Power	3.5 kWe	2 kWe	Minutes
Electrical Pwr Management	2-3 kWe	2-3 kWe	Continuous
Electrical Pwr to Grid	30 kWe	10.5 kWe	Hours to Continuous
Power Draw/Supply	5.5 kWe/30 kWe	5.5kWe/10.5 kWe	
Notes	*Limited to 15 kWe based on maximum design temp of Heater*	*This is the maximum power to grid measured to date*	

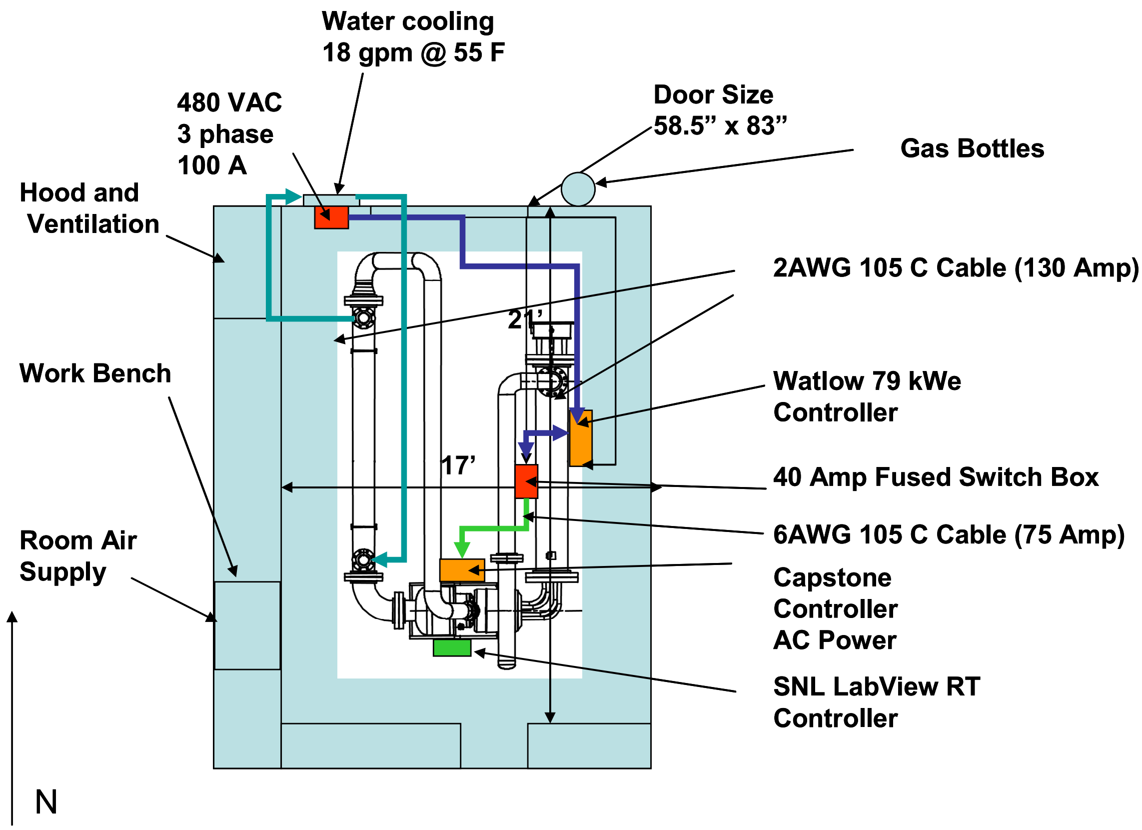

Figure 5.17: Electrical connection and cooling water supply for the SBL-30 as located in building 6585 room 2504. All power is supplied by the 480 3phase 100 amp service from the wall. The cooling water is provided by the building facilities manager.

The electrical circuit for the Watlow heater controller was purchased from Watlow, and it is shown in Figure 5.18. The Watlow heater control box is interlocked through the door to remove electrical service power to the heater when the service box door is open. It also has a manual switch that must be turned to off before the door can be opened. The circuitry within the heater box then splits into two 50 kWe Dynamite DC2T-60F0-0000 SCR controllers. The SCR controllers switch at the zero crossing intervals and the fractional power is determined by dwell time when no current is allowed to flow. For 50% power, the SCR switches the current on for 3 cycles of the 60 Hz power supply, and then off for 3 cycles. Similarly 25% power uses a dwell time of 6 cycles for the off mode and 3 for the on. The amount of power draw is controlled by a 4-20mA current loop that is set by the RT_CBC_Controller. The internals of the box was wired and provided by Watlow and the electrical circuit for this controller is shown in Figure 5.18. Two thermocouple high temperature limit circuitry interrupts the current draw if the heater element temperatures exceed their maximum temperature limits. One thermocouple is connected to the heater element at the hot outlet side of the heater and is set to a value at or below 1450 F = (1061K), and the other thermocouple measures the gas exit temperature and is set to a value below 1350 F = 1005 K. These thermocouples are also monitored by the RT_CBC_Controller.

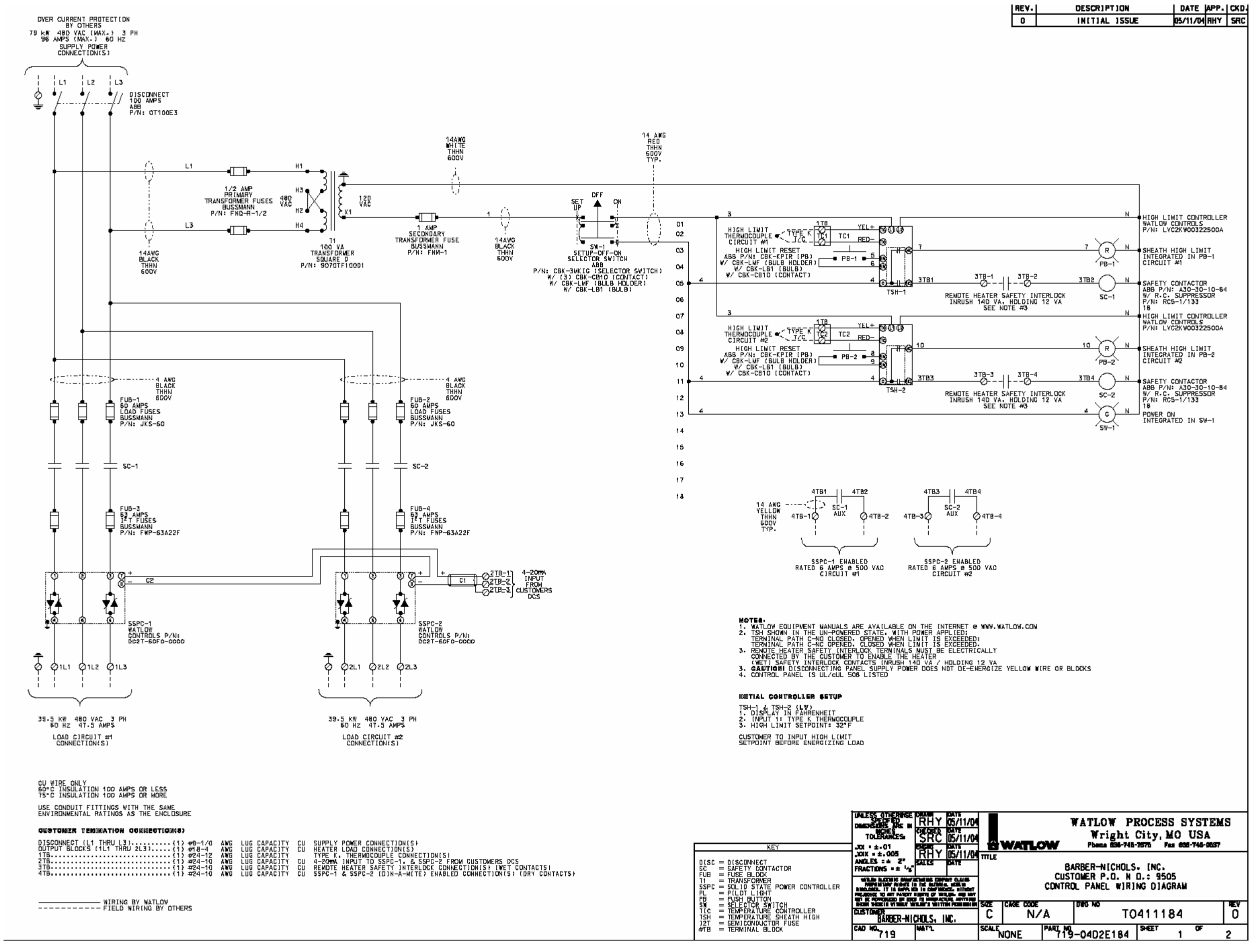

Figure 5.18: Electrical Power circuit for the heater provided by Watlow.

5.4 Gas Cooler Description

The gas cooler provides waste heat rejection capability for the Sandia Brayton Loop. It uses a Basco/Whitlock, Buffalo, NY, shell and tube counter flow heat exchanger. Water flows in the shell portion and the gas/nitrogen flowing in the tubes. It was designed to reject 68.9 kW of heat for a water flow rate of 18 gallons per minute (1.089 kg/s) with a water temperature difference of 15.1 K. The design can accommodate even higher flow rates, up to 50 gallons per minute, thus if we upgrade the power capability of the heater, we can still use the same gas chiller as it is oversized for our nominal operations. Photos of the chiller and the gas inlet passages are shown in Figure 5.19 and Figure 5.20. The cooling water available within laboratory 6585/2504 provides 18 gallons per minute of cooling water at 55 F.

Table 5-6: Basco/Whitlock gas chiller hydraulic and heat transfer properties used in the RPCSIM model for the Sandia Brayton Loop

Hydraulic and Heat Transfer Properties of the Gas Cooler Heat Exchanger	
Mass of Heat Exchanger	114 kg
Area of Water Flow Leg in Heat Exchanger	10.109 m^2
Area of Gas leg in Heat Exchanger	8.0870 m^2
Length of Wtr leg in Heat Exchanger	2.896 m
Length of Gas Leg in Heat Exchanger	2.896 m
Effective Wall thickness of Heat Exchanger	1.587 mm
Hydraulic Diameter of Water Leg	21.3 mm
Hydraulic Diameter of Gas Heat Exchanger leg	25.4 cm
Flow area in HP Heat Exchanger Leg	.019 m^2
Flow area in LP Heat Exchanger Leg	.008867 m^2

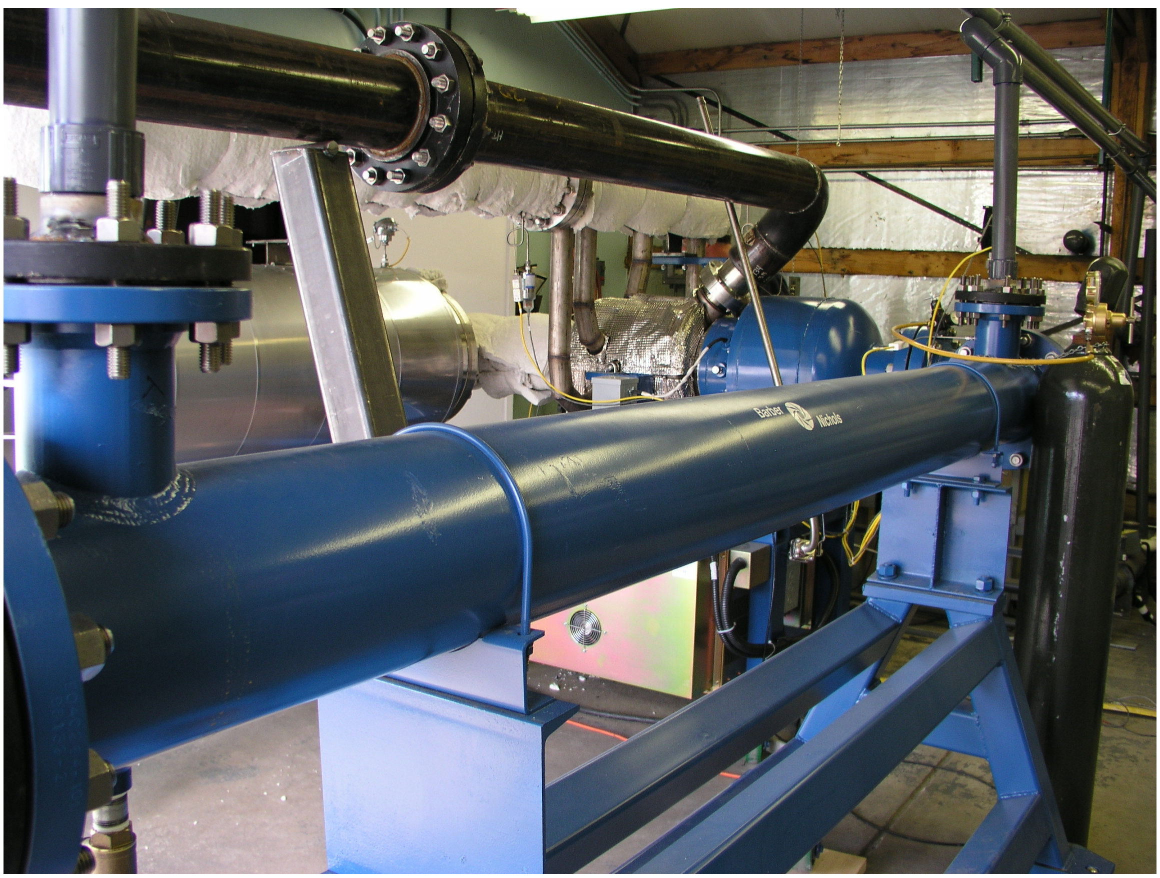

Figure 5.19: Image of the Basco/Whitlock shell and tube gas chiller. Inlet water flows from the upper right side of the image to the lower left, while gas flows in the opposite direction.

Figure 5.20: View of the Basco/Whitlock shell and tube heat exchanger gas inlet flange, showing the stainless steel tubes.

May 06 02 10:46a Roger Shultz 303-670-0802 p.2
MAY-06-2004 12:30 P.03/03

API Heat Transfer

Basco/Whitlock Shell and Tube Heat Exchanger

		JOB NO.	
CUSTOMER	BARBER NICHOLS	REFERENCE NO.	
ADDRESS		PROPOSAL NO.	JHB03-16980
PLANT LOCATION		DATE	06 MAY 2004
SERVICE OF UNIT	NITROGEN COOLER	ITEM NO.	101 REVISION 02
SIZE 08-114	TYPE "-EM"	(HORZ.) (VERT.)	CONNECTED IN
SQ.FT.SURF/UNIT (GROSS) (EFF.) 107.3	SHELLS/UNIT ONE	SQ.FT.SURF/SHELL (GROSS) (EFF.)	107.3

PERFORMANCE OF ONE UNIT

		SHELL SIDE	TUBE SIDE
FLUID CIRCULATED		WATER	NITROGEN
TOTAL FLUID ENTERING	LB/HR	24750	2088
VAPOR	LB/HR		
LIQUID	LB/HR	24750	
STEAM	LB/HR		
NON-CONDENSABLES	LB/HR		2088
FLUID VAPORIZED OR CONDENSED	LB/HR		
STEAM CONDENSED	LB/HR		
SPECIFIC GRAVITY			
VISCOSITY @ TEMP	cP @ °F	@	@
MOLECULAR WEIGHT			
SPECIFIC HEAT	BTU/LB-°F		
THERMAL CONDUCTIVITY	BTU/HR-FT-°F		
LATENT HEAT	BTU/LB		
TEMPERATURE IN	°F	70.0	540.0
TEMPERATURE OUT	°F	79.5	95.0
OPERATING PRESSURE	PSIA		35.0
NO. PASSES PER SHELL		ONE	ONE
VELOCITY	FT/SEC		
PRESSURE DROP	PSI	2.5	0.2
FOULING RESISTANCE (Min)	°F-FT²-HR/BTU	0.001	0.001
HEAT EXCHANGED 235500	BTU/HR	MTD CORRECTED	149 °F
TRANSFER RATE - SERVICE 14.9		CLEAN	BTU/HR-FT²-°F

CONSTRUCTION OF ONE SHELL

		SHELL SIDE	TUBE SIDE
DESIGN PRESSURE	PSIG	150	150
TEST PRESSURE	PSIG	Per Code	Per Code
DESIGN TEMPERATURE (Max/Min)	°F	500 / +20	600 / +20

TUBES 304SS SA249	NO. 70 OD 0.625" BWG 18	LENGTH 9'-6"	PITCH 0.78125" Tri
SHELL Carbon Steel	ID OD 8.625"	SHELL COVER	(INTEG)(REMOV)
BONNET/CHANNEL ————		CHANNEL COVER	
TUBESHEET-STATIONARY 304 SS		TUBESHEET-FLOATING	
BAFFLES-CROSS Carbon Steel	TYPE	FLOATING HEAD COVER	
BAFFLES-LONG	TYPE	IMPINGEMENT PROTECTION	No
TUBE SUPPORTS			
TUBE TO TUBESHEET JOINT	Mechanically Rolled & Double Grooved		
GASKETS ————		PACKING	
CONNECTIONS-SHELL SIDE	IN 4"	OUT 4"	RATING 150# RFSO
BONNET/CHANNEL SIDE	IN 8" Axial	OUT 8" Axial	RATING 300# RF
CORROSION ALLOWANCE - SHELL SIDE	1/16" on C. Steel	TUBE SIDE	None
CODE REQUIREMENTS	ASME Sec. VIII, Div. 1 (Latest Addenda)	TEMA CLASS	"C"
OTHER			
REMARKS			

Customer's 8" 300# ANSI RF pipe flanges to bolt directly to tubesheets.
Cooling water must be the first stream turned on and the last stream turned off.
Fixed tubsheet heat exchanger. Do not thermally shock.

• API Basco • 2777 Walden Avenue, Buffalo, NY 14225 • (716) 684-6700 Fax: (716) 684-2129

• www.apiheattransfer.com

Figure 5.21: Gas cooler specifications (1).

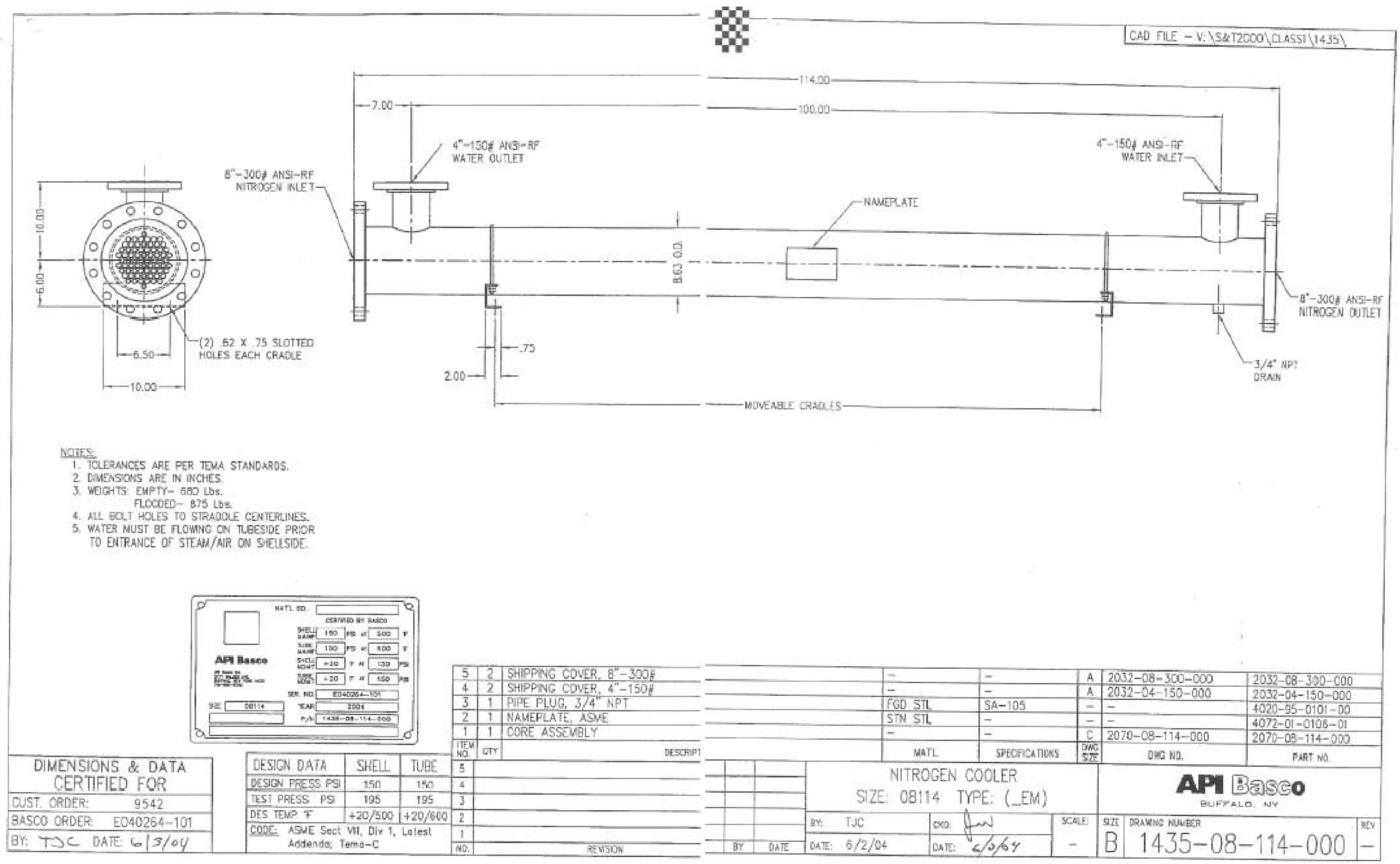

Figure 5.22: Gas cooler design specifications.

5.5 Ducting and Instrumentation Description

A schematic of the Sandia Brayton Loop is shown in Figure 5.23. This figure shows the location of the pressure and temperature sensors used in the loop. Since the time of writing of this report a few addition sensors have been added. The major sensors consist of temperature and pressure measurements at either the entrance or exit of every major component. The stations are labeled 1-6 by using the same nomenclature as described earlier. The manufacturer used a different numbering scheme when installing the instrumentation. This nomenclature starts with 100 (at the turbine inlet) and then progresses around the loop in increments of 100. The loop also contains a flow orifice at station 6B. The orifice is has a diameter of ½ the ducting inside diameter and the pressure taps are at ½ and 1 times the diameter of the ducting. The ½ diameter tap is located down stream of the orifice. For the gas temperature we use the temperature sensor located at station 6. The flow is calculated using the methods described in ASME MFC-3M-1989. In all cases type K thermocouples are used. For the gas temperature measurements the thermocouples are 1/8" diameter ungrounded sheathed thermocouples. Other pressure tapes not shown in the diagram are located on the inlet and outlet flange of the Watlow heater. Similarly a number of thermocouples were added to provide measurements of hot duct wall temperatures. A detailed list of instrumentation and the feedthrough type used at each gas state-point measurement location is provided in Table 5-7.

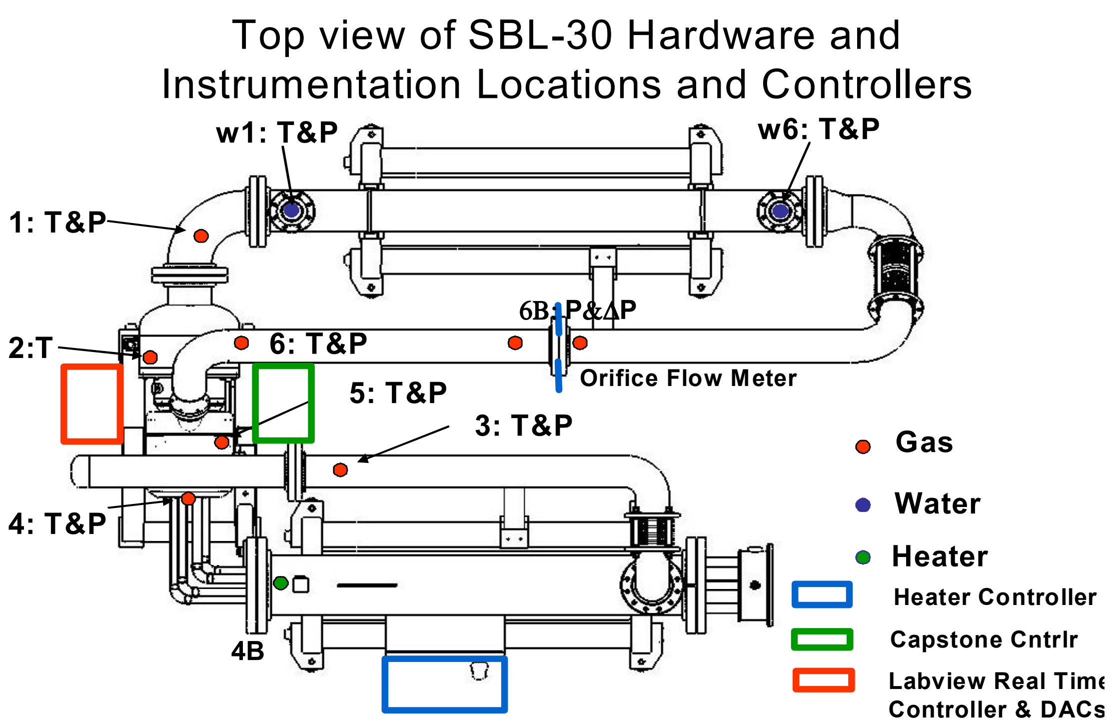

Figure 5.23: Top view schematic of Sandia Brayton Loop and location of major temperature and pressure sensors, and the controllers.

Table 5-7: Description of instrumentation, feedthroughs, and connectors at each station identified in Figure 5.23.

1. TC, Type K on SS Swagelok, T400

   PT on SS Swagelok hardware, Setra Systems, C280E, 1277375, 0-25 psia, P400

2. PT on SS Swagelok hardware, Setra Systems, C280E, 2369046, 0-100 psig, P500

   5B ¾” pipe, steel flange, ¾” cast iron nipple, 3/4”-1” elbow, brass adaptor, rubber vacuum hose with hose clamps, CC Valve (100 psi, electric), ¾” steel tube, manual valve (Whitey, SS-65TSW16P 2200 psi CF3M), ¾” steel tube; tee off ¾” pipe to PT 2373889, 0-25 psig, P200

3. TC, Type K on SS Swagelok, T601

   PT on SS Swagelok hardware, Setra Systems, C280E, 2369045, 0-100 psig, P601

4. TC, Type K on SS Swagelok, T100

   PT on SS Swagelok hardware, Setra Systems, C280E, 2373889, 0-25 psig, P200

   4B TC, Type K on SS Swagelok, TC, Type K on SS Swagelok

5. TC, Type K on SS Swagelok, T200 on housing dome
6. TC, Type K on SS Swagelok, T300

   PT on SS Swagelok hardware, Setra Systems, C280E, x297734, 0-25 psia,

   6B PT on SS Swagelok hardware, Setra Systems, C280E, 1277377, 0-25 psia

   ΔPT, Setra, 2301001PD2F11B, 0-1 psid

   W1 TC, Type K on SS Swagelok, T700

   W2 TC, Type K on SS Swagelok, T701; PT 2372251, 0-50 psig, P701

Two photos of the instrumentation and the feed through ports are shown in Figure 5.24 and in Figure 5.25. Figure 5.24 shows the turbine inlet temperature port and the pressure port. Both measurements are made on one of the six heater outlet tubes. Also, if one looks closely, the turbine exit temperature and pressure ports can also be seen. They are mounted directly to the bell housing near the center of the dome. Figure 5.25 shows the temperature and pressure feed through used for the compressor inlet. Also shown in this figure is the inlet gas feed through which the system is filled.

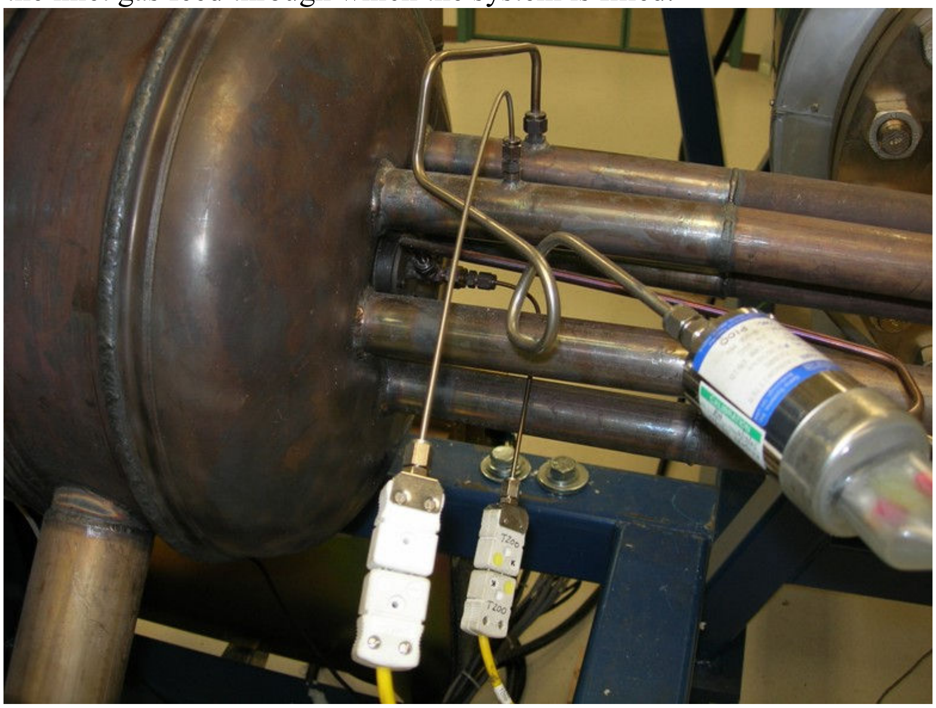

Figure 5.24: Turbine inlet temperature and pressure sensors and their feed through ports. Note that these instruments measure the gas temperature and pressure in one of the six heater exit tubes.

Figure 5.25: Compressor inlet temperature and pressure feed through port and sensors.

An important parameter that is used in the dynamic model is the volume and mass of each duct and component. The volume of the components in the high and low pressure legs are given in Table 5-8. Stainless steel was used for all hot ducts and carbon steel was used for the low temperature ducts which consist of the Gas cooler inlet ducting and the compressor inlet ducting. The summed volumes and the resulting stored energy are given in Table 5-9. The differential pressure (absolute minus ambient) is used in these calculations. The total stored energy in the gas loop at the values of the respective pressure relief valve settings is 0.163 MJ. The total volume of the gas loop is 0.57 m^3(20 cf). For comparison, the volume of the room that the unit is in is about 97 m^3 (3400 cf).a

Table 5-8: Volumes on the components in the gas loop.

Component: Pipes & Ducts	Inner Diam	Inner Diam	Length	Vol
	(in)	(m)	(m)	(m3)
Low-Pressure Leg				
Turbine Housing	17.760	0.451	0.480	0.077
Recup-to-Gas-Cooler Small Pipe	4.760	0.121	0.130	0.001
Gas-Cooler Inlet First Elbow	6.352	0.161	0.380	0.008
Gas-Cooler Inlet Line	6.352	0.161	3.250	0.066
Gas-Cooler Inlet Second Elbow	6.352	0.161	0.380	0.008
Cooler Inlet Bellows	6.625	0.168	0.410	0.009
Gas-Cooler Inlet Elbow	6.352	0.161	0.740	0.015
Gas Cooler Tubes	0.527	0.013	189.0	0.027
Compressor Inlet Elbow	7.9810	0.203	0.5100	0.016
Compressor Inlet Pipe	7.9810	0.203	0.2000	0.006
Filter Housing	20.000	0.508	0.470	0.095
Generator Housing	13.500	0.343	0.200	0.018
High-Pressure Leg				
Recup-to-Heater Small Pipes	2.635	0.067	2.500	0.009
Recup-to-Heater Manifold	5.761	0.146	1.120	0.019
Heater Inlet Large Pipe	6.060	0.154	1.500	0.028
Heater Inlet First Elbow	6.060	0.154	0.380	0.007
Heater Inlet Bellows	6.625	0.168	0.230	0.005
Heater Inlet Second Elbow	6.060	0.154	0.300	0.006
Gas Heater Inlet Pipe	6.352	0.161	0.180	0.004
Gas Heater Shell	11.380	0.289	2.300	0.151
Gas Heater Element Tubes	0.430	0.011	-124.2	-0.012
Turbine Inlet Pipes	1.402	0.036	4.860	0.005
Turbine Inlet Elbows	1.402	0.036	0.120	0.000

Table 5-9: Total volume gas loop.

Low-Pressure Leg Total Vol (m3)	0.348
Low-Pressure Leg Pressure (MPa_g)	0.206
Low-Pressure Leg Energy (MJ)	0.036
High-Pressure Leg Total Vol (m3)	0.221
High-Pressure Leg Pressure (MPag)	0.413
High-Pressure Leg Energy (MJ)	0.046
Total loop volume (m3)	0.569

Table 5-10: Duct and component volumes, mass, length, and hydraulic diameter.

Duct or Component ID		Volume (liter)	Length (m)	Hydraulic Diameter (m)	Mass (kg)
V_{11}	Compressor Inlet Duct	127 liter	0.662 m	..4048 m	60.748
V_{22}	Compressor Outlet Duct	3 liter	0.10 m	0.4 m	0.252
V_{23}	High Pressure leg of Recuperator	20 liter	0.25 m	rcp	250
V_{33}	Heater Inlet Duct	77 liter	4,239 m	0.307 m	121.78
V_{34}	Reactor Coolant Volume or Length	139 liter	2.235 m	rx	---
V_{44}	Heater Outlet Duct Volume	5 liter	1.067	..0696 m	9.6769
V_{55}	Turbine Outlet Duct	3 liter	0.1 m	.4 m	0.25196
V_{56}	Low Pressure leg of Recuperator	20 liter	0.25 m	rcp	250
V_{66}	Gas Chiller Inlet Duct	108 liter	5.004 m	0.3226 m	70.425
V_{61}	Gas Chiller	27 liter	2.5 m	gcx	114

6 Summary and Observations

The data presented in this report provides a more detailed data base for modeling closed Brayton cycles than has been generally available. Overall a large number of tests have been performed in FY06 and much of this data is provided in this document and in the data CD that will be made available with this report.

This data contains steady-state data, transient data, and the results from a range of working fluids which span a range of thermo-physical gas properties from ideal gases and gas mixtures to very non-ideal gases such as CO_2 (far from the critical point). The steady state data that is provided contains information that can be used to validate the characteristic flow curves used in the current steady-state and dynamic models. Other steady-state data is provided that requires steady-state or dynamic models of the entire Brayton loop to predict the operating behavior of the closed Brayton loop. The transient test data is summarized and provided in this report, but still requires comparisons with models to be complete.

The data provided here a significantly expanded database for model comparisons and validation, but clearly more data is required to support modeling of control options, especially techniques that use bypass control methods. It is also desirable to perform additional inventory and throttle valve control tests. The bypass and throttle valve control tests were not performed because they require hardware modifications to the Sandia Brayton loop which were not within the resource scope of the FY06 Tasks. The data provided will support the development of S-CO2 model development and verification. This data is intended to provide an initial database for model evaluation, but it is recognized that higher fidelity experiments with S-CO2 are needed before larger systems can be designed and constructed.

The follow-on activities that are recommended include bypass flow control testing and modifications to the heater operating control system to allow simulation of the response from a nuclear reactor with various types of feedback mechanisms. Although additional testing with this loop will provide useful data for improved models, eventually testing of small scale supercritical CO2 loops is also required if one is to actively advance the state-of-knowledge for these unique Brayton cycles.

A follow-on report (July, 2006) will provide results and summaries of the modeling efforts for the test results described in this report. The July deliverable report will contain modeling results from SNL, and results to date from the MIT, ANL, and INL tasks. These initial comparisons will provide insight on the validity, strengths, and weaknesses of the current models.

References

ASME, "Measurement of Fluid flow in Pipes Using Orifice, Nozzle, and Venturi", ASME MFC-3M-1989, Reaffirmed 1995, 1989.

Balje O. E., *Turbomachines: A Guide to Design, Selection and Theory,* John Wiley and Sons, New York, 1981.

Barber-Nichols Inc, 6325 West 55th Avenue, Arvada, CO 80002, http://www.barber-nichols.com, 2006.

Bragg-Sitton S. and J.P. Holloway. "Reactor Start-up and Control Methodologies: Consideration of the Space Radiation Environment," in *Proceedings of Space Technology and Applications International Forum (STAIF-2004)*, pp 614-622, February, 2004.

Brey, H. L. "Current Status and Future Development of Modular High Temperature Gas Cooled Reactor Technology," IAEA, Tecdoc=(electronic version), 1999-2000.

Brunhouse J. S. Jr. and G. W. Titus, "Nitrogen, Air Acceptable to Cool ML-1", *Nucleonics*, February 1961.

CBC pressure safety data package (Lipinski, Wright, 2005).

Capstone Turbine Corporation, 21211 Nordhoff Street, Chatsworth, CA 91311, http://www.microturbine.com

Frutschi Hans Ulrich, "Closed-Cycle Gas Turbines, Operating experience and Future Potential", ASME Press, 2005.

Galvas, M.R. "Fortran Program for Predicting Off-Design Performance of Centrifugal Compressors," NASA TN D-7487, 1973.

Japikse, D. and N.C. Baines. *Introduction to Turbomachinery*, Concepts ETI Inc. and Oxford University Press, 1997.

Japikse, D. *Centrifugal Compressor Design and Performance*, Concepts ETI Inc. 1996.

Lipinski R.J. and S.A. Wright. "A Gas-Cooled-Reactor Closed-Brayton-Cycle Demonstration with Nuclear Heating," in *Proceedings of Space Technology and Applications International Forum (STAIF-2005)*, February, 2005.

Mason Lee S., Richard K. Shaltens, and William D. Espinos. "Experimental Data for two Different alternator Configurations in a Solar Brayton Power System", NASA Technical Memorandum 107509, IECEC-97481, *Proceedings of the 32 Intersociety Energy Conversion engineering Conference*, Honolulu, Hawaii, July-August 1997.

NASA, Software Repository, https://technology.grc.nasa.gov/software/index.asp, 2005.

Pope M. A. Driscoll M. and Hejzlar P. "Reactor Physics Studies in Support of GFR Core Design*", Transactions of the American Nuclear Society, Proceeding of GLOBAL '03*, New Orleans, LA, Nov. 16-21, 2003.

Saito, S., et. al, "Design of High Temperature engineering Test Reactor (HTTR), JAREI 1332, 6 1994.

Suid L. H., *The Army's Nuclear Power Program: The Evolution of a Support Agency*, Greenwood Press, NY 1990.

Walsh P.P. and P. Fletcher. Gas Turbine Performance, ASME Press, 1998.

Wasserbauer, C.A. and A.J.Glassman. "FORTRAN Program for Predicting Off-Design Performance of Radial-Inflow Turbines," NASA TN D-8063, 1975.

Watlow Electric Manufacturing Company, 12001 Lackland Road, St. Louis, Missouri, USA 63146, www.watlow.com, 2005.

Weitzberg, A. "Liquid Metal Cooled Reactor Concept for Nuclear Space Initiative Electric Propulsion Missions," Design Data Package to Department of Energy Office of Space and Defense Power systems Space Reactor Programs Team, October, 2002.

Wilson D. G., *The Design of High-Efficiency Turbomachinery and Gas Turbines*, MIT Press, Cambridge, Massachusetts, 1988.

Wollman M, "The Reactor Module for Project Prometheus", proceedings of the "Space Nuclear Conference 2005", Embedded Topical Meeting at the 2005 ANS Annual Meeting", June 5-9, San Diego, 2005.

Wright S. A., "Preliminary Results of Dynamic System Model for a Closed-Loop Brayton Cycle Coupled to a Nuclear Reactor," in *Proceedings of the 1st International Energy Conversion Engineering Conference*, 17 - 21 Portsmouth, VA, Aug. 17-21, 2003.

Wright, S.A. "Dynamic Model of a Space Reactor Brayton-Cycle System," *Transactions of the American Nuclear Society Proceedings*, Washington, DC, November, 2003.

Wright, S. A. and Beets R., "Application of Digitally-Controlled-Reactor Architecture to Space Reactors", *in Proceedings of the American Nuclear Society Meeting*, Washington DC, November, 2003.

Wright, S. A., and R. J. Lipinski. "Pin-Type Gas Cooled Reactor for Nuclear Electric Propulsion," in *Proceedings* of *Space Technology and Applications International Forum (STAIF-2003)*, edited by M. El-Genk, AIP Conference Proceedings 654, New York, pp. 408-419, 2003.

Wright, S.A., R. Fuller, , R. J. Lipinski, K. Nichols, and N. Brown. "Operational Results of a Closed Brayton Cycle Test-Loop," in proceedings of *Space Technology and Applications International Forum (STAIF-2005)*, edited by M. El-Genk, AIP Conference Proceedings, New York, 2005.

Wright, S.A and Lipinski, R. J. "Gas Cooled Space Fission Electric Power and Propulsion Systems," Design Data Package Prepared by Sandia National Laboratories for U.S. Department of Energy Office of Space and Defense Power Systems Space Reactor Programs Team, April 17, 2003a.

Wright S.A. and T. Sanchez. "Dynamic Modeling and Control of Nuclear Reactors Coupled to Closed-Loop Brayton Cycle Systems using SIMULINK™ ," in *Proceedings of Space Technology and Applications International Forum (STAIF-2005)*, February, 2005.

Wright, S. A and Lipinski, R. J., "Advanced High Efficiency Direct Cycle Gas Power Conversion Systems for Small Special Purpose Nuclear Power Reactors", SAND 2006-2518, 2006.